Modeling Cystic Fibrosis Chronic Infection Using an Engineered Mucus-like Hydrogel

by

Courtney O'Brien

Submitted in partial fulfilment of the requirements
for the degree of Master of Applied Science

at

Dalhousie University
Halifax, Nova Scotia
October 2022

Dalhousie University is located in Mi'kma'ki,
the ancestral and unceded territory of the Mi'kmaq.
We are all Treaty people.

Table of Contents

List of Tables

List of Figures

Abstract

Airway mucus provides protection to airway epithelial surfaces by trapping and clearing harmful pathogens. In cystic fibrosis, a genetic disorder that primarily impacts the respiratory system, airway mucus has altered properties including increased solids content and viscoelasticity. These altered properties cause mucus clearance mechanisms to fail and create a microenvironment primed for chronic airway infections. These complex polymicrobial infections show increased resistance to antibiotics and are associated with poor patient prognosis. Current *in vitro* models of cystic fibrosis airway infections fail to combine the key elements needed to fully represent this microenvironment and also lack the ability to capture major aspects of chronic airway infections in cystic fibrosis. In this study, mucus-like hydrogels with varied compositions and viscoelastic properties reflecting relative differences between healthy airway mucus and cystic fibrosis airway mucus were developed. Models of the cystic fibrosis and healthy airway microenvironments were created by combining the mucus-like hydrogels with relevant pathogens, human bronchial epithelial cells, and a common antibiotic used to treat airway infections in patients with cystic fibrosis. This research project demonstrated that antibiotic resistance was not solely dependent on the altered properties of the mucus-like hydrogels but was also influenced by culture conditions including microbe species, whether the culture was monomicrobial or polymicrobial, and the presence of epithelial cells. In addition, our cystic fibrosis airway model showed the ability to mimic important features that are characteristic of chronic cystic fibrosis airway infections including sustained polymicrobial growth and increased antibiotic tolerance. This model has the potential to be used to investigate antibiotic resistance and polymicrobial interactions in chronic cystic fibrosis airway infections and can also be adapted to study microbe behavior in other mucus-related diseases.

List of Abbreviations and Symbols Used

AA	Antibiotic-antimycotic
AMP	Antimicrobial peptide
ANOVA	Analysis of variance
ASM	Artificial CF sputum medium
ATPS	Aqueous two-phase system
BHI	Brain Heart Infusion
CF	Cystic fibrosis
CFU	Colony forming unit
CFTR	Cystic fibrosis transmembrane conductance regulator
DAPI	4′,6-diamidino-2-phenylindole
DEX	Dextran
DI	Deionized
DMEM	Dulbecco's Modified Eagle Medium
DNA	Deoxyribonucleic acid
ENaC	Epithelial sodium channel
FBS	Fetal bovine serum
G'	Storage (or elastic) modulus
G''	Loss (or viscous) modulus
GC	Growth control
GDL	Glucono-delta-lactone
GFP	Green fluorescent protein
HA	Hyaluronic acid
hBD	Human β-defensin

HBE	Human bronchial epithelial
HEPES	4-(2-hydroxyethyl)-1-piperazineethanesulfonic acid
ISO	International Organization for Standardization
LB	Luria-Bertani
LVR	Linear viscoelastic region
MIC	Minimum inhibitory concentration
MSA	Mannitol salt phenol red agar
OD_{600}	Optical density at 600 nm wavelength
PDMS	Polydimethylsiloxane
PEG	Polyethylene glycol
PGM	Porcine gastric mucins
PBS	Phosphate-buffered saline
RFP	Red fluorescent protein
RPMI	Roswell Park Memorial Institute
SC	Sterility control
SCFM	Synthetic CF sputum medium
SCV	Small colony variant
SD	Standard deviation
UV	Ultraviolet
w/v	Weight per volume

Acknowledgements

I would first like to acknowledge and thank my supervisor, Dr. Brendan Leung, for providing the opportunity to join his lab. Your guidance throughout this experience has helped me to develop both as a researcher and as a person since beginning this program. I am forever grateful for your support and encouragement. I would also like to thank the rest of my committee members, Dr. Zhenyu Cheng and Dr. Daniel Boyd, for their insightful questions and comments as well as for their helpful suggestions. Additionally, I would like to thank Dr. Alison Scott for help and expertise with the hydrogel rheology aspects of the project.

Thank you to all of the present and past members of the Leung Lab, as well as other SBME students, for the helpful discussions, pep-talks, and friendship. I appreciate each and every one of you. To Dr. Naeimeh Jafari, Sarah Spencer, and Andy Haung, thank you for providing help with various experiments and troubleshooting.

To my family and friends, thank you for your constant support and words of encouragement. I couldn't have done it without you. Thank you to my parents who have been so supportive through this program and acted as a practice audience for all of my presentations. A final special thank you to Mark for always encouraging me to do my absolute best. You have always believed in me and never let me stop believing in myself.

CHAPTER 1. Introduction

1.1 Functions and properties of airway mucus in health and disease

Mucus is a viscoelastic biological material that coats a multitude of internal epithelial surfaces of the body including the respiratory, digestive, and reproductive tracts [1], [2]. In the respiratory tract, the mucus layer functions as a selective physicochemical barrier by defending the body from pathogens and toxins in inspired air [2], [3]. These potential sources of infection or damage are trapped within the mucus which is continuously cleared from the lungs through cough or mucociliary clearance [3], [4]. Mucociliary clearance is achieved through cilia beating freely within the periciliary layer beneath the mucus layer and sweeping mucus up and out of the airway [5]. The biophysical properties of airway mucus are crucial as they allow for the defense and clearance functions of the mucus layer to be effective [6].

Healthy airway mucus is mainly composed of water with a solids content of approximately 1 to 3% [7], [8]. Airway mucus solids components include mucins and other proteins, salts, lipids, DNA, and cellular debris [7], [8]. The viscoelastic properties of airway mucus are mainly owing to mucins, which are high molecular weight glycoproteins that make up a significant portion of the mucus solids content [4], [6]. The protein core of mucins make up approximately 20% of their molecular mass while sugar side chains make up approximately 80% [9], [10]. Mucins are classified as either secreted mucins or membrane-tethered mucins with the secreted mucins, also known as gel-forming mucins, making up the mucus gel network [2], [11]. The monomers of the secreted mucins link through disulfide bonds to form large chain polymers [2]. These mucin polymers then form the viscoelastic gel network of airway mucus through physical

entanglements and reversible hydrophobic interactions as well as through electrostatic interactions between charged sugar side groups which stabilize the network [2], [10], [12]. Airway mucus is well hydrated due to the high level of mucin glycosylation, and this hydration, in combination with the network formed by secreted mucins, is why airway mucus is generally referred to as a hydrogel [13]. While there have been a number of individual mucin genes discovered, the secreted gel-forming mucins MUC5B and MUC5AC are the two major mucins within airway mucus [4], [14].

The viscoelasticity of healthy airway mucus is highly regulated through ion channels on the mucosal epithelia which control mucus hydration [3], [15]. This regulation of hydration is provided by the epithelial sodium channel (ENaC), which is responsible for sodium absorption, and the cystic fibrosis transmembrane conductance regulator (CFTR), which is responsible for chloride ion secretion [3]. These channels regulate airway surface hydration by controlling the concentration of sodium and chloride ions in the airway lumen which results in passive transport of H_2O through osmosis [3]. Airway mucus properties and the mucosal microenvironment are altered in a number of conditions such as cystic fibrosis (CF), chronic obstructive pulmonary disease, and asthma, and these altered properties often lead to infection and impaired lung function [3].

1.2 Altered airway mucus properties in cystic fibrosis

CF is a genetic disease caused by mutations of the *CFTR* gene which results in dysfunction of the CFTR protein. CF affects many systems, including the pancreas, liver, and digestive system, but the major and most detrimental impacts of CF are to the

respiratory system [16]. Within the airways, CFTR mutations lead to decreased chloride ion secretion and an upregulation of sodium absorption through the ENaC which result in fluid hyperabsorption and mucus layer dehydration (Figure 1) [3], [6].

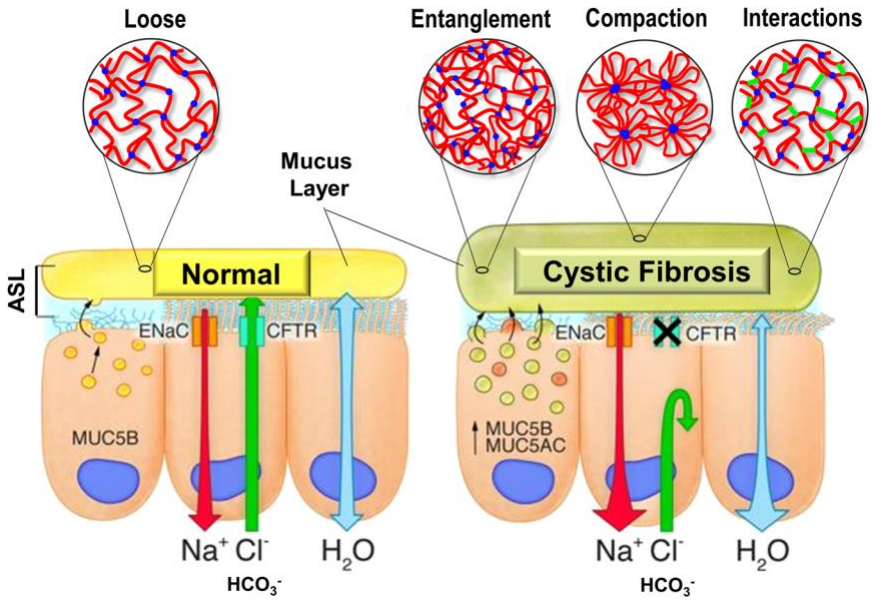

Figure 1: Schematic of airway mucus in healthy and CF airways. Airway hydration is maintained within healthy airways through functioning ion channels, including ENaC and CFTR. In CF, CFTR mutations cause the airway surface to be dehydrated which leads to changes in mucus properties and in the mucosal microenvironment. Reprinted with permission from Wiley Online Library [6].

Dehydrated mucus within the CF airway lumen, coupled with impaired mucus clearance and the continuous secretion of mucus into the airways, leads to mucus buildup and the formation of hypoxic mucus plugs [17]. Mucin production and secretion by the airway epithelium have also been found to be increased in CF airways [18]. Airway mucus in CF has increased viscoelasticity [19], [20], solids/mucin concentration [7], [8], [18], and DNA content [21], [22], as well as decreased water content [7], [8] and pH [23] relative to healthy airway mucus. While healthy airway mucus typically has approximately 1 to 3% solids, CF airway mucus has been found to have 5 to 7% solids, and this value may be underestimated due to sputum collection techniques and the inability for the more

adherent mucus to be collected [7], [8]. The secreted mucin concentration within CF airway mucus also appears to increase 3 to 5-fold relative to healthy airway mucus [8].

The viscoelastic properties of CF airway mucus have been thoroughly investigated as they are one of the major changes between healthy and CF airway mucus. Both healthy and CF airway mucus are generally characterized as elastically dominant materials as their storage modulus, G', is typically greater than their loss modulus, G'' [24]–[27]. CF airway mucus has been consistently found to have greater viscoelastic moduli, denoting a greater resistance to deformation, than healthy airway mucus [19], [20]. The magnitude of this difference has not been well-defined as differences in mucus sample collection and measurement methods, as well as differences in patient age, patient disease status, and patient disease progression, result in study-to-study and patient-to-patient variations in the viscoelastic properties of CF airway mucus [19], [20], [28]. There is also variation within patients as airway mucus is heterogeneous and mucus properties vary between different parts of the airways [18], [28].

The altered viscoelastic properties and dehydration of CF airway mucus significantly impair mucus clearance mechanisms in CF patients. The dehydrated airway mucus and reduced periciliary layer volume due to airway fluid hyperabsorption result in cilia compression and the inability for cilia to properly beat, leading to stagnant and stationary airway mucus [29], [30]. Airway mucus dehydration in CF also causes the mucus to become adherent to the airway surface [29], [31]. This is not only detrimental to mucociliary clearance, but also to cough clearance mechanisms [32]. Both the adhesive and cohesive strength of airway mucus has been found to be increased when airway mucus concentration is increased [32]. This has implications in the inability for CF

patients to clear thickened airway mucus through cough [32]. The impaired mucus clearance and altered properties of CF airway mucus lead to mucus stasis and buildup and a microenvironment primed for chronic infection [33].

1.3 Airway infections in cystic fibrosis

Lung infections frequently occur in CF patients, as evidenced by the Cystic Fibrosis Annual Data Report 2019, which showed that over 60 percent of young CF patients and over 80 percent of older CF patients in the USA were infected with at least one microorganism [34]. Chronic lung infections are common in CF because the thick, dehydrated, and stagnant airway mucus becomes colonized by multiple species of opportunistic pathogens that are not properly cleared due to impaired clearance mechanisms [17]. The two most commonly recognized pathogens in CF airway infections are *Pseudomonas aeruginosa* and *Staphylococcus aureus*, although a number of other, less prevalent pathogens are also known to infect CF patient airways; including *Haemophilus influenzae* and bacteria from the *Burkholderia cepacian* complex group [34], [35]. CF airway infections are complex, polymicrobial, and vary between patients [36], [37]. The complex polymicrobial nature of CF airway infections further complicates treatment of these infections, with the presence of an antibiotic sometimes increasing total bacteria load in *in vitro* studies [38]. Bacterial diversity and composition of CF airway infections have been found to vary with many factors including patient age [39] and disease stage and progression [40].

Many of the species that infect CF patient airways are known to form bacterial biofilms within the adherent and impacted mucus [17], [41]–[43]. Bacterial biofilms in

CF are microcolonies of bacteria surrounded by a protective extracellular matrix that contains exopolysaccharides, DNA, and proteins [44], [45]. These biofilms are difficult to eradicate and show increased resistance to antibiotics and host immune defense when compared to planktonic bacteria due to reduced antibiotic penetration and metabolic adaptation [46], [47]. Increased mucus concentration, as found in CF airway mucus, is thought to be a factor that influences the growth of stronger and more robust biofilms which are more resistant to killing by antibiotics [48]–[50]. For example, *P. aeruginosa* grown in CF-mimicking media has been found to grow biofilms with altered architecture and increased biofilm matrix components that show a greater resistance to antibiotics relative to *P. aeruginosa* biofilms grown in standard bacteria culture medium [49]. In addition, biofilms that are polymicrobial have been found to have a greater resistance to antibiotics than biofilms with a single species [51]. Bacteria within chronic CF airway infections are also known to adapt to a small colony variant (SCV) phenotype, which are persistent and highly adherent biofilm formers that are characteristic of chronic infections and are more resistant to both antibiotic challenges and environmental stress [52], [53]. Along with the increased resistance to antibiotics in CF airway infections due to biofilm formation and phenotypic changes, host defense is also impacted in the CF airways. Neutrophil motility and ability to capture and kill bacteria has been found to be decreased within concentrated, CF-like airway mucus [54].

Bacterial airway infections in CF are commonly treated through inhaled, oral, or intravenous antibiotics. Because many microbes that infect the CF airways have the ability to resist antibiotic killing through biofilm formation, mutation or gene transfer, and intrinsic resistance, these airway infections are often difficult to treat [55], [56].

Treatment is further complicated because the complex polymicrobial infections found within the CF airway require advanced treatment strategies based on which species are present [56]. Additional treatment challenges include samples taken for microbe identification represent only discrete sections of the airway and laboratory isolation techniques lack the ability to identify all species present within a sample [55]. These hard-to-treat lung infections that develop in CF airways lead to inflammation, decreased lung function, and progressive lung disease and are known to be the primary cause of mortality in CF patients [57].

1.4 *Pseudomonas aeruginosa* and *Staphylococcus aureus* in cystic fibrosis airway infections

As previously mentioned, *P. aeruginosa*, a Gram-negative opportunistic pathogen, and *S. aureus*, a Gram-positive opportunistic pathogen, are the two most common microbes found to infect CF patient airways (Figure 2). These classifications of Gram-negative and Gram-positive are owing to their cell wall compositions, with Gram-negative bacteria having a thin peptidoglycan layer and protective outer membrane and Gram-positive bacteria having a thicker peptidoglycan layer and no outer membrane.

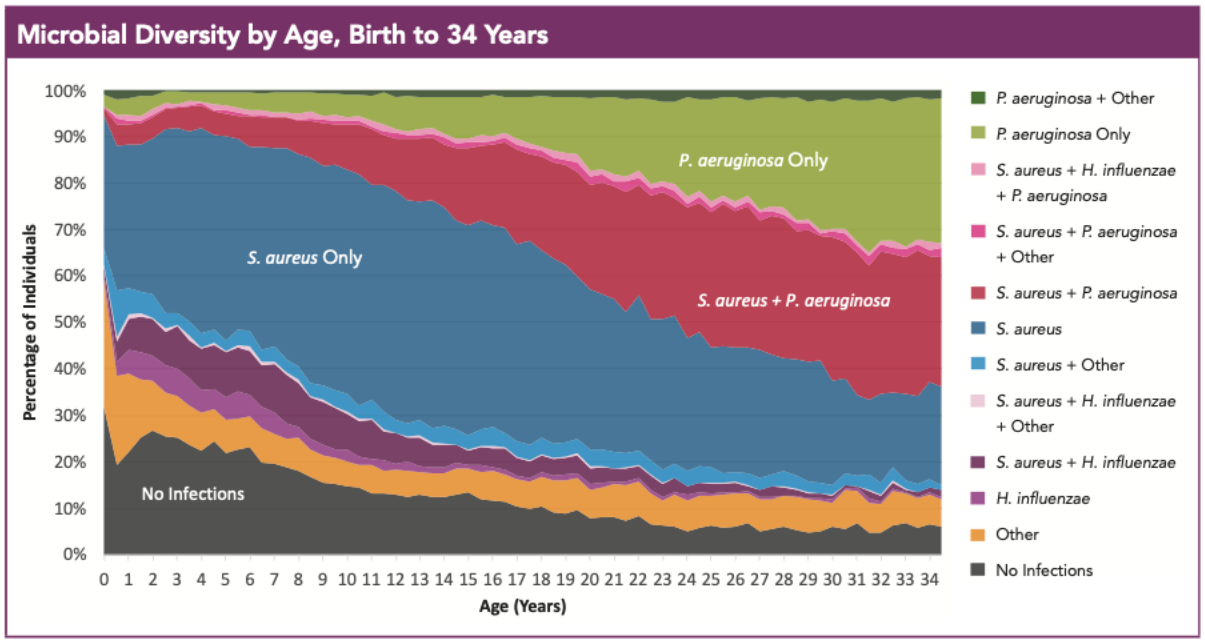

Figure 2: Microbes infecting the airways of CF patients by age. Younger patients are most commonly infected with *S. aureus*. *P. aeruginosa* infections as well as co-infections with *P. aeruginosa* and *S. aureus* become more common as patients age. Figure contains data collected from US CF patients. Reprinted with permission from Cystic Fibrosis Foundation [34].

It has been well established that *S. aureus* is an early colonizer of CF patient airways, infecting CF patient airways from a very young age, with almost 60% age two-and-under US CF patients having cultured positive for the pathogen during 2019 [34]. After early colonization, these *S. aureus* infections are persistent, with *S. aureus* continuing to be one of the most common microbes infecting CF patients in all age groups [34], [58], [59]. *S. aureus* has been found to resist antibiotic treatment, particularly when it is in the biofilm mode of growth which is known to occur within CF airway mucus [60]–[62]. *S. aureus* has also been found to adapt to the CF airway environment by changing to a SCV phenotype [58], [63].

P. aeruginosa infections are most common in adult CF patients [34], [59]. Approximately 44% of US CF patients cultured positive for *P. aeruginosa* in 2019 [34].

Similarly to *S. aureus*, *P. aeruginosa* is known to form biofilms in the CF airways and these biofilms are more resistant to antibiotic killing [42], [64], [65]. This antibiotic resistance has been found to be increased when *P. aeruginosa* converts to a mucoid phenotype that is associated with alginate overproduction and often occurs during CF airway infection [17], [66], [67]. *P. aeruginosa* within the CF airways also appears to undergo other adaptive changes over the course of persistent infection, including an increase in multidrug resistant phenotypes [68]. *P. aeruginosa* also has the ability to adapt to a SCV phenotype in CF-like conditions [69]; these highly adherent *P. aeruginosa* SCVs have been isolated from CF patient airways [70], [71]. Additionally, *P. aeruginosa* interactions with mucin proteins have been investigated, with some sources finding that mucins cause the dispersal of *P. aeruginosa* biofilms [72], [73], while others have noted *P. aeruginosa* attachment to mucins through adhesin-mucin interactions [50], [74]. *P. aeruginosa* in CF is associated with more aggressive infections, worsening patient conditions, and mortality [75], [76].

P. aeruginosa and *S. aureus* are also frequently found to co-infect and exist within dual-species biofilms in the airways of patients with CF [34], [77]. Although *P. aeruginosa* is the more common microbe infecting adult CF patient airways, it does not appear to outcompete and replace *S. aureus in vivo*; in a longitudinal study of CF patients, the prevalence of *S. aureus*/*P. aeruginosa* co-infections was found to increase over time [77]. When the two species are co-existing, the presence of *S. aureus* is hypothesized to induce changes in *P. aeruginosa*, as *S. aureus* exoproducts have been found to alter *P. aeruginosa* biofilm architecture and increase *P. aeruginosa* resistance to antibiotics [78]. Similarly, co-culture of *S. aureus* and *P. aeruginosa* has been found to

increase the antibiotic resistance and surface attachment capacity of *S. aureus* [79]. There is also evidence that, in co-culture, the presence of *S. aureus* induces selection of *P. aeruginosa* SCVs [80] and the presence of *P. aeruginosa* induces selection of *S. aureus* SCVs [79], [81], [82], which increases the ability for these pathogens both to co-exist and to persist in infections of the CF airways.

P. aeruginosa has often been observed to outcompete *S. aureus in vitro*, although this competition is reduced when the *P. aeruginosa* strains are isolated from later stage chronic infections, implying that coexistence between the two species is the result of adaptive changes of *P. aeruginosa* in these chronic infections [80], [83]. Competition between the two species may cause changes to *S. aureus* which allow it to survive and coexist with *P. aeruginosa* in a viable but non-cultivable state, which is a state of low metabolic activity used by bacteria as a survival strategy [84]. An additional promotion of coexistence between the two species is that *S. aureus* provides carbon sources for *P. aeruginosa* [81], [85]. Interactions between *P. aeruginosa* and *S. aureus in vitro* and whether they compete or coexist appears to be dependent on many different factors including the relative concentration of bacteria, the availability of oxygen, and the point of infection from which they were isolated [85]–[87]. The ability for *S. aureus* to coexist with *P. aeruginosa* has also been associated with increased phenotypic and genotypic diversity of the *S. aureus* population within the infected CF airway [82].

1.5 Mucus-mimetic materials

The many host and microbe interactions with airway mucus that occur in the airway *in vivo* emphasize the importance of a representative mucus-like layer to be included

within *in vitro* models of the airway. Fresh, native airway mucus is difficult to source and can easily be diluted or contaminated, and the mucus generated by human bronchial epithelial (HBE) cells *in vitro* is secreted in restrictively small quantities [10], [27]. Due to the drawbacks of using native mucus and mucus secreted by cells in culture, there has been a focus on developing mucus-mimetic materials.

A number of different materials have been used as mucus-mimetic materials to model the healthy or diseased airway microenvironment. One such material is an artificial CF sputum medium (ASM) comprised mainly of purified mucins, DNA, NaCl, and amino acids, deployed as a CF mucus-mimetic to study bacterial growth [88]–[90]. A more complex material that has been developed to mimic the nutritional microenvironment of CF mucus is synthetic CF sputum medium (SCFM), the components of which include a number of free amino acids, glucose, and lactate [91]. SCFM has also been modified with the addition of other CF mucus components including mucins and DNA to better mimic the composition of CF sputum. This modified version of SCFM, along with the original SCFM, have been used to observe the growth, biofilm formation, and diversification of *P. aeruginosa* in CF-like conditions [92]–[95].

While ASM and modified SCFM have been shown to support *in vitro* bacterial behavior similar to what occurs in the CF airways *in vivo*, neither of these materials have the hallmark viscoelastic properties of CF airway mucus. Both ASM and modified SCFM have shown viscous behavior rather than the viscoelastic solid behavior that is characteristic of CF airway mucus [96], [97]. Despite mucin proteins being the main structural and gel-forming component in native healthy and CF airway mucus, and mucin proteins being a component of both ASM and SCFM, mucus-mimetic materials cannot

rely on purified mucins to provide the same structural properties. It has been shown that purified mucins have different rheological properties than natural mucus [98] and that purified mucins alone do not accurately model native mucus [20], [99], [100]. Despite this, mucins remain an important addition to artificial mucus due to the interactions that occur between mucins and bacteria.

To better recapitulate the viscoelastic properties of native airway mucus, ASM has been combined with gel-forming polymers, such as poly(acrylic) acid [96], [101]. Others have opted for a simplified approach with less components, mainly relying on a combination of porcine gastric mucins (PGM, the most commonly used source of commercially available purified mucins) with gel-forming polymers to artificially recapitulate the viscoelastic properties of native airway mucus. PGM has been combined with artificial materials, such as glutaraldehyde [102], and while this material had viscoelastic properties within the targeted range, the use of this material is not ideal as it is potentially cytotoxic and could be damaging to mammalian cells if used within an *in vitro* airway model. Natural materials, such as hyaluronic acid (HA) [103] and sodium alginate [104], [105], have also been combined with PGM to create airway mucus-mimetic hydrogels. These natural materials are favorable for use within *in vitro* airway models as they are typically cytocompatible and less foreign to microbes and mammalian cells. Natural polymers, such as HA and sodium alginate, can also be crosslinked to form hydrogels with networks, water content, and viscoelastic properties similar to those that make up native airway mucus. Due to the importance of mucus viscoelasticity *in vivo*, it is important that the viscoelastic properties of mucus-mimetics are comparable to those of native airway mucus.

1.6 Current models of the cystic fibrosis airway microenvironment

Issues with current models of the CF microenvironment have precipitated the need for a representative *in vitro* model capable of supporting the concurrent growth of bronchial epithelial cells and multiple CF pathogens. Many of the current models being used to study the CF microenvironment are *in vivo* animal models. These models, which include small animal models, such as mice [106], [107], and larger animal models, such as pigs [23], [108], are limited in their ability to be used to study CF chronic infections. Mouse CF models do not develop spontaneous CF lung infections and thus do not accurately recapitulate human CF lung disease [109]. Conversely, pig models of CF can more accurately represent human CF lung disease but their use remains limited by shortened lifespans due to meconium ileus or other CF complications [110]–[112], making CF lung disease in these models difficult to study. Studying CF chronic infections *in vivo* using animal models also requires a large amount of resources.

Due to the limitations with *in vivo* animal models of CF airways, many *in vitro* CF airway models have been developed and explored. A number of these *in vitro* studies have investigated interactions between mammalian cells and *P. aeruginosa* and/or *S. aureus* [81], [113]–[115]. However, without a mucus-like layer in these systems, they are not fully representative of the CF microenvironment. Some of these systems rely on collecting the mucus secreted by mammalian cells in culture, but sourcing this mucus, especially in quantities needed for analysis, is labor and time intensive [27]. Other *in vitro* CF models focus on the growth behavior of CF pathogens when cultured with CF mucus or mucus-mimetics without the inclusion of mammalian cells [88], [101], [116], [117]. Mammalian cells are an important inclusion within an *in vitro* CF airway model as

they allow for the observation of host-microbe interactions and render the model more representative of the native CF airway microenvironment. Additionally, many of the models that do include mucus or a mucus-like component only incorporate one species of bacteria into their models rather than modeling the more complex polymicrobial interactions that occur within the CF airways. The CF airway microenvironment has also been modeled through infecting *ex vivo* porcine bronchiolar tissue with either *P. aeruginosa* or *S. aureus* in the presence of SCFM to observe bacterial growth and biofilm formation [94], [118]. This model lacks both the viscoelastic microenvironment of native CF airway mucus as well as live mammalian cells for observation of host-microbe interactions.

Recently, a CF airway chip has been developed that combines primary human lung microvascular endothelial cells, healthy or CF HBE cells, and *P. aeruginosa* to model the CF airway microenvironment [119]. The CF airway chip showed increased mucus secretion, cilia density, and *P. aeruginosa* growth relative to the healthy airway chip. As the CF airway chip relies on mucus secreted by the HBE cells within the chip, the properties of the mucus cannot be modified to represent different stages of CF airway mucus dysfunction, such as a mucus plug, and are, therefore, only representative of mucus secreted by a monolayer of cultured cells. Additionally, on-a-chip technologies like the CF airway on a chip are technically challenging and require expertise to fabricate and operate. While the CF airway chip does show promise as an *in vitro* model of the CF airway microenvironment, there remains a need for a simpler, more tunable approach to modeling this system.

The limitations of animal CF models, as well as the aforementioned issues with current *in vitro* CF models, create the need for an *in vitro* polymicrobial infection model of the CF microenvironment with a simple yet representative mucus-like component.

1.7 Research aims, objectives, and hypothesis

The overall aim of this project was to develop *in vitro* models of the healthy and CF airway mucus microenvironments for the study of bacteria behavior and response to relative changes in airway mucus properties and composition, as seen in CF airway infections. Both models included mucus-like hydrogels overlaid on top of a layer of cells from a human bronchial epithelial cell line (16-HBE). Relevant CF pathogens, *P. aeruginosa* and *S. aureus*, were cultured over top of the mucus-like hydrogels in the presence of a relevant CF antibiotic, ciprofloxacin. The major difference between the two airway models were the properties and composition of the mucus-like hydrogels within the models, with a healthy mucus-like hydrogel being included within the healthy airway model and a CF mucus-like hydrogel being included within the CF airway model. The hydrogels included a crosslinkable gel component to obtain mucus-like viscoelastic properties and a mucin protein component to capture one of the major changes in composition between healthy and CF airway mucus. This was done to capture known relative differences between healthy and CF airway mucus within the airway models. A schematic of the healthy and CF airway models can be found in Figure 3 below.

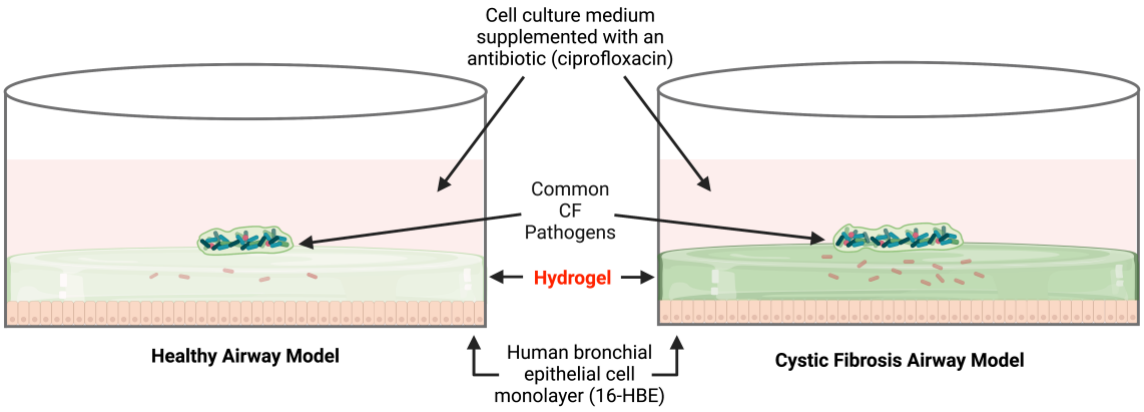

Figure 3: Schematic of the healthy and CF airway models. The base of both models was cells from a human bronchial epithelial cell line (16-HBE). Layered on top of the 16-HBE cells were the healthy and CF mucus-like hydrogels, with the darker color of the CF mucus-like hydrogel signifying increased solids and mucin concentration. Common CF pathogens, *Pseudomonas aeruginosa* (rod-shaped) and *Staphylococcus aureus* (cocci-shaped), were deposited over top of the mucus-like hydrogels. Cell culture medium supplemented with a relevant CF antibiotic (ciprofloxacin) was also included over the model. Schematic created with BioRender.com.

It was hypothesized that the differences in viscoelastic properties and composition between the mucus-like hydrogels within the *in vitro* airway models would impact microbial colony response and cause increased resistance to eradication through antibiotics. To achieve the overall aim of this project, there were three main objectives:

Objective 1: Develop healthy and CF mucus-like hydrogels with differing compositions and viscoelastic properties that are simple to prepare and accessible for use within other laboratories. These mucus-like hydrogels must meet a set of detailed selection criteria that were developed based on physiological mucus properties as well as experimental requirements.

Objective 2: Establish a bacterial culture over the mucus-like hydrogels using an aqueous two-phase system (ATPS). Ensure that, after a short incubation period to establish the bacterial culture, the outer liquid portion of the ATPS could be removed

while the majority of the bacteria would remain on top of or within the mucus-like hydrogel layer beneath.

Objective 3: Layer the mucus-like hydrogels over top of a human airway epithelial cell layer and deposit relevant CF pathogens onto the mucus-like hydrogels, and then expose the healthy and CF *in vitro* airway models to a relevant CF antibiotic. Observe how bacteria growth and how bacteria response to antibiotics is impacted by the differences in mucus-like hydrogel properties and composition between the healthy and CF mucus-like hydrogels.

The healthy and CF *in vitro* airway models developed in this research are useful for observing mono- and polymicrobial behavior and response to relative changes within their microenvironment. This can provide a better understanding of how the physical properties and composition of airway mucus relate to the altered bacterial behavior and resistance to antibiotics that is observed in CF airway infections. This can also provide a system to study the microbe-microbe interactions that occur in multi-species infections of the CF airway. Additionally, there is potential for the CF airway model to be used as a platform for *in vitro* antimicrobial testing as the inclusion of important features of the CF airway microenvironment, including a mucus-like hydrogel and multiple species of bacteria, improve the relevance of the model compared to standard monomicrobial *in vitro* models.

As mentioned in Objective 1, a set of detailed selection criteria were developed to ensure compatibility with mammalian cell culture and to obtain hydrogels that reflect important differences between healthy and CF airway mucus. The selection criteria include:

- The healthy and CF mucus-like hydrogels must not reduce 16-HBE cell viability below 80% when co-cultured for 48 hours. The International Organization for Standardization (ISO) 10993-5:2009 standard states that a cell viability reduction of greater than 30% (less than 70% of cells viable) is deemed cytotoxic [120]. While the cytotoxicity assessment procedure of the mucus-like hydrogels for this project does not match the test procedure set out in ISO standard 10993-5:2009, the quantitative evaluation for cytotoxicity based on less than 70% of cells viable was used as a guide. Cell viability of 80% or less was then chosen as a more conservative evaluation of cytotoxicity than ISO 10993-5:2009.
- The solids content and mucin protein concentration of the healthy and CF mucus-like hydrogels must be different. The relative difference between the solids content of the two hydrogels and the relative difference between the mucin protein concentration of the two hydrogels should be similar to the relative differences between native CF and healthy airway mucus.
- The healthy and CF mucus-like hydrogels must show elastically dominant behavior (i.e. the storage modulus (G') must be greater than the loss modulus (G'') for both of the chosen mucus-like hydrogels).
- The viscoelastic properties of the healthy and CF mucus-like hydrogels must be significantly different.
- The healthy and CF mucus-like hydrogels must have viscoelastic properties within the same order of magnitude as physiological airway mucus.
- The healthy and CF mucus-like hydrogels must gel within 1 hour or less. This is because cell culture medium cannot be added to the culture while the mucus-like

hydrogels are solidifying over top of the 16-HBE cells. Therefore, the gelation time must be kept short enough to prevent 16-HBE cell death due to lack of cell culture medium.

CHAPTER 2. Materials and Methods

2.1 Hydrogel preparation

2.1.1 Hyaluronic acid hydrogels

The HA hydrogels were prepared using the HyStem® Thiol-Modified Hyaluronan Hydrogel Kit (Advanced Biomatrix). This kit consisted of a thiol-modified hyaluronan (Glycosil®), a thiol-reactive crosslinker (polyethylene glycol diacrylate, Extralink®-Lite), and degassed/deionized water. To prepare the hydrogels, the thiol-modified hyaluronan and thiol-reactive crosslinker were reconstituted with degassed/deionized water and allowed to mix on a shaker for approximately 60 minutes. A 100 mg/mL solution of Mucin Type II (PGM, Sigma-Aldrich) was also prepared. The mucin powder was sterilized by spreading the dry mucin powder in a petri dish, completely saturating the powder with 95% ethanol, and placing the petri dish into a 70°C oven for 24 hours. After 24 hours, the mucin powder was collected and solubilized with phosphate-buffered saline (PBS). The thiol-modified hyaluronan and mucin solution were first mixed by pipette and after mixing, the thiol-reactive crosslinker was added to the mixture and the hydrogels were deposited into the wells and allowed to solidify. HA hydrogels were tested at thicknesses of 1.5 mm, 2 mm, and 2.5 mm. The formulations of the HA-based hydrogels that were tested included HA concentrations of 4 mg/mL and 8 mg/mL, crosslinker concentrations of 0.5 mg/mL and 1 mg/mL, and mucin concentrations of 0%, 1.5% and 5% (w/v). HA and crosslinker concentrations were chosen based on manufacturer recommendations.

2.1.2 Alginate hydrogels crosslinked with $CaCO_3$/GDL

The first alginate hydrogel crosslinking method investigated was a combination of $CaCO_3$ and glucono-delta-lactone (GDL). Stock sodium alginate solutions were prepared at a concentration of 30 mg/ml alginic acid sodium salt (low viscosity, MP Biomedicals) in PBS. To sterilize the alginic acid sodium salt, the powder was placed into a 50 ml Falcon tube and the tube was placed horizontally into an ultraviolet (UV) light sterilizing chamber for 60 minutes (with the tube being rotated once every 20 minutes). For later trials, HEPES buffer was also added to the stock sodium alginate solution at a concentration of 75 mM. To sterilize the $CaCO_3$ and GDL, the powders were weighed and added to microcentrifuge tubes and were steam sterilized in an autoclave. The mucin solution was prepared as stated in Section 2.1.1 except the concentration of the stock solution was increased to 200 mg/mL. After all hydrogel components were sterilized, the $CaCO_3$ powder was solubilized in PBS and mixed with the alginate solution and the mucin solution to make the hydrogel mixture. The GDL powder was then solubilized in PBS and mixed with the hydrogel mixture. The hydrogels were vortexed, deposited into the wells (of a 48-well plate) at a thickness of 1.5 mm (based on volume deposited), and allowed to crosslink within a cell culture incubator at 37°C and 5% CO_2 for 45 minutes. Formulations of the alginate hydrogels crosslinked with $CaCO_3$/GDL that were tested include crosslinker concentrations of 0.3% CaCO3 with 1.1% GDL and 0.45% CaCO3 with 1.6% GDL, mucin concentrations of 0%, 1%, and 4%, and an alginate concentration of 1%.

2.1.3 Alginate crosslinked with $CaCl_2$

The second alginate hydrogel crosslinking method that was investigated was $CaCl_2$. Sodium alginate stocks containing 75 mM HEPES were prepared as stated in Section 2.1.2. Stock calcium chloride solutions were prepared by solubilizing calcium chloride in deionized (DI) water at a concentration of 10 mg/ml. For use within the hydrogels, the higher concentration stock $CaCl_2$ solution was diluted with 0.9% NaCl in DI water directly prior to use. The calcium chloride and the NaCl solutions were sterilized using filter sterilization with a 0.22 μm filter. The mucin solutions were prepared as stated in Section 2.1.2. To prepare the hydrogels, alginate and mucin solutions were first mixed and diluted with PBS. The $CaCl_2$ stock solutions were then diluted with the NaCl solution and rapidly mixed by pipette with the rest of the hydrogel components. The hydrogel mixture was then deposited into the wells at a thickness of 1.5 mm (based on volume deposited) and allowed to solidify, as previously stated. The first $CaCl_2$-crosslinked hydrogel formulations tested were combinations of 1% (weight per volume, w/v) alginate (with no HEPES buffer), 0.67 mg/ml $CaCl_2$ crosslinker, and mucin concentrations ranging from 0% up to 5% (w/v). The second iteration of $CaCl_2$-crosslinked alginate hydrogel formulations tested had combinations of 1% and 1.5% (w/v) alginate, 0.67 mg/ml and 1 mg/ml $CaCl_2$ crosslinker, and 0%, 1%, and 4% mucins. The third iteration of $CaCl_2$-crosslinked alginate hydrogel formulations tested had combinations of 1% and 1.5% alginate, 0.5 mg/ml and 0.6 mg/ml $CaCl_2$ crosslinker, and 0%, 1%, and 4% mucins. The formulations from the third iteration were considered the potential mucus-like hydrogel formulations and were further assessed for use within the final models.

2.1.4 Alginate cushion

A thin layer of $CaCl_2$-crosslinked alginate hydrogel with 0% mucin concentration was also incorporated into the model. This thin layer of alginate beneath the mucin-containing mucus-like hydrogels is referred to as the alginate cushion. The alginate cushion was incorporated into the model to improve 16-HBE cell adhesion, as the $CaCl_2$-crosslinked alginate hydrogels with high mucin concentrations were resulting in reduced cell adhesion after incubation. This strategy was chosen, as opposed to choosing an alternate mucin source, because the majority of current mucus mimetics and mucus-mimicking media use this source of commercially available porcine gastric mucins. It was desirable to continue using this widely used mucin source for this research. The alginate cushion was prepared with the same steps as outlined in Section 2.1.3. Potential alginate cushion formulations investigated include alginate concentrations of 10 and 15 mg/ml and $CaCl_2$ concentrations of 0.1, 0.2, 0.3, 0.4 and 0.5 mg/ml. The final alginate cushion formulation was chosen based on crosslinking time using a plate tilt test. 500 µl of the potential alginate cushion formulations were added to the wells of a 24-well plate and the plate was periodically tilted to determine whether the hydrogels were solidified based on hydrogel movement. The height of the alginate cushion was chosen based on the ability for the chosen formulation to spread over the entirety of the bottom of the well.

2.2 Mammalian cell culture conditions

A human bronchial epithelial cell line, 16-HBE, was used for this study. The 16-HBE cell line (16HBE14o-) was kindly provided by Dr. Geoff Maksym, Dalhousie University. 16-HBE cells were incubated at 37ºC and 5% CO_2. Dulbecco's Modified Eagle Medium

(DMEM, Thermo Fisher Scientific, Gibco, Cat. No. 11965092) and Gibco Ham's F-12 nutrient mixture (F-12, Thermo Fisher Scientific, Gibco, Cat. No. 11765054) were mixed at a 1:1 ratio and supplemented with 10% fetal bovine serum (FBS, Thermo Fisher Scientific, Gibco) and 1% antibiotic-antimycotic (AA, 100x, Thermo Fisher Scientific, Gibco, Cat. No. 15240062) for all 16-HBE cell growth and maintenance. For initial experiments in this study, media was changed at the beginning of each early experiment to Roswell Park Memorial Institute (RPMI Medium 1640, Thermo Fisher Scientific, Gibco, Cat. No. 11875093) media supplemented with 1% FBS and 1% AA to promote slower cell growth and avoid cells becoming over confluent. This step was based on another similar study [121] but was found to be unnecessary under the experimental conditions of this research. Therefore, DMEM/F-12 media was used for the majority of experiments. RPMI media with 1% FBS was used for HA hydrogel cytotoxicity experiments and initial alginate hydrogel cytotoxicity experiments. DMEM/F-12 media was used for the majority of alginate hydrogel cytotoxicity experiments and for all other experiments post-cytotoxicity testing, including all microbe-mammalian co-culture experiments.

For experiments with HA hydrogel formulations, a custom cell culture plate insert was developed using polydimethylsiloxane (PDMS). The use of a custom PDMS cell culture plate insert with shallow and small diameter wells was necessary as the HA hydrogel kit used for this study contained a limited volume. To create the custom cell culture plate insert, the SYLGARD™ 184 Silicone Elastomer Kit (Dow) was used. The liquid components supplied in the kit were mixed at a 10:1 ratio as per kit instructions and poured into a 60 mm cell culture plate up to PDMS thicknesses of 1.5, 2, or 2.5 mm.

The PDMS-containing cell culture plates were placed into a vacuum chamber to be degassed and then incubated in a 60ºC oven for 24 hours to cure. Once the PDMS was cured, a scalpel was used to carefully remove the PDMS sheets from the 60 mm cell culture plate. A 4 mm diameter biopsy punch was used to create 12 evenly spaced "wells" within the PDMS and then the PDMS was sterilized by UV sterilization and inserted into a new 60 mm cell culture plate (Figure 4). Approximately 1 x 10^6 16-HBE cells were seeded into the 60 mm cell culture plate with the custom PDMS insert. The cells were grown for 24 hours in the 60 mm cell culture plate prior to use for experiments.

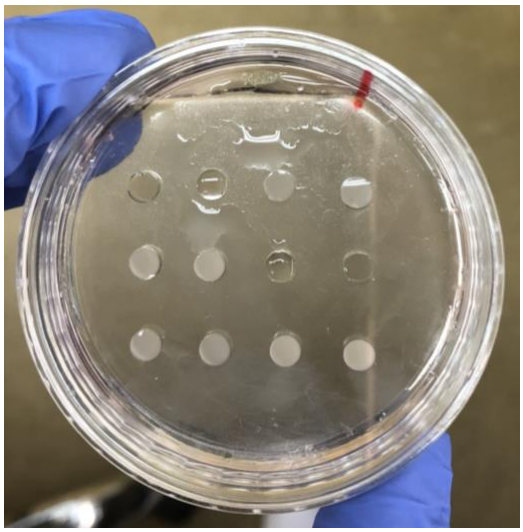

Figure 4: Custom PDMS plate insert within 60 mm cell culture plate for use with HA hydrogels. In this figure, HA hydrogels have been added to the individual 4mm diameter wells.

For all experiments with alginate hydrogel formulations, 48-well cell culture plates were used. 16-HBE cells were seeded at a cell density of approximately 50000 to 55000 cells/well. Wells were coated with fibronectin (Thermo Fisher Scientific) prior to cell seeding to encourage cell adhesion. The cells were grown for 24 hours in the 48-well plate prior to use for experiments.

2.3 Cytotoxicity assessment of hydrogels

To assess the cytotoxicity of potential hydrogel formulations, 16-HBE cells were first cultured as stated in Section 2.2 above. After 24 hours of cell growth, the potential mucus-like hydrogel formulations were added to the individual wells. Crosslinking time was dependent on the components of the hydrogel, with the HA hydrogels being allowed to crosslink for 50 minutes, the $CaCO_3$/GDL alginate hydrogels being allowed to crosslink for 45 minutes, and the $CaCl_2$ alginate hydrogels being allowed to crosslink for 35 minutes, all within a cell culture incubator at 37°C and 5% CO_2.

For the experiments where the alginate cushion was included, the cushion hydrogel was first added to the individual wells at a thickness of approximately 0.4 mm (based on volume deposited) and allowed to crosslink within a cell culture incubator at 37°C and 5% CO_2 for 10 minutes. The mucus-like hydrogel formulations were then added over top of the cushion at a thickness of approximately 1.1 mm (based on volume deposited). After the hydrogels were solidified, 250 µl of cell culture medium was added over top of the hydrogels when a 48-well plate was used. When the custom PDMS plate insert was used for the HA-based hydrogels, a total of 5 ml of cell culture medium was added to each plate, submerging the hydrogels and the PDMS plate insert. The cells and hydrogels were then cultured together for 48 hours at 37ºC and 5% CO_2. After 48 hours, the cell culture medium and hydrogels were removed. For initial cytotoxicity experiments, hydrogels were removed using liquid aspiration, but this method was later changed and the hydrogels were instead removed using pipette aspiration with a 1000 µl pipette.

After the cell culture medium and hydrogels were removed from the 16-HBE cells, a live/dead assay consisting of calcein AM and ethidium homodimer-1 (Thermo Fisher

Scientific) and a Hoechst stain (Hoechst 33342, Thermo Fisher Scientific) was performed to assess cell viability. Calcein AM and ethidium homodimer-1 were both diluted together in PBS to final concentrations of 2 μM and 4 μM, respectively, and Hoechst was diluted in PBS to a concentration of 8.1 μM. To stain the 16-HBE cells, the cells were rinsed and then incubated with the calcein AM/ethidium homodimer-1 stain at 37ºC for 30 minutes. The cells were then rinsed again and incubated with the Hoechst stain for 10 minutes at room temperature. The cells were rinsed a final time and then covered with PBS for imaging. The EVOS™ FL Auto 2 Imaging System (Thermo Fisher Scientific) was used to collect phase contrast and fluorescence images and to visualize live cells (green fluorescent protein channel, GFP), dead cells (red fluorescent protein channel, RFP), and cellular DNA (DAPI channel). ImageJ was used for image processing and cell viability quantification. Cell viability for each condition was calculated based on cell counts using Equation 1.

$$Cell\ viability\ (\%) = \left(\frac{Total\ cells - Dead\ cells}{Total\ cells}\right) \times 100\% \qquad (1)$$

2.4 Viscoelastic characterization of hydrogels

The storage (elastic, G') and loss (viscous, G'') moduli of the 12 potential mucus-like hydrogel formulations were measured. As described in Section 2.1.3, these formulations were combinations of 1% and 1.5% alginate, 0.5 mg/ml and 0.6 mg/ml $CaCl_2$ crosslinker, and 0%, 1%, and 4% mucins. A controlled-stress/controlled-rate rheometer (AR2000, TA Instruments) with a 40 mm diameter/2º cone geometry was used to measure the moduli. Use of the rheometer was kindly provided by Dr. Alison Scott, Dalhousie University. The

temperature was kept constant at 23ºC using a Peltier plate and a solvent trap was used to prevent evaporation of the hydrogels. Strain sweeps were performed to determine the linear viscoelastic region (LVR) of each hydrogel. Strain sweeps were performed from 0.1% to 1000% strain at an angular frequency of 1 rad/s. Frequency sweeps were then performed to determine the frequency-dependent storage modulus and loss modulus of each hydrogel. Frequency sweeps were performed from 0.1 to 100 rad/s at strains found to be within the LVR of each hydrogel, which ranged from 1% to 2% strain. Each hydrogel formulation was tested three times.

To conduct the measurements, the hydrogels were first prepared as outlined in Section 2.1.3, with 1 ml of each hydrogel being prepared in microcentrifuge tubes. For each measurement, a pipette was used to deposit 590 µl of the hydrogel onto the Peltier plate. Hydrogels were deposited directly after mixing the crosslinker and tests were conducted 15 or 20 minutes after deposition to allow the hydrogels to solidify. Strain and frequency sweeps were repeated three times for each hydrogel formulation.

2.5 Bacteria strains and culture conditions

P. aeruginosa CF18 and *S. aureus* ATCC 6538 were used for this study. *P. aeruginosa* CF18 is a CF clinical strain isolated from the airways of a child (< 24 months) (WOLFGANG 2003) with CF and was kindly provided by Dr. Zhenyu Cheng, Dalhousie University. Frozen stocks of *P. aeruginosa* CF18 were stored in Luria-Bertani (LB) broth containing 25% (v/v) glycerol stored at -80ºC. For use of the bacteria within experiments, frozen stocks were streaked on 1.5% (w/v) LB agar (Sigma-Aldrich) plates and incubated overnight at 37ºC, 5% CO_2 for 16 to 18 hours. Overnight cultures were

prepared by using a loop to pick single colonies from the streaked plates and inoculating 5 ml of bacteria culture broth. LB broth was used for *P. aeruginosa* overnight cultures and Brain Heart Infusion (BHI) broth was used for *S. aureus* overnight cultures. The inoculated broth was placed in a shaking incubator shaking at 200 rpm and 37ºC for 16 to 18 hours.

2.6 Preparation of aqueous two-phase system

The ATPS formulations used for this research consisted of polyethylene glycol (PEG) and dextran (DEX). To prepare the ATPS formulations, 5% (w/v) PEG (35 kDa, Sigma-Aldrich) and 5% (w/v) DEX (500 kDa, Pharmacosmos) were dissolved together in LB broth as well as in DMEM/F-12 cell culture medium supplemented with 10% FBS. The cell culture medium used for ATPS preparation did not contain any antibiotics or antimycotics. The solutions were then mixed on a rocking platform shaker (VWR) until the PEG and DEX were fully dissolved. Once fully dissolved, the solutions were filter sterilized using suction filtration with a 0.22 µm filter. After filtration, the solutions were centrifuged for 90 minutes at 3000 x g to separate the PEG-rich phase and the DEX-rich phase, which were then collected and stored at 4ºC. For one preliminary experiment assessing the containment of *P. aeruginosa* within an ATPS, a 5% PEG/5% DEX ATPS was used where both phases were dissolved in DMEM/F-12 supplemented with 10% FBS. For all other experiments, the ATPS that was used was a combination of the PEG-rich phase of the DMEM/F-12 ATPS formulation (to support 16-HBE cell growth) with the DEX-rich phase from the LB broth ATPS formulation (to support microbe growth).

2.7 Assessment of *Pseudomonas aeruginosa* containment within aqueous two-phase system

The ability for *P. aeruginosa* CF18 monoculture growth to be confined within an ATPS was assessed. *S. aureus* ATCC 6538 containment within an ATPS had already been established by previous lab members. For this experiment, a 5%/5% PEG/DEX ATPS made with DMEM/F-12 cell culture medium supplemented with 10% FBS (without antibiotic or antimycotic) was used. The ATPS was prepared as described in Section 1.6. *P. aeruginosa* CF18 from an overnight culture was suspended in the DEX-rich phase of the ATPS at optical densities (measured at 600 nm, OD_{600}) of 0.01, 0.1, and 0.5. OD_{600} is an approximation of bacteria concentration within a liquid sample. OD_{600} values were measured using the Varioskan Lux plate reader (Thermo Fisher Scientific). 250 µl of the PEG-rich phase was added to the wells of a 48-well plate and a BioMek 4000 Automated Liquid Handler (Beckman Coulter) was used to deposit a 0.5 µl droplet of the inoculated DEX-rich phase into each of the wells. The plate was then imaged once per hour for 18 hours using the EVOS™ FL Auto 2 Imaging System (Thermo Fisher Scientific) while being incubated using the EVOS™ Onstage Incubator (Thermo Fisher Scientific) at 37ºC and 5% CO_2.

2.8 Assessment of short-term bacteria culture establishment over healthy and CF hydrogels using an aqueous two-phase system

An ATPS was used to establish a short-term confined bacteria culture over top of the healthy and CF hydrogels. To assess whether the culture was confined, the alginate cushion and the chosen healthy and CF mucus-like hydrogels were first deposited into

wells of a 48-well plate at a total height of approximately 1.5 mm (based on volume deposited). 250 µl of the PEG-rich phase from a 5%/5% PEG/DEX ATPS in DMEM/F-12 was then added over top of the hydrogels. *P. aeruginosa* CF18 and *S. aureus* ATCC 6538 from overnight cultures were suspended in monoculture and co-culture in the DEX-rich phase of a 5%/5% PEG/DEX ATPS in LB broth. The bacteria monocultures were suspended within the DEX-rich phase at an OD_{600} of 0.01 and the bacteria co-cultures were suspended within the DEX-rich phase at an OD_{600} of 0.005 for each species giving a total OD_{600} of 0.01. A BioMek 4000 Automated Liquid Handler (Beckman Coulter) was used to deposit a 0.5 µl droplet of the inoculated DEX-rich phase into each of the wells. The plate was then incubated for 5 hours at 37ºC and 5% CO_2. After 5 hours, the liquid PEG phase and the hydrogel phase of each culture condition were removed separately using a pipette and were added to microcentrifuge tubes. Both phases were vortexed for 60 seconds and centrifuged at 16000 x g for 10 minutes to pellet bacteria. After centrifugation, the supernatant from each condition was removed, the hydrogel phases were resuspended in 150 µl of PBS, and the PEG phases were resuspended in 250 µl. The samples were then serially diluted with PBS in a 96-well plate. Samples from monoculture conditions were diluted from 10^{-1} to 10^{-6} and 20 µl of each dilution was spot plated onto LB agar (for *P. aeruginosa* monoculture) and BHI agar (for *S. aureus* monoculture). Initially, samples from co-culture conditions were diluted from 10^{-1} to 10^{-6} and 20 µl of each dilution was spot plated onto mannitol salt phenol red agar (MSA, selective for *S. aureus*, Millipore) and cetrimide agar (selective for *P. aeruginosa*, Oxoid). The *S. aureus* grew on the MSA as expected but *P. aeruginosa* growth on the cetrimide was inconsistent and did not follow the growth expected from serial dilutions.

Spread plating, spot plating, and gliding drop plating techniques were used to assess *P. aeruginosa* growth on cetrimide. After investigation, it was determined that *P. aeruginosa* CF18 and *S. aureus* ATCC 6538 were distinguishable when spread plated on LB agar based on colony color and morphology. The *S. aureus* growth on LB agar was also found to be consistent with *S. aureus* growth on MSA. The samples from co-culture conditions were then diluted from 10^{-2} to 10^{-5} for PEG phase samples and 10^{-4} to 10^{-7} for hydrogel samples and 100 µl of each dilution was spread plated onto LB agar. Agar plates were incubated for 16 to 18 hours at 37ºC and 5% CO_2 and colonies were counted for colony forming unit (CFU) determination within the PEG phase and hydrogel phase of each condition. Equation 2 was used to calculate the concentration of viable bacteria within each condition.

$$N = \frac{C}{V \times D} \tag{2}$$

In Equation 2, N is the concentration of viable bacteria in CFU/ml, C is the number of colonies counted, V is the volume of sample plated in ml, and D is the dilution factor.

2.9 Determination of ciprofloxacin minimum inhibitory concentration for bacteria monocultures and co-cultures

The minimum inhibitory concentration (MIC) of ciprofloxacin was determined for *P. aeruginosa* CF18 and *S. aureus* ATCC 6538 in monoculture and in co-culture using a broth microdilution procedure [122]. Prior to this procedure, the correlation between OD_{600} and CFU/ml was first determined for *P. aeruginosa* CF18 and *S. aureus* ATCC 6538. Overnight cultures of *P. aeruginosa* and *S. aureus* were diluted to an OD_{600} of 0.01, serially diluted in PBS from 10^{-4} to 10^{-7}, and 100 µl of each dilution was spread

plated on LB agar. The plates were incubated at 37ºC and 5% CO_2 for 16 to 18 hours. After incubation, the colonies were counted and the CFU/ml corresponding to the plated OD_{600} of 0.01 was calculated using Equation 2. This was repeated in triplicate using overnight cultures from three separate colonies for both species of bacteria.

Once the correlation between OD_{600} and CFU/ml was determined for *P. aeruginosa* CF18 and *S. aureus* ATCC 6538, overnight cultures of both species in LB broth were diluted to ~ 1 x 10^8 CFU/ml and, for a co-culture of the two species, the overnight cultures were diluted and mixed to a total concentration of ~ 1 x 10^8 CFU/ml. The solutions were then further diluted 1:100 in LB broth so each solution had total bacteria concentration of 1 x 10^6 CFU/ml. To determine the ciprofloxacin MIC, 50 µl of ciprofloxacin at different dilutions (diluted in LB broth) was mixed with 50 µl of the diluted bacteria cultures in the wells of a 96-well plate for a final bacteria concentration of 5 x 10^5 CFU/ml within each well. The ciprofloxacin concentrations tested were 0.06, 0.125, 0.25, 0.5, 1, 2, 4, 8, 16, and 32 µg/ml. For the three culture conditions (*P. aeruginosa* monoculture, *S. aureus* monoculture, and co-culture of the two species) a growth control (GC) and sterility control (SC) was also included. The GC was 50 µl of bacteria solution with 50 µl of LB broth and the SC was 100 µl of LB broth with no inoculation. All empty wells were filled with sterile PBS. The 96-well plate was incubated at 37ºC and 5% CO_2 for 16 to 18 hours. The plate was incubated at 5% CO_2 to match later experimental conditions for experiments involving mammalian cells. The MIC for each culture condition was determined to be the lowest tested concentration of ciprofloxacin that resulted in no visible bacteria growth. The test was repeated twice for the three culture conditions.

2.10 Assessment of bacteria growth when cultured with healthy and CF hydrogels in the presence of ciprofloxacin

Prior to culturing the *P. aeruginosa* CF18 and *S. aureus* ATCC 6538 within the airway models, the growth of the bacteria with the mucus-like hydrogels in the presence of ciprofloxacin was first assessed without the inclusion of 16-HBE cells. The cultures were prepared as described in Section 2.8, with an ATPS being used to deposit the bacteria over top of the healthy and CF mucus-like hydrogels. Also as described in Section 2.8, the plate was cultured for 5 hours at 37ºC and 5% CO_2. After 5 hours, the PEG-rich phase of the ATPS was carefully removed through pipetting and was replaced with DMEM/F-12 supplemented with 10% FBS and 0.5 µg/ml ciprofloxacin. The plate was then cultured for an additional 43 hours at 37ºC and 5% CO_2, for a total culture period of 48 hours. After the 43-hour culture period, 50 µl of the liquid phase from each culture condition was carefully collected through pipetting and was deposited into microcentrifuge tubes. The remainder of the liquid phase was then carefully removed and disposed of. This was done to avoid collecting any of the bacteria at the liquid-hydrogel interface and to avoid collecting the hydrogel itself. Once the liquid phase was removed, the hydrogel phase from each culture condition were collected and deposited into microcentrifuge tubes. The hydrogel phases were prepared as described in Section 2.8 and the liquid phases were vortexed for 60 seconds each. The samples were then serially diluted with PBS in a 96-well plate. Samples from monoculture conditions were diluted from 10^{-1} to 10^{-7} and a combination of spot plating and spread plating techniques were used. A combination of spot and spread plating was used for the monoculture dilutions because there is only space for six spot plating dilutions on one agar plate. For six of the

seven dilutions, 20 µl of each dilution was spot plated onto LB agar, with 100 µl of the seventh dilution spread plated onto LB agar. Samples from co-culture conditions were diluted from 10^{-1} to 10^{-6} and 100 µl of each dilution was spread plated onto LB agar. Co-culture dilutions were spread plated because colonies of the two species were not distinguishable when spot plating was tested. The concentration of viable bacteria in the liquid and hydrogel phase for each culture condition was then determined as described in Section 2.8.

2.11 Assessment of mammalian-microbe culture without ciprofloxacin

P. aeruginosa CF18 and *S. aureus* ATCC 6538 were cultured within the airway models without ciprofloxacin to assess their impact on 16-HBE cell viability. 16-HBE cells were seeded into a fibronectin-coated 48-well plate at a seeding density of approximately 55000 cells/well. The cells were cultured at 37ºC and 5% CO_2 for 24 hours, growing to approximately 60% confluency. After the 24-hour culture period, the cultures were prepared as described in Section 2.8, with an ATPS being used to deposit the bacteria over top of the healthy and CF mucus-like hydrogels. Also as described in Section 2.8, the plate was cultured for 5 hours at 37ºC and 5% CO_2. After 5 hours, the PEG-rich phase of the ATPS was carefully removed through pipette aspiration and was replaced with DMEM/F-12 supplemented with 10% FBS (without antibiotic or antimycotic). The plate was then cultured for an additional 1 or 19 hours, representing total culture periods of 6 and 24 hours, respectively. After both of these culture periods, the liquid phases and hydrogel phases from each culture condition were prepared as described in Section 2.10 and, once prepared, were serially diluted with PBS in a 96-well

plate. Samples from the 6-hour monoculture conditions were diluted from 10^{-1} to 10^{-8} and 20 µl of the first 6 dilutions were spot plated while 100 µl of the last dilution was spread plated, all on LB agar. Samples from the 24-hour monoculture conditions were diluted from 10^{-1} to 10^{-10} and 20 µl of each dilution was spot plated on LB agar. Samples from the 6-hour and 24-hour co-culture conditions were diluted from 10^{-1} to 10^{-8} and 100 µl of each dilution was spread plated on LB agar. The concentration of viable bacteria in the liquid and hydrogel phase for each culture condition of both culture periods was then determined as described in Section 2.8. After the 6- and 24-hour culture periods, 16-HBE cell viability was also assessed using a live/dead assay and a Hoechst stain as described in Section 2.3.

2.12 Assessment of healthy and CF airway models

To establish the healthy and CF airway models, which combine mammalian-microbe culture with the mucus-like hydrogels and a relevant CF antibiotic, 16-HBE cells were first seeded into a fibronectin-coated 48-well plate at a seeding density of approximately 55000 cells/well. The cells were cultured at 37ºC and 5% CO_2 for 24 hours, growing to approximately 60% confluency. After the 24-hour culture period, the cultures were prepared as described in Section 2.8, with an ATPS being used to deposit the bacteria over top of the healthy and CF mucus-like hydrogels. Also as described in Section 2.8, the models were cultured for 5 hours at 37ºC and 5% CO_2. After 5 hours, the PEG-rich phase of the ATPS was carefully removed through pipette aspiration and was replaced with DMEM/F-12 supplemented with 10% FBS and 0.5 µg/ml ciprofloxacin. The models were then cultured for an additional 43 hours. After 43 hours, the liquid phases and

hydrogel phases from each culture condition were prepared as described in Section 2.10 and, once prepared, were serially diluted with PBS in a 96-well plate. Samples from monoculture conditions were diluted from 10^{-1} to 10^{-7} and a combination of spot plating and spread plating techniques were used. For six of the seven dilutions, 20 µl of each dilution was spot plated onto LB agar, with 100 µl of the seventh dilution spread plated onto LB agar. Samples from co-culture conditions were diluted from 10^{-1} to 10^{-7} and 100 µl of each dilution was spread plated on LB agar. The concentration of viable bacteria in the liquid and hydrogel phase for each culture condition was then determined as described in Section 2.8. After the full 48-hour culture period, 16-HBE cell viability was also assessed using a live/dead assay and a Hoechst stain as described in Section 2.3. A schematic of the final assessment of the airway models can be found in Figure 5 below.

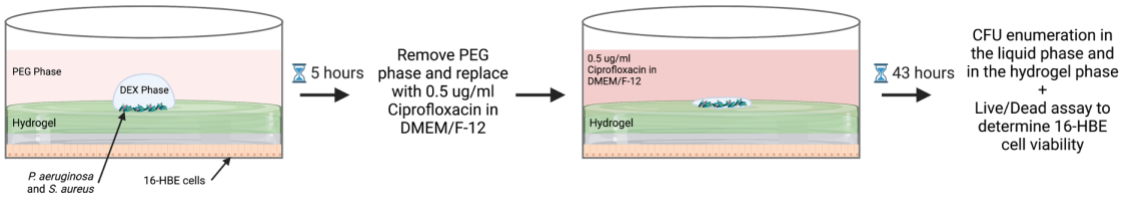

Figure 5: Schematic of the final airway model assessment. For the final assessment, both the healthy and CF airway models were composed of a mucus-like hydrogel overlaid onto a layer of 16-HBE cells. An ATPS was used to deposit *P. aeruginosa* and *S. aureus*, in monoculture or co-culture, over top of the mucus-like hydrogels. The models were cultured for 5 hours and then the PEG phase of the ATPS was removed and replaced with 0.5 µg/ml ciprofloxacin in DMEM/F-12. This was then cultured for another 43 hours and, after this culture period, the concentration of viable bacteria within the liquid and hydrogel phases were determined through CFU enumeration and 16-HBE cell viability was assessed using a live/dead assay and DNA stain. Schematic created with BioRender.com.

2.13 Statistical analysis

GraphPad Prism (Version 9.4.1) was used for statistical analysis of bacterial abundance and potential mucus-like hydrogel rheology data. Statistical significance of

bacterial abundance was determined using two-way analysis of variance (ANOVA) with p values represented as *$p < 0.05$, **$p < 0.01$, ***$p < 0.001$. Statistical significance of potential mucus-like hydrogel rheology data when comparing increased crosslinker concentration and increased alginate concentration were determined using Welch's t-test with p values represented as $^{a}p < 0.05$ (when comparing G' values) and $^{b}p < 0.05$ (when comparing G'' values). Statistical significance of potential mucus-like hydrogel rheology data when comparing increased mucin concentration was determined using one-way ANOVA with p values of $p < 0.05$ indicated by matching superscripts.

CHAPTER 3. Results

3.1 Selection of potential mucus-like hydrogel formulations based on cytotoxicity assessments

The viability of 16-HBE cells was assessed after 48 hours of culture with HA hydrogels and alginate hydrogels. 16-HBE cell viability under these conditions is described in the following sections.

3.1.1 Hyaluronic acid hydrogels

16-HBE cell viability results after 48 hours of culture with the HA hydrogels was similar for all three hydrogel thicknesses tested. Also, cell viability did not appear to differ greatly with changes in HA concentration or crosslinker concentration, but did appear to depend on changes in mucin concentration. 16-HBE cells incubated with HA hydrogels containing 0% mucins showed high cell viability with few non-viable cells. 16-HBE cells incubated with HA hydrogels containing 1.5% and 5% mucins showed all non-viable cells with no remaining live cells, and cell adherence was also found to be generally poor. Cell adherence was found to be greater for HA hydrogels containing 5% mucins than for HA hydrogels containing 1.5% mucins (Figure 6). Based on these results, all tested formulations of HA hydrogels containing mucins were deemed cytotoxic after 48 hours of culture with 16-HBE cells.

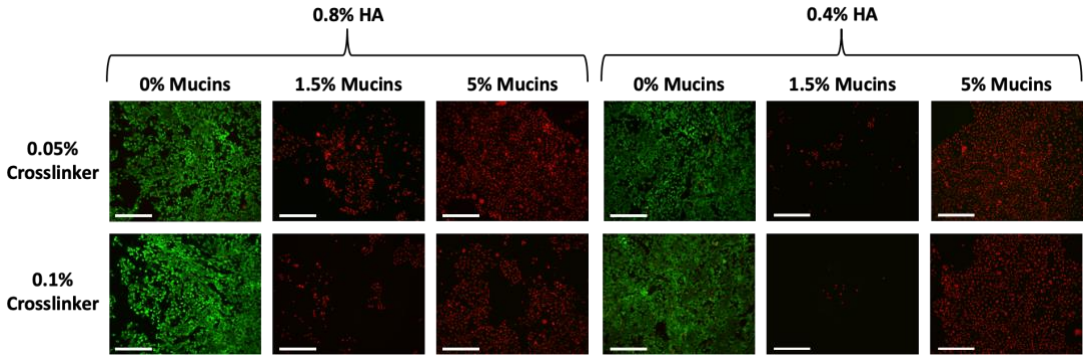

Figure 6: Cell viability of 16-HBE cells cultured beneath 1.5 mm thick HA-based hydrogels for 48 hours. Live/dead assay with calcein AM and ethidium homodimer-1 performed after 48 hours of culture. Green cells are viable and red cells are non-viable. Images captured on EVOS™ FL Auto 2 Imaging System using GFP and RFP channels. Scale bar = 275 μm.

3.1.2 Alginate hydrogels crosslinked with $CaCO_3$/GDL

Alginate-based hydrogels were also investigated as potential mucus-like hydrogels. The first alginate crosslinking method that was investigated was a combination of $CaCO_3$ and glucono-delta-lactone (GDL). This crosslinking method works by mixing low solubility $CaCO_3$ with a sodium alginate solution and then adding GDL to acidify the mixture. This acidification releases the calcium ions from the $CaCO_3$ which form crosslinks between the alginate strands. Initial testing of the alginate hydrogels crosslinked with $CaCO_3$ and GDL showed poor cytocompatibility with no viable cells remaining for the hydrogels containing 1% and 4% mucins (Figure 7).

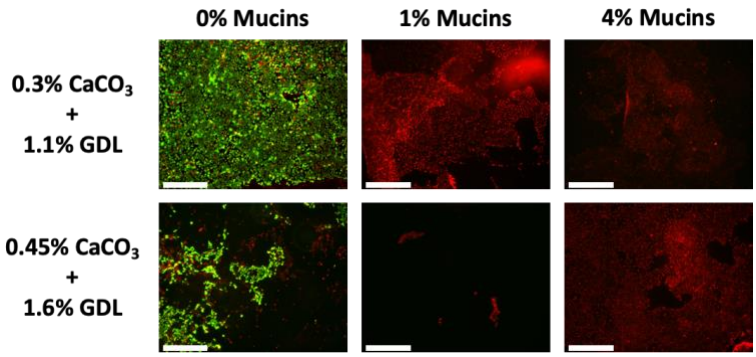

Figure 7: Cell viability of 16-HBE cells cultured beneath 1% (w/v) alginate hydrogels crosslinked with $CaCO_3$/GDL. Live/dead assay with calcein AM and ethidium homodimer-1 performed after 48 hours of culture. Green cells are viable and red cells are non-viable. Images captured on EVOS™ FL Auto 2 Imaging System using GFP and RFP channels. Scale bar = 650 μm.

The same hydrogel formulations were retested with HEPES buffer added to the system. Results were similar to the previous trial, although cell viability was improved for the 0% mucin hydrogels. Cell adherence and cell viability were poor for both the 1% and 4% mucin hydrogels (Figure 8). Across all trials, cell viability did not appear to differ greatly between the two crosslinker concentrations tested. Based on these results, all tested formulations of alginate crosslinked with $CaCO_3$/GDL that contained mucins were deemed cytotoxic after 48 hours of culture with 16-HBE cells.

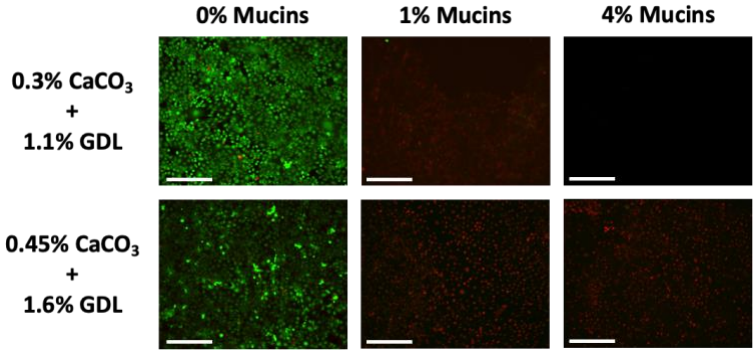

Figure 8: Cell viability of 16-HBE cells cultured beneath 1% (w/v) alginate hydrogels crosslinked with $CaCO_3$/GDL and containing HEPES buffer. Live/dead assay with calcein AM and ethidium homodimer-1 performed after 48 hours of culture. Green cells are viable and red cells are non-viable. Images captured on EVOS™ FL Auto 2 Imaging System using GFP and RFP channels. Scale bar = 275 μm.

3.1.3 Alginate hydrogels crosslinked with $CaCl_2$

The second alginate crosslinking method that was investigated was $CaCl_2$. This crosslinking method works through calcium ions from highly soluble $CaCl_2$ replacing sodium ions in the sodium alginate and forming crosslinks between the alginate strands. The initial test was to assess cell viability of 16-HBE cells incubated with $CaCl_2$-crosslinked alginate hydrogels containing a wide range of mucin concentrations. Lower and higher mucin concentrations needed to be developed to represent the relative difference in mucin concentration between CF and healthy airway mucus. The hydrogel formulations tested were combinations of 1% alginate, 0.67 mg/ml $CaCl_2$ crosslinker, and mucin concentrations ranging from 0% up to 5% (0 mg/mL up to 50 mg/mL). There were few non-viable 16-HBE cells observed for mucin concentrations up to 4%. Above 4% mucins, cell viability and cell adhesion were reduced (Figure 9).

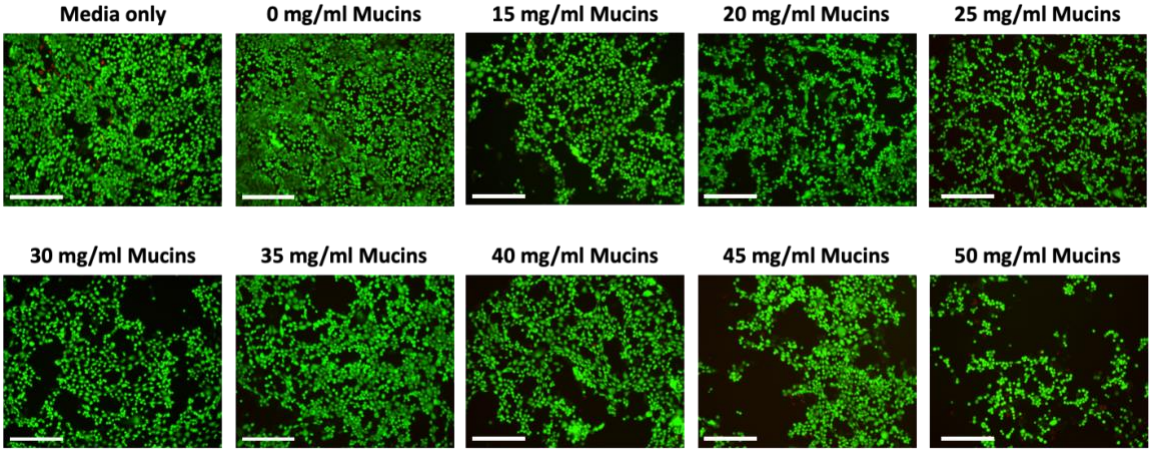

Figure 9: Cell viability of 16-HBE cells cultured beneath $CaCl_2$-crosslinked alginate hydrogels with varying mucin concentrations. Live/dead assay with calcein AM and ethidium homodimer-1 performed after 48 hours of culture. Green cells are viable and red cells are non-viable. Images captured on EVOS™ FL Auto 2 Imaging System using GFP and RFP channels. Scale bar = 275 μm.

The following test involved reducing the range of mucin concentrations but increasing the range of alginate and crosslinker concentrations in the hydrogel

formulations. The formulations tested for this iteration were combinations of 1% and 1.5% alginate, 0.67 and 1 mg/mL $CaCl_2$ crosslinker, and 0%, 1%, and 4% mucins. For this experiment and all experiments moving forward, HEPES buffer was incorporated into the hydrogels to attempt to improve 16-HBE cell viability and adhesion by better maintaining a physiological pH. Cell viability was high across all conditions but the hydrogels were found to begin solidifying while pipetting which lead to uneven hydrogel thicknesses within the wells (Figure 10).

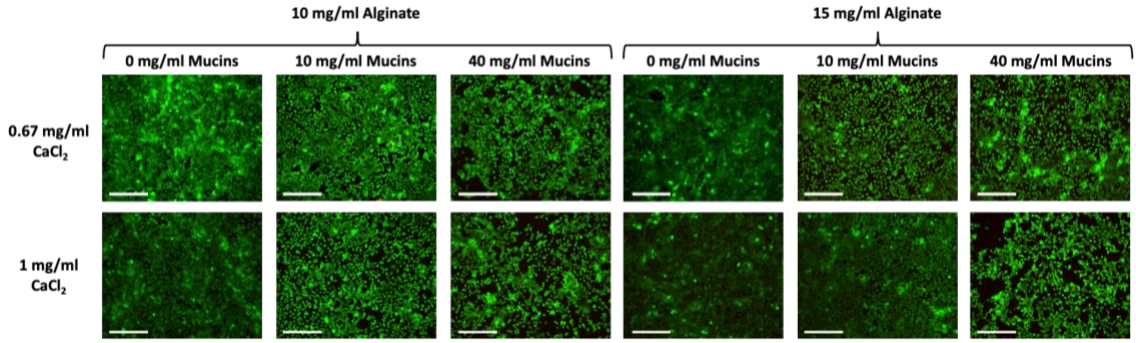

Figure 10: Cell viability of 16-HBE cells cultured beneath $CaCl_2$-crosslinked alginate hydrogels with varied alginate, mucin, and $CaCl_2$ crosslinker concentrations. Live/dead assay with calcein AM and ethidium homodimer-1 performed after 48 hours of culture. Green cells are viable and red cells are non-viable. Images captured on EVOS™ FL Auto 2 Imaging System using GFP and RFP channels. Scale bars = 275 μm.

To reduce the uneven pipetting occurring with the previous trials, crosslinker concentrations within the hydrogel formulations were reduced. The new hydrogel formulations tested were combinations of 1% and 1.5% alginate, 0.5 and 0.6 mg/mL $CaCl_2$ crosslinker, and 0%, 1%, and 4% mucins. With these formulations, the uneven pipetting issue was resolved and average cell viability was above 96% for all formulations (Figure 11) but overall cell adhesion was lacking, particularly for the 4% mucin hydrogel formulations.

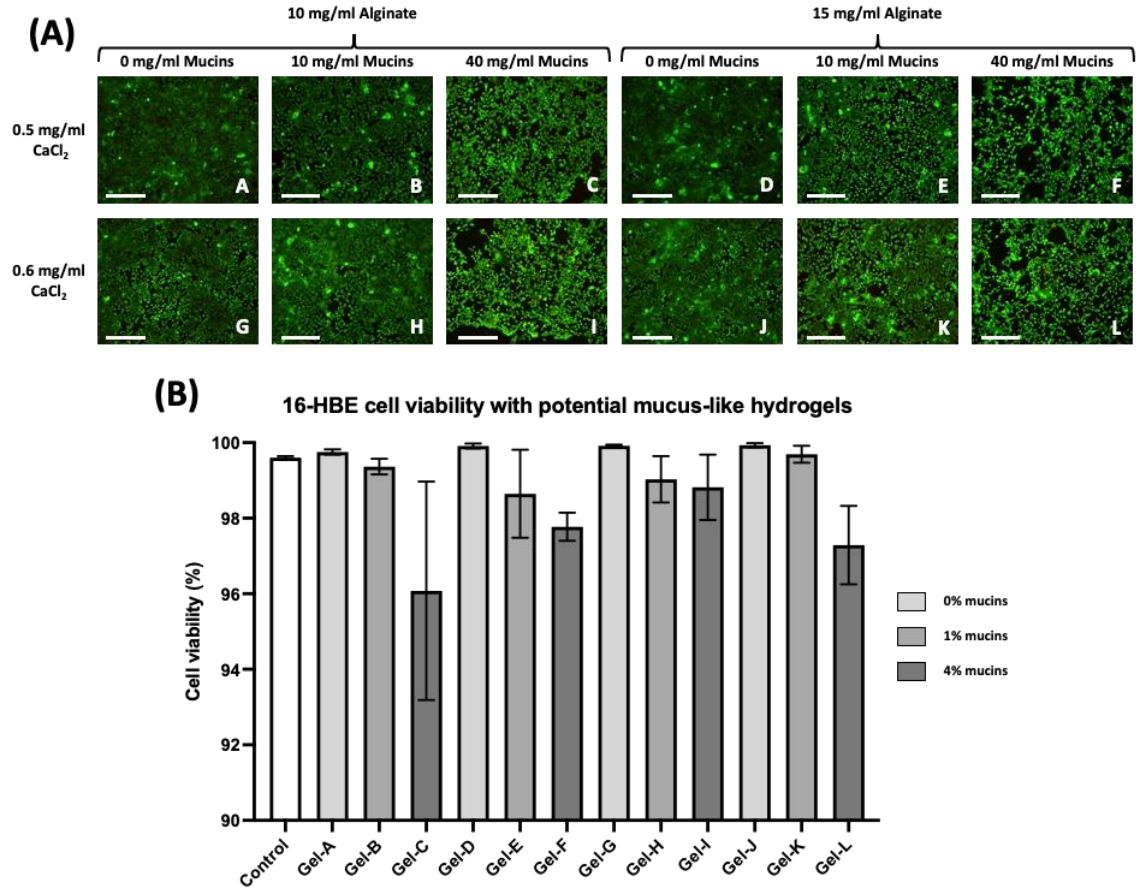

Figure 11: Cell viability of 16-HBE cells cultured beneath $CaCl_2$-crosslinked alginate hydrogels with reduced $CaCl_2$ crosslinker concentrations. (A) Live/dead assay with calcein AM and ethidium homodimer-1 performed after 48 hours of culture. Green cells are viable and red cells are non-viable. Images captured on EVOS™ FL Auto 2 Imaging System using GFP and RFP channels. Naming convention of hydrogels shown in bottom right corner of each image, with hydrogels named Gel-A through Gel-L. Representative images chosen from three biological replicates. Scale bar = 275 μm. **(B)** Average 16-HBE cell viability (%) ± standard deviation (SD) shown for each hydrogel formulation. Data averaged from three biological replicates.

3.1.4 Alginate hydrogels crosslinked with $CaCl_2$ including alginate cushion

To improve cell adhesion, an approximately 0.4 mm thick layer of $CaCl_2$-crosslinked alginate hydrogel with a 0% mucin concentration was added on top of the 16-HBE cells and below the mucus-like hydrogel formulations. This thin alginate hydrogel layer was added to act as a buffer between the 16-HBE cells and the mucus-like hydrogels and was named the "alginate cushion". The alginate cushion formulation was chosen based on

gelation time. Alginate hydrogels with combinations of 1% and 1.5% alginate, 0.1, 0.2, 0.3, 0.4, and 0.5 mg/mL $CaCl_2$, and 0% mucins were assessed as potential alginate cushion formulations. The formulation chosen for the alginate cushion was 1.5% alginate, 0.5 mg/mL $CaCl_2$ crosslinker, and 0% mucins because this formulation was found to solidify after 10 minutes. The alginate cushion volume (and thus height) to be used with the mucus-like hydrogels was chosen by pipetting varying volumes of the chosen alginate cushion formulation into a 48-well plate and determining the lowest volume that would spread and cover the bottom of the well. Volumes tested ranged from 20 μL to 70 μL at 10 μL increments and the chosen alginate cushion volume was 40 μL.

Once the alginate cushion formulation was chosen, it was combined with the potential mucus-like hydrogel formulations. The mucus-like hydrogel formulations tested with the inclusion of the alginate cushion were combinations of 1% and 1.5% alginate, 0.5 and 0.6 mg/ml $CaCl_2$ crosslinker, and 0%, 1%, and 4% mucins. The alginate cushion was added at a thickness of approximately 0.4 mm with the mucus-like hydrogel being added overtop at a thickness of 1.1 mm, keeping the total hydrogel thickness at approximately 1.5 mm (Figure 12). A total hydrogel thickness of 1.5 mm was chosen to approximate a build-up of mucus in the bronchi/bronchioles, which have been found to generally range in diameter from 1 to approximately 6 mm [123].

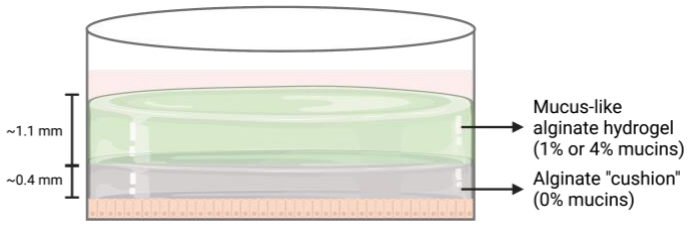

Figure 12: Schematic of the alginate cushion. An approximately 0.4 mm thick alginate cushion layer was added to the bottom of each well (on top of a layer of 16-HBE cells for

experiments including 16-HBE cells) with an approximately 1.1 mm thick mucus-like hydrogel layer added over top. Schematic created with BioRender.com.

With the addition of the alginate cushion, cell adhesion was generally improved (Figure 13).

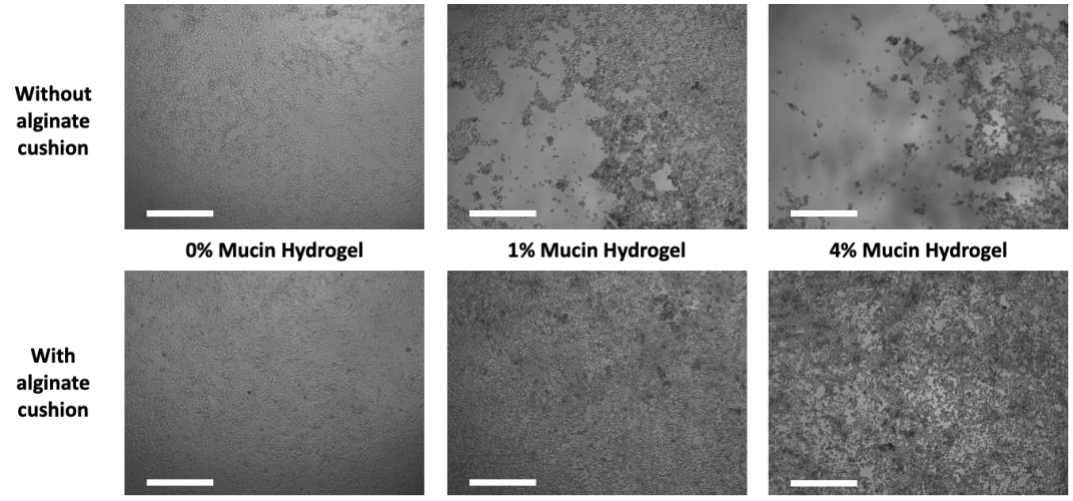

Figure 13: Representative images of 16-HBE cell adhesion after culture beneath $CaCl_2$-crosslinked alginate hydrogel formulations without (top row) and with (bottom row) the addition of an alginate cushion layer. Phase contrast images captured on EVOS™ FL Auto 2 Imaging System. Scale bar = 650 μm.

16-HBE cell viability was also high after the addition of the alginate cushion with an average cell viability of 98% or greater for all formulations (Figure 14).

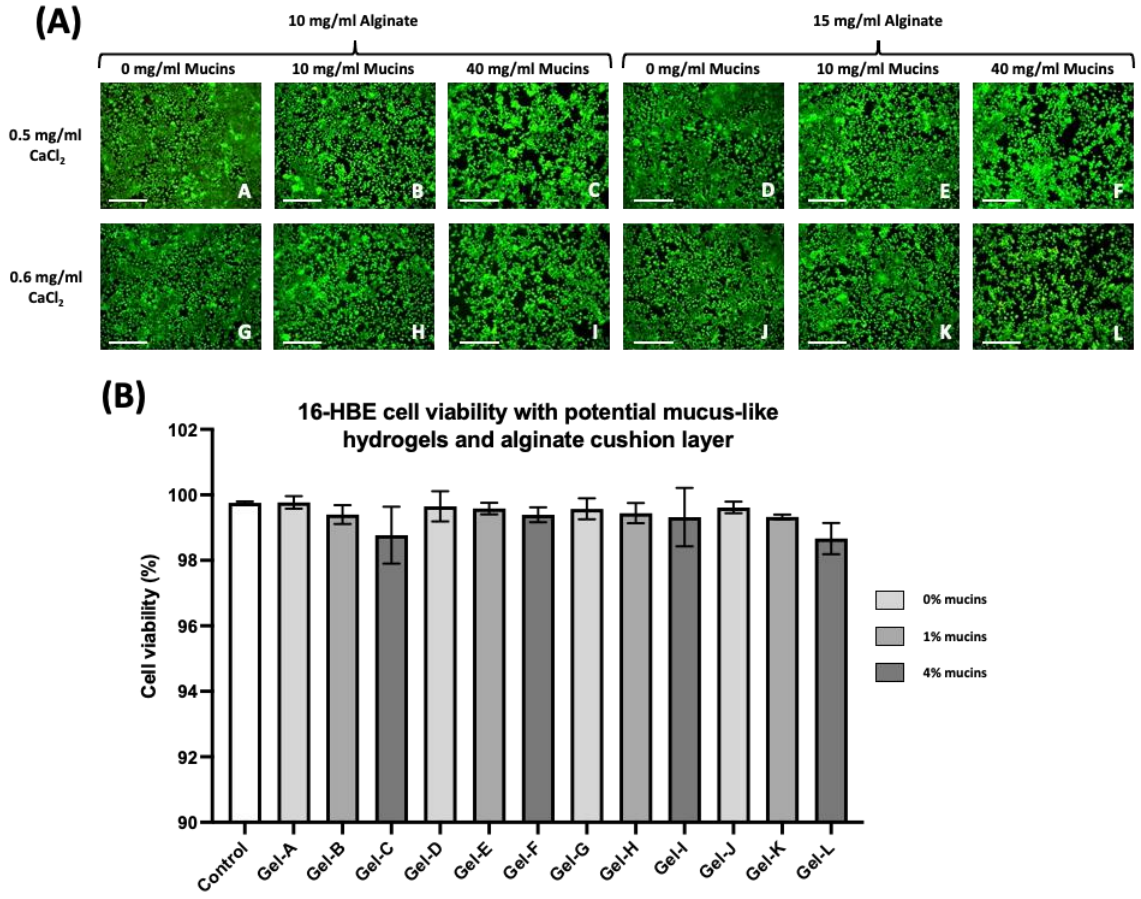

Figure 14: Cell viability of 16-HBE cells cultured beneath $CaCl_2$-crosslinked alginate hydrogels with the addition of an alginate cushion layer. (A) Live/dead assay with calcein AM and ethidium homodimer-1 performed after 48 hours of culture. Green cells are viable and red cells are non-viable. Images captured on EVOS™ FL Auto 2 Imaging System using GFP and RFP channels. Naming convention of hydrogels shown in bottom right corner of each image, with hydrogels named Gel-A through Gel-L. Representative images chosen from three biological replicates. Scale bar = 275 μm. **(B)** Average 16-HBE cell viability (%) ± SD shown for each hydrogel formulation. Data averaged from three biological replicates.

Based on hydrogel cytotoxicity testing, twelve formulations were chosen as potential mucus-like hydrogel formulations for the final airway models (with the inclusion of the alginate cushion layer). The twelve formulations can be found summarized in Table 1 below.

Table 1: Potential mucus-like hydrogel formulations chosen based on 16-HBE cytotoxicity after 48 hours of culture.

	1% alginate			1.5% alginate		
	0% mucin	1% mucin	4% mucin	0% mucin	1% mucin	4% mucin
0.5 mg/ml $CaCl_2$	Gel-A	Gel-B	Gel-C	Gel-D	Gel-E	Gel-F
0.6 mg/ml $CaCl_2$	Gel-G	Gel-H	Gel-I	Gel-J	Gel-K	Gel-L

The four formulations with 1% mucins (Gels B, E, H and K) were potential healthy mucus-like hydrogels as a relatively lower mucin concentration is more representative of healthy airway mucus. The four formulations with 4% mucins (Gels C, F, I, and L) were potential CF mucus-like hydrogel formulations as the relatively higher mucin concentration is more representative of CF airway mucus. The four formulations with 0% mucins were not intended to be used for the final models but were included in testing and analysis as a control. This was necessary to observe how the inclusion of mucins in the hydrogels affected hydrogel cytotoxicity and viscoelastic properties.

3.2 Selection of healthy and CF mucus-like hydrogels based on viscoelastic characterization

Once the potential mucus-like hydrogels were chosen based on cytocompatibility, the viscoelastic properties of the twelve potential hydrogel formulations were measured and analyzed to select final hydrogel formulations to represent the CF and healthy mucus-like hydrogels. The viscoelastic properties that were measured were the storage modulus, G', and the loss modulus, G''. These properties are the two components of the complex modulus which is a measure of the overall resistance to deformation of a material. When deformation is imposed on a material, the storage modulus represents the deformation

energy that becomes stored within a material and is used for elastic deformation while the loss modulus represents the deformation energy that is dissipated due to viscous flow. An increase in one or both of these properties is an increase in the overall complex modulus which indicates an increased resistance to deformation of a material. The general trend that emerged was that the viscoelastic properties of the hydrogels appeared to be dependent on changes in crosslinker concentration, changes in alginate concentration, and changes in mucin concentration. When crosslinker concentration was increased, the viscoelastic properties of the hydrogels tended to increase, although this increase was less pronounced for the hydrogels with a higher mucin concentration (Table 2). Plots comparing viscoelastic properties of the potential mucus-like hydrogel formulations when crosslinker concentration was varied can be found in Appendix A.

Table 2: Storage (G') and loss (G'') moduli of potential mucus-like hydrogel formulations paired by constant mucin and alginate concentration to demonstrate how crosslinker concentration impacts viscoelastic properties. Values in table were measured at an angular frequency of 1 rad/s. Values are the average ± SD from three independent measurements. [a]Indicates statistical significance between G' of the two formulations being compared and [b]indicates statistical significance between G'' of the two formulations being compared ($P < 0.05$).

		G' (Pa)	G'' (Pa)
0% mucin 1% alginate	**Gel-A (0.5 mg/ml $CaCl_2$)**	13.600 ± 3.170	1.300 ± 0.382[b]
	Gel-G (0.6 mg/ml $CaCl_2$)	30.283 ± 9.229	2.400 ± 0.381[b]
0% mucin 1.5% alginate	**Gel-D (0.5 mg/ml $CaCl_2$)**	15.596 ± 9.801	2.030 ± 0.554[b]
	Gel-J (0.6 mg/ml $CaCl_2$)	34.593 ± 8.580	3.224 ± 0.413[b]
1% mucin 1% alginate	**Gel-B (0.5 mg/ml $CaCl_2$)**	10.039 ± 3.127[a]	1.326 ± 0.351
	Gel-H (0.6 mg/ml $CaCl_2$)	22.830 ± 4.826[a]	3.003 ± 1.010
1% mucin 1.5% alginate	**Gel-E (0.5 mg/ml $CaCl_2$)**	11.118 ± 3.571	2.902 ± 0.761
	Gel-K (0.6 mg/ml $CaCl_2$)	19.970 ± 4.826	3.224 ± 0.798
4% mucin 1% alginate	**Gel-C (0.5 mg/ml $CaCl_2$)**	10.729 ± 2.907	2.759 ± 0.555
	Gel-I (0.6 mg/ml $CaCl_2$)	17.463 ± 3.535	3.654 ± 0.797
4% mucin 1.5% alginate	**Gel-F (0.5 mg/ml $CaCl_2$)**	16.590 ± 5.801	4.998 ± 1.733
	Gel-L (0.6 mg/ml $CaCl_2$)	19.970 ± 2.523	5.817 ± 0.260

When the alginate concentration was increased, the storage moduli of the hydrogels were very similar but the loss modulus tended to increase (Table 3). Plots comparing viscoelastic properties of the potential mucus-like hydrogel formulations when alginate concentration was varied can be found in Appendix B.

Table 3: Storage (G') and loss (G'') moduli of potential mucus-like hydrogel formulations paired by constant mucin and crosslinker concentration to demonstrate how alginate concentration impacts viscoelastic properties. Values in table were measured at an angular frequency of 1 rad/s. Values are the average ± SD from three independent measurements. [b]Indicates statistical significance between G'' of the two formulations being compared ($P < 0.05$). No statistical significance was found for any of the G' values being compared.

		G' (Pa)	G'' (Pa)
0% mucin 0.5 mg/ml $CaCl_2$	**Gel-A (1% alginate)**	13.600 ± 3.170	1.300 ± 0.382
	Gel-D (1.5% alginate)	15.596 ± 9.801	2.030 ± 0.554
0% mucin 0.6 mg/ml $CaCl_2$	**Gel-G (1% alginate)**	30.283 ± 9.229	2.400 ± 0.381
	Gel-J (1.5% alginate)	34.593 ± 8.580	3.224 ± 0.413
1% mucin 0.5 mg/ml $CaCl_2$	**Gel-B (1% alginate)**	10.039 ± 3.127	1.326 ± 0.351
	Gel-E (1.5% alginate)	11.118 ± 3.571	2.902 ± 0.761
1% mucin 0.6 mg/ml $CaCl_2$	**Gel-H (1% alginate)**	22.830 ± 4.826	3.003 ± 1.010
	Gel-K (1.5% alginate)	19.970 ± 4.826	3.224 ± 0.798
4% mucin 0.5 mg/ml $CaCl_2$	**Gel-C (1% alginate)**	10.729 ± 2.907	2.759 ± 0.555
	Gel-F (1.5% alginate)	16.590 ± 5.801	4.998 ± 1.733
4% mucin 0.6 mg/ml $CaCl_2$	**Gel-I (1% alginate)**	17.463 ± 3.535	3.654 ± 0.797[b]
	Gel-L (1.5% alginate)	19.970 ± 2.523	5.817 ± 0.260[b]

When the mucin concentration was increased, the storage modulus tended to decrease and the loss modulus tended to increase (Table 4). Plots comparing viscoelastic properties of the potential mucus-like hydrogel formulations when mucin concentration was varied can be found in Appendix C.

Table 4: Storage (G') and loss (G'') moduli of potential mucus-like hydrogel formulations grouped by constant alginate and crosslinker concentration to demonstrate how mucin concentration impacts viscoelastic properties. Values in table were measured at an angular frequency of 1 rad/s. Values are the average ± SD from three independent measurements. Matching [a] or [b] indicates statistical significance between G'' values. No statistical significance was found for any of the G' values being compared.

		G' (Pa)	G'' (Pa)
1% alginate 0.5 mg/ml $CaCl_2$	**Gel-A (0% mucin)**	13.600 ± 3.170	1.300 ± 0.382[a]
	Gel-B (1% mucin)	10.039 ± 3.127	1.326 ± 0.351[b]
	Gel-C (4% mucin)	10.729 ± 2.907	2.759 ± 0.555[a,b]
1.5% alginate 0.5 mg/ml $CaCl_2$	**Gel-D (0% mucin)**	15.596 ± 9.801	2.030 ± 0.554[a]
	Gel-E (1% mucin)	11.118 ± 3.571	2.902 ± 0.761
	Gel-F (4% mucin)	16.590 ± 5.801	4.998 ± 1.733[a]
1% alginate 0.6 mg/ml $CaCl_2$	**Gel-G (0% mucin)**	30.283 ± 9.229	2.400 ± 0.381
	Gel-H (1% mucin)	22.830 ± 4.826	3.003 ± 1.010
	Gel-I (4% mucin)	17.463 ± 3.535	3.654 ± 0.797
1.5% alginate 0.6 mg/ml $CaCl_2$	**Gel-J (0% mucin)**	34.593 ± 8.580	3.224 ± 0.413[a]
	Gel-K (1% mucin)	19.970 ± 4.826	3.224 ± 0.798[b]
	Gel-L (4% mucin)	19.970 ± 2.523	5.817 ± 0.260[a,b]

Based on the measured viscoelastic properties and the mucus-like hydrogel selection criteria, Gel-E was chosen as the healthy mucus-like hydrogel and Gel-L was chosen as the CF mucus-like hydrogel. All potential hydrogel formulations showed elastically dominant behavior (G' > G'') and all potential hydrogel formulations were within the same order of magnitude as physiological airway mucus. Gel-E and Gel-L were primarily chosen based on their difference in viscoelastic properties. Gel-B was also considered for the healthy mucus-like hydrogel as it also met the criteria, but through cytotoxicity testing it was found that Gel-B was more prone to hydrogel contraction during culture which was undesirable. The viscoelastic properties of the alginate cushion were not measured as the thicker mucus-like hydrogel makes up the majority of the hydrogel layer within the models and is the main interface with the bacteria while the alginate cushion is

a relatively thinner layer. The viscoelastic properties, G' and G'', of the chosen mucus-like hydrogels plotted against angular frequency can be found in Figure 15. A comparison of the viscoelastic properties of the chosen mucus-like hydrogels at selected high and low angular frequencies can be found in Appendix D.

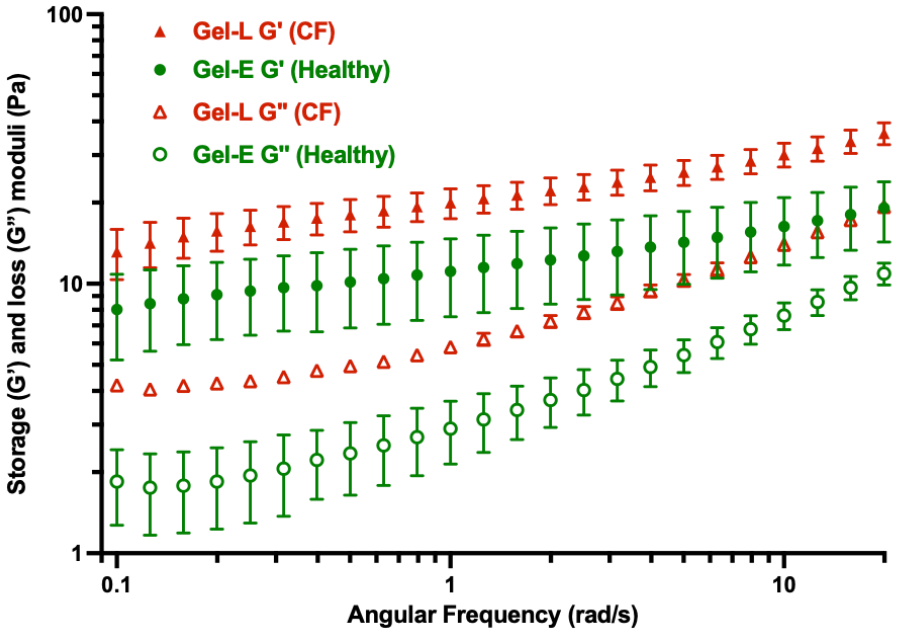

Figure 15: Viscoelastic properties of the chosen mucus-like hydrogel formulations. The properties of the CF mucus-like hydrogel, Gel-L, are shown in red and the properties of the healthy mucus-like hydrogel, Gel-E, are shown in green. Storage moduli, G', represented by solid icons and loss moduli, G'', represented by open icons. Data shown from an angular frequency range of 0.1 to 20 rad/s. Values are the average ± SD from three independent measurements.

The measured viscoelastic properties of the chosen hydrogels were also compared to literature viscoelastic properties of healthy and CF mucus (Figure 16).

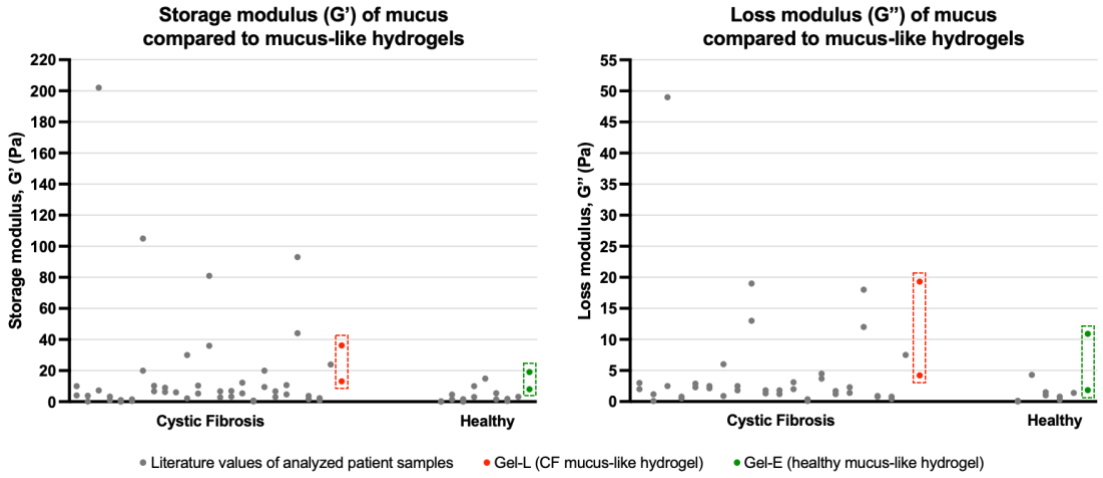

Figure 16: Viscoelastic properties of the chosen mucus-like hydrogels compared to the viscoelastic properties of healthy and CF mucus in literature. The properties of the CF mucus-like hydrogel, Gel-L, are shown in red and the properties of the healthy mucus-like hydrogel, Gel-L, are shown in green. The grey icons represent viscoelastic properties of CF and healthy mucus found in literature. Icons in line vertically represent the properties measured at lower and higher angular frequencies. The lower and higher angular frequencies of the mucus-like hydrogels were 0.1 and 20 rad/s while literature values were measured at frequencies ranging from 0.1 up to 100 rad/s. Literature values obtained from [19]–[21], [24], [25], [27], [28], [96], [124]–[129].

A summary of how the chosen mucus-like hydrogels meet the hydrogel selection criteria can be found in Table 5.

Table 5: Chosen mucus-like hydrogels compared to the hydrogel selection criteria.

Selection criteria	Gel-E (healthy mucus-like hydrogel) and Gel-L (CF mucus-like hydrogel)
The healthy and CF mucus-like hydrogels must not reduce cell viability below 80% when co-cultured for 48 hours.	Average cell viability after 48 hours of culture with Gel-E and Gel-L (including the addition of the alginate cushion) is above 98%.
The solids content and mucin protein concentration of the healthy and CF mucus-like hydrogels must be different. The relative difference should be similar to the relative differences between native healthy and CF airway mucus.	Gel-E has 2.6% (w/v) solids and 1% (w/v) mucin proteins, while Gel-L has 5.6% (w/v) solids and 4% (w/v) mucin proteins.

Selection criteria	Gel-E (healthy mucus-like hydrogel) and Gel-L (CF mucus-like hydrogel)
The healthy and CF mucus-like hydrogels must show elastically dominant behavior (i.e. G' > G'')	Both Gel-E and Gel-L show elastically dominant behavior with greater storage moduli than loss moduli.
The viscoelastic properties of the healthy and CF mucus-like hydrogels must be significantly different.	The storage moduli and loss moduli of Gel-L are significantly greater than the storage moduli and loss moduli of Gel-E.
The healthy and CF mucus-like hydrogels must have viscoelastic properties within the same order of magnitude as physiological airway mucus.	The storage and loss moduli of both healthy and CF mucus reported in literature generally range from 0.1 to 100 Pa with a small number of values > 100 Pa reported for the storage modulus of CF mucus. The storage and loss moduli of Gel-L and Gel-E are within this order of magnitude.
The healthy and CF mucus-like hydrogels must gel within 1 hour or less.	Gel-E and Gel-L, as well as the rest of the 12 potential mucus like hydrogel formulations, gel within less than 1 hour based on tube inversion.

To summarize, the chosen healthy mucus-like hydrogel formulation, Gel-E, consists of 1.5% alginate, 0.5 mg/ml $CaCl_2$, and 1% mucins. The chosen CF mucus-like hydrogel formulation, Gel-L, consists of 1.5% alginate, 0.6 mg/ml $CaCl_2$, and 4% mucins.

3.3 Preliminary observation of *Pseudomonas aeruginosa* CF18 growth within aqueous two-phase system

P. aeruginosa CF18 was grown within a 5% PEG/5% DEX ATPS on tissue culture plastic (with no hydrogels) for 18 hours as a preliminary assessment of bacteria containment within the DEX phase (Figure 17). Both phases of the ATPS used for this experiment were solubilized in DMEM/F-12 cell culture medium supplemented with 10% FBS but this was adapted and all other experiments that include an ATPS are 5%

PEG in DMEM/F-12 cell culture medium supplemented with 10% FBS with 5% DEX in LB broth.

After 6 hours of culture, *P. aeruginosa* seeded at 0.01 OD_{600} was contained while *P. aeruginosa* seeded at 0.1 OD_{600} was beginning to breach the DEX phase and *P. aeruginosa* seeded at 0.5 OD_{600} was no longer contained. After 12 hours, *P. aeruginosa* was no longer contained within the DEX droplet for any of the three conditions. Preliminary ATPS containment on tissue culture plastic was not assessed for *S. aureus* ATCC 6538 as this was previously investigated and confirmed by another lab member.

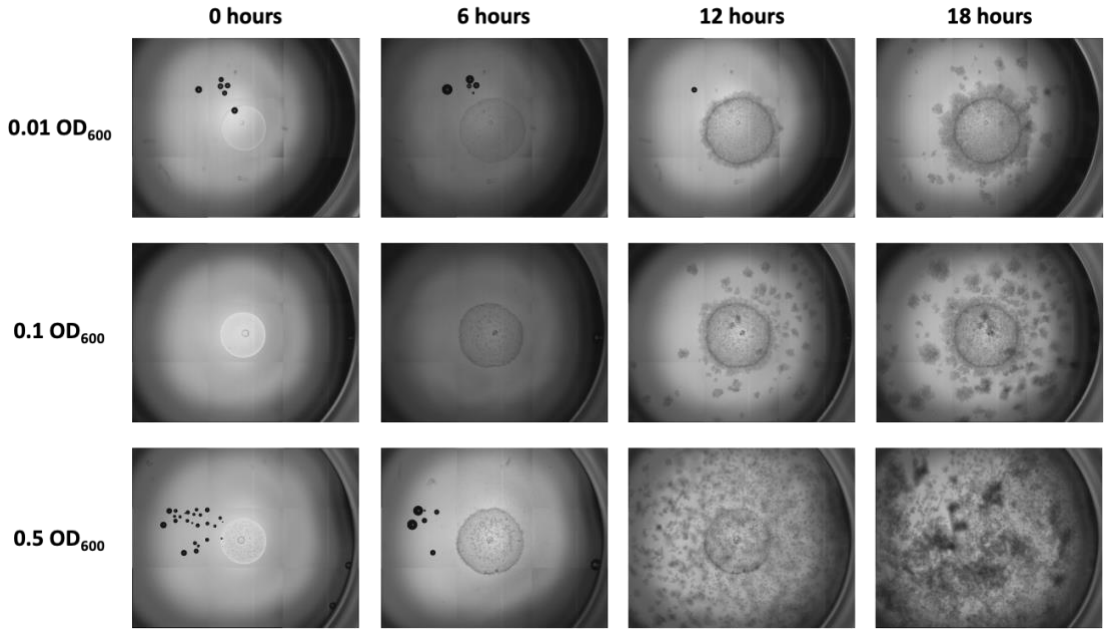

Figure 17: Preliminary observation of *P. aeruginosa* CF18 containment within 5% PEG/5% DEX ATPS on tissue culture plastic at different bacteria seeding densities. Timelapse imaging completed over 18 hours using EVOS™ FL Auto 2 Imaging System (Thermo Fisher Scientific) while being incubated using the EVOS™ Onstage Incubator.

3.4 Short-term confined culture of bacteria with healthy and CF mucus-like hydrogels using an aqueous two-phase system

The ability to establish a short-term confined culture of *P. aeruginosa* CF18 and *S. aureus* ATCC 6538 on top of/within the mucus-like hydrogels was assessed. Establishing a short-term confined culture of these microbes over the hydrogels was the first step towards the final microbe-mammalian airway models.

3.4.1 Viable *Pseudomonas aeruginosa* within PEG and hydrogel phases after 5 hours

After 5 hours of growth within the ATPS, the majority of viable *P. aeruginosa* was collected with the hydrogel phase for both the *P. aeruginosa* monoculture and the *P. aeruginosa* co-culture with *S. aureus* (Figure 18). The hydrogel phase had a minimum of six times the viable bacteria relative to the PEG phase for all conditions. The differences between viable *P. aeruginosa* within the hydrogel phase and PEG phase for each respective culture condition was found to be statistically significant.

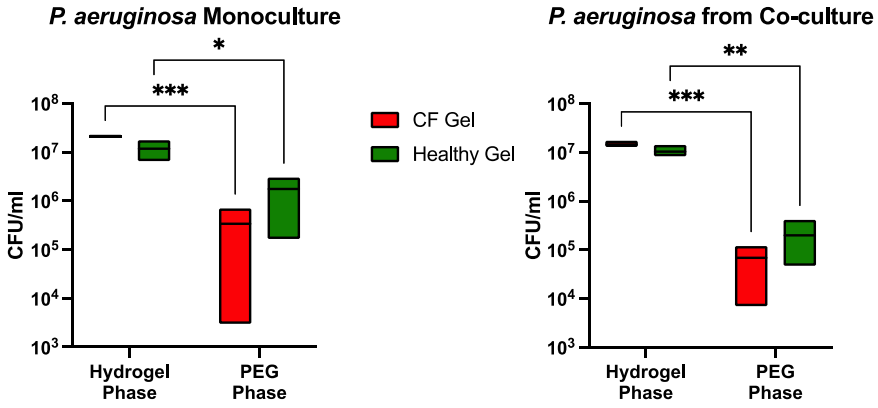

Figure 18: Concentration of viable *P. aeruginosa* (CFU/ml) within healthy and CF models after short-term (5 hour) monoculture and co-culture. *P. aeruginosa* grown in monoculture on the left and *P. aeruginosa* grown in co-culture with *S. aureus* on the right. The bars span from the minimum to the maximum value with the line within the bars representing the average value from three biological replicates (n = 3). P values obtained using two-way ANOVA. *p < 0.05, **p < 0.01, ***p < 0.001.

3.4.2 Viable *Staphylococcus aureus* within PEG and hydrogel phases after 5 hours

After 5 hours of growth within the ATPS, the majority of viable *S. aureus* was collected within the hydrogel phase for both the *S. aureus* monoculture and the *S. aureus* co-culture with *P. aeruginosa* (Figure 19). The hydrogel phase had a minimum of six times the viable bacteria relative to the PEG phase for all conditions. The differences between viable *S. aureus* within the hydrogel phase and PEG phase for each respective culture condition was found to be statistically significant, with the exception of the healthy co-culture condition. Despite the lack of statistical significance for the healthy co-culture condition, the hydrogel phase was found to have a greater concentration of viable *S. aureus* than the PEG phase for all three biological replicates.

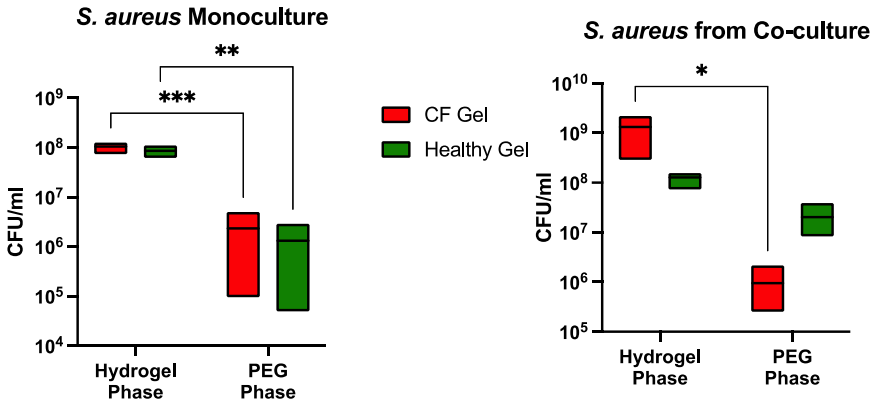

Figure 19: Concentration of viable *S. aureus* (CFU/ml) within healthy and CF models after short-term (5 hour) monoculture and co-culture. *S. aureus* grown in monoculture on the left and *S. aureus* grown in co-culture with *P. aeruginosa* on the right. The bars span from the minimum to the maximum value with the line within the bars representing the average value from three biological replicates (n = 3). P values obtained using two-way ANOVA. *p < 0.05, **p < 0.01, ***p < 0.001.

The results of the short-term *P. aeruginosa* and *S. aureus* cultures over the hydrogels show that the majority of bacteria growth is on top of and/or within the hydrogel layer (as opposed to within the liquid PEG phase). The results also show that the PEG phase can be removed without removing the bulk of the bacteria. An early trend also appeared to be

emerging from this data which showed that both the *P. aeruginosa* and the *S. aureus* preferred to grow with the CF mucus-like hydrogel.

3.5 Ciprofloxacin MIC for *Pseudomonas aeruginosa* CF18 and *Staphylococcus aureus* ATCC 6538 in monoculture and co-culture

The MIC of ciprofloxacin was assessed for *P. aeruginosa* and *S. aureus* in monoculture and co-culture. Ciprofloxacin, a broad-spectrum fluoroquinolone antibiotic that inhibits DNA replication, was chosen for antibiotic experiments because it is used to treat *P. aeruginosa* infections in CF [130]–[132] and has also been found to be effective against *S. aureus* in literature [62]. Following the broth dilution method of MIC determination by Wiegand et al. [122], the correlation between *P. aeruginosa* and *S. aureus* OD_{600} and CFU was first determined. A *P. aeruginosa* CF18 OD_{600} of 0.01 correlated to approximately 3.8×10^7 CFU/ml. An *S. aureus* OD_{600} of 0.01 correlated to approximately 3.5×10^7 CFU/ml. The ciprofloxacin MIC of *P. aeruginosa* in monoculture, *S. aureus* in monoculture, and *P. aeruginosa* and *S. aureus* in co-culture was determined to be 0.125 μg/ml.

3.6 Bacteria growth when cultured with healthy and CF hydrogels in the presence of ciprofloxacin

After confirming that an ATPS can be used to establish a short-term confined bacteria culture over top of the CF and healthy mucus-like hydrogels, their growth was investigated when cultured with the two different hydrogels in the presence of ciprofloxacin. For this experiment, 16-HBE cells were not included within the culture.

The growth of these two microbes when cultured with 16-HBE cells and the mucus-like hydrogels in the presence of ciprofloxacin is discussed in Section 3.8 as these are the conditions of the healthy and CF airway models.

To investigate microbe growth in the presence of ciprofloxacin, a 5-hour confined monoculture and co-culture of *P. aeruginosa* and *S. aureus* was first established over the mucus-like hydrogels using an ATPS. Ciprofloxacin was then added to the cultures at a concentration of 0.5 μg/ml and, after 43 additional hours, the concentration of viable bacteria within the liquid and hydrogel phases of the cultures was determined. A ciprofloxacin concentration of 0.5 μg/ml (4x MIC) was used because when 0.125 μg/ml (MIC) and 0.25 μg/ml (2x MIC) were trialed for this experiment, there was a large amount of visible growth on the liquid surface of the cultures. This was a visual indication that the ciprofloxacin concentration could be further increased to better control bacteria growth within the cultures.

3.6.1 Viable *Pseudomonas aeruginosa* within liquid and hydrogel phases after 48 hours culture with ciprofloxacin

After 5 hours of growth within the ATPS and an additional 43 hours of culture in the presence of ciprofloxacin, the *P. aeruginosa* appeared to show increased resistance to ciprofloxacin when grown with the CF mucus-like hydrogel. For both the *P. aeruginosa* monoculture and the *P. aeruginosa* co-culture with *S. aureus*, the concentration of viable *P. aeruginosa* in both phases was generally higher for the culture with the CF mucus-like hydrogel (Figure 20). While the magnitude of growth and the relative difference between the CF and healthy cultures varied, this trend was observed for the hydrogel phase of all replicates and for the liquid phase of all replicates but one. Additionally, the

concentration of viable *P. aeruginosa* within the liquid phase of the healthy co-culture with *S. aureus* was much lower than in any of the other conditions for all replicates. The differences in viable *P. aeruginosa* concentration between the CF and healthy conditions were not statistically significant. Results from individual biological replicates were plotted to demonstrate trends in relative growth between the models despite differences in growth magnitude between replicates.

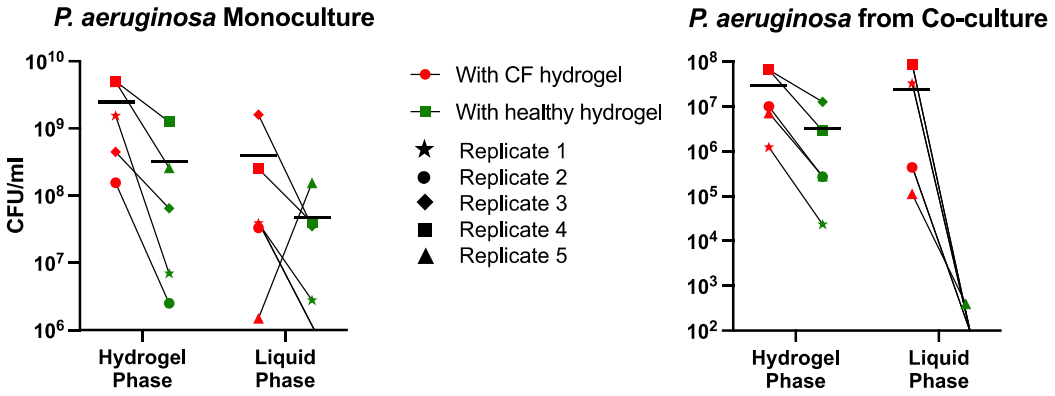

Figure 20: Concentration of viable *P. aeruginosa* (CFU/ml) grown with healthy and CF mucus-like hydrogels after 48 hours total of monoculture and co-culture in the presence of 0.5 µg/ml ciprofloxacin and without 16-HBE cells. *P. aeruginosa* grown in monoculture on the left and *P. aeruginosa* grown in co-culture with *S. aureus* on the right. The values from each biological replicate are indicated by a different icon and horizontal black bars represent the mean (n = 5). Values from *P. aeruginosa* grown with the CF and healthy hydrogels from the same biological replicate are connected by a line. Any missing icons or lines passing through the x-axis indicate a value of zero.

3.6.2 Viable *Staphylococcus aureus* within liquid and hydrogel phases after 48 hours culture with ciprofloxacin

After 5 hours of growth within the ATPS and an additional 43 hours of culture in the presence of ciprofloxacin, the *S. aureus* in monoculture appeared to show increased resistance to ciprofloxacin when grown with the CF mucus-like hydrogel (Figure 21), although for some replicates this trend was less pronounced than the *P. aeruginosa* monoculture. For the *S. aureus* monoculture, the concentration of viable *S. aureus* in both

phases was generally higher for the culture with the CF mucus-like hydrogel. For the *S. aureus* co-culture with *P. aeruginosa*, the trends were not as consistent, particularly for the hydrogel phase. The concentration of viable *S. aureus* in the liquid phase of the co-culture was generally higher for the culture with the CF mucus-like hydrogel, similarly to what was observed for the *S. aureus* monoculture. The concentration of viable *S. aureus* in the hydrogel phase of the co-culture showed a mixed response to the ciprofloxacin. Three biological replicates showed a greater concentration of viable *S. aureus* for the culture with the healthy mucus-like hydrogel and two showed a greater concentration of viable *S. aureus* for the culture with the CF mucus-like hydrogel. The differences in viable *S. aureus* concentration between the CF and healthy conditions were not statistically significant. Results from individual biological replicates were plotted to demonstrate trends in relative growth between the models despite differences in growth magnitude between replicates.

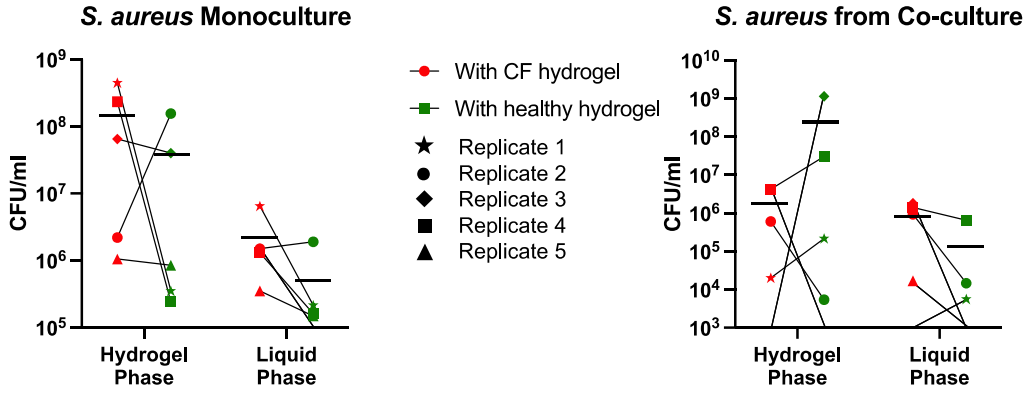

Figure 21: Concentration of viable *S. aureus* (CFU/ml) grown with healthy and CF mucus-like hydrogels after 48 hours total of monoculture and co-culture in the presence of 0.5 μg/ml ciprofloxacin and without 16-HBE cells. *S. aureus* grown in monoculture on the left and *S. aureus* grown in co-culture with *P. aeruginosa* on the right. The values from each biological replicate are indicated by a different icon and horizontal black bars represent the mean (n = 5). Values from *S. aureus* grown with the CF and healthy hydrogels from the same biological replicate are connected by a line. Any missing icons or lines passing through the x-axis indicate a value of zero.

3.7 Bacteria growth and 16-HBE cell viability when cultured with healthy and CF hydrogels without ciprofloxacin

The growth of *P. aeruginosa* and *S. aureus* and their impact on 16-HBE viability when cultured with the mucus-like hydrogels without the inclusion of ciprofloxacin was also investigated. A 5-hour confined monoculture and co-culture of *P. aeruginosa* and *S. aureus* was first established over the mucus-like hydrogels using an ATPS. After 5 hours, the liquid PEG phase of the ATPS was removed and replaced with DMEM/F-12 supplemented with 10% FBS. Following an additional 1 hour and 19 hours of culture (for a 6-hour or 24-hour total culture time, respectively), the concentration of viable bacteria within the liquid and hydrogel phases of the cultures was determined. 16-HBE cell viability was also visually assessed at the 6-hour and 24-hour timepoints of all culture conditions.

3.7.1 Viable *Pseudomonas aeruginosa* within liquid and hydrogel phases after 6 and 24 hours culture with no ciprofloxacin

The concentration of viable *P. aeruginosa* grown in monoculture was much greater at the 24-hour culture timepoint relative to the 6-hour culture timepoint (Figure 22). After 24 hours, viable bacteria concentrations were greater than 10^{10} CFU/ml for both phases of the healthy and CF hydrogel culture conditions. The 6-hour timepoint showed much less viable bacteria, with viable bacteria concentrations less than 10^{8} CFU/ml for both phases of the healthy and CF hydrogel culture conditions. While the concentration of viable *P. aeruginosa* varied greatly between culture timepoints, *P. aeruginosa* growth was similar between the healthy and CF hydrogel culture conditions. Only the liquid phase of the 24-hour culture timepoint showed a major difference in *P. aeruginosa* growth between the

two mucus-like hydrogels, with the liquid phase of the healthy hydrogel culture having a much larger concentration of viable *P. aeruginosa* than the liquid phase of the CF hydrogel culture.

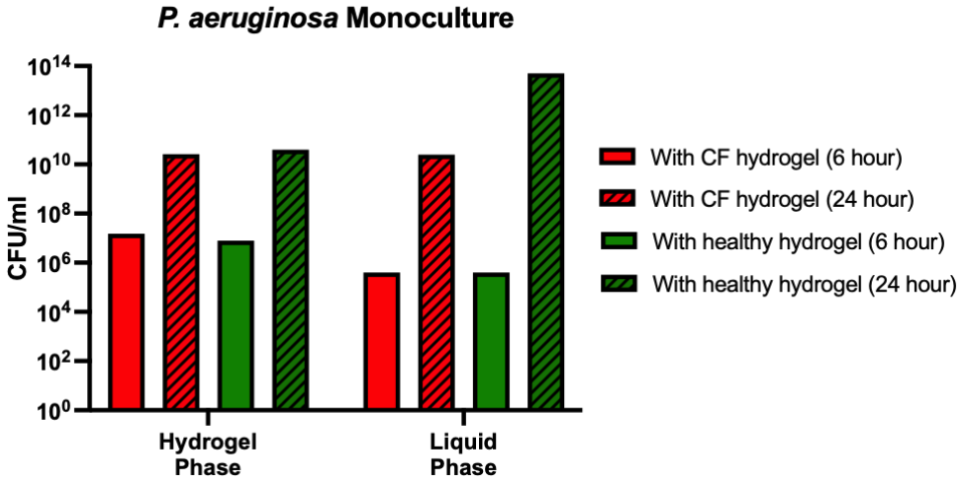

Figure 22: Concentration of viable *P. aeruginosa* (CFU/ml) grown in monoculture with 16-HBE cells and healthy and CF mucus-like hydrogels for a total of 6 and 24 hours. No ciprofloxacin was included within this experiment.

Similarly to the *P. aeruginosa* monoculture results above, the concentration of viable *P. aeruginosa* when grown in co-culture with *S. aureus* was much greater at the 24-hour culture timepoint relative to the 6-hour culture timepoint (Figure 23). After 24 hours, viable bacteria concentrations were greater than 10^{11} CFU/ml for both phases of the healthy and CF hydrogel culture conditions. The 6-hour timepoint showed much less viable bacteria, with viable bacteria concentrations less than 10^{7} CFU/ml for both phases of the healthy and CF hydrogel culture conditions. *P. aeruginosa* growth was also similar between the two mucus-like hydrogel formulations at the 6-hour culture timepoint and the 24-hour culture timepoint.

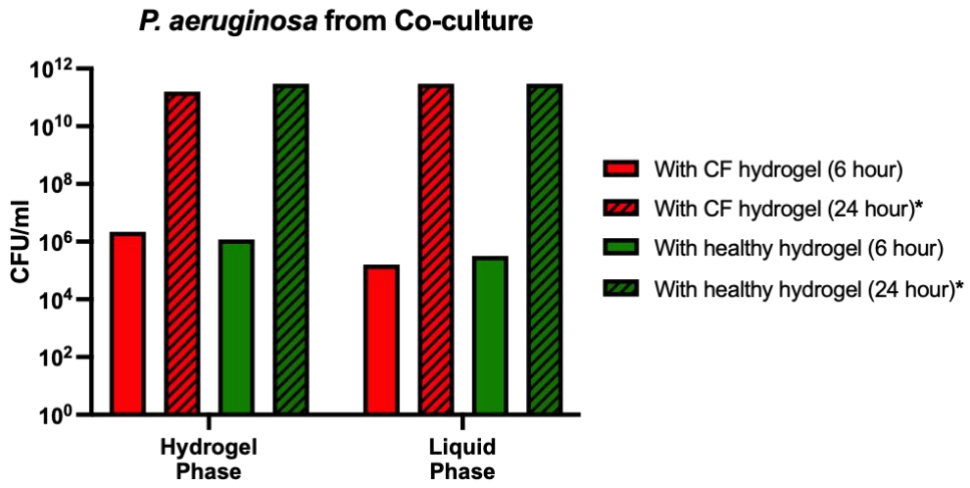

Figure 23: Concentration of viable *P. aeruginosa* (CFU/ml) grown in co-culture with *S. aureus* and with 16-HBE cells and healthy and CF mucus-like hydrogels for a total of 6 and 24 hours. No ciprofloxacin was included within this experiment. *CFU/ml values from all 24-hour culture conditions, except for the hydrogel phase of the CF mucus-like hydrogel, outgrew the highest plated dilution and were found to be > 3 x 10^{11} CFU/ml. These values were represented as 3 x 10^{11} CFU/ml on the above plot for comparison purposes.

3.7.2 Viable *Staphylococcus aureus* within liquid and hydrogel phases after 6 and 24 hours culture with no ciprofloxacin

The concentration of viable *S. aureus* grown in monoculture was greater at the 24-hour culture timepoint relative to the 6-hour culture timepoint (Figure 24). Between the hydrogel phases of the 6-hour and 24-hour timepoints, there was at least a 10-fold increase in viable *S. aureus* concentration. Between the liquid phases of the 6-hour and 24-hour timepoints, there was at least a 3-fold increase in viable *S. aureus* concentration. *S. aureus* growth was also similar between the two mucus-like hydrogel formulations at the 6-hour culture timepoint, while results suggested that there was slightly greater *S. aureus* growth for the CF hydrogel culture relative to the healthy hydrogel culture at the 24-hour timepoint.

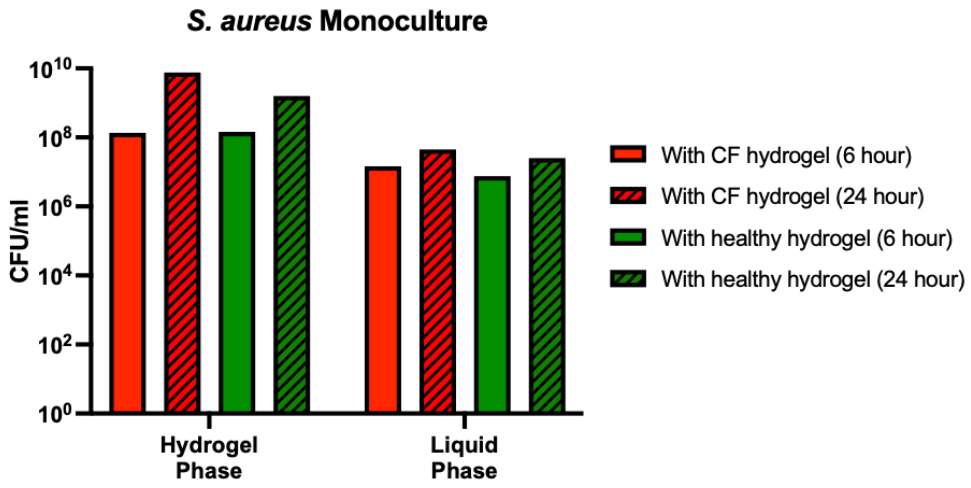

Figure 24: Concentration of viable *S. aureus* (CFU/ml) grown in monoculture with 16-HBE cells and healthy and CF mucus-like hydrogels for a total of 6 and 24 hours. No ciprofloxacin was included within this experiment.

The growth of *S. aureus* appeared to be impacted by the presence of *P. aeruginosa* for both the hydrogel phases and the liquid phases of the co-cultures (Figure 25). Between 6 and 24 hours of culture, the hydrogel phase of the CF mucus-like hydrogel culture showed very similar *S. aureus* growth while the hydrogel phase of the healthy mucus-like hydrogel culture showed a 3-fold increase in viable *S. aureus* concentration. The liquid phases of both mucus-like hydrogel cultures showed no viable *S. aureus* after 24 hours. For both culture timepoints, results suggested that the hydrogel phase of the CF mucus-like hydrogel culture had a slightly greater concentration of viable *S. aureus* relative to the healthy mucus-like hydrogel culture.

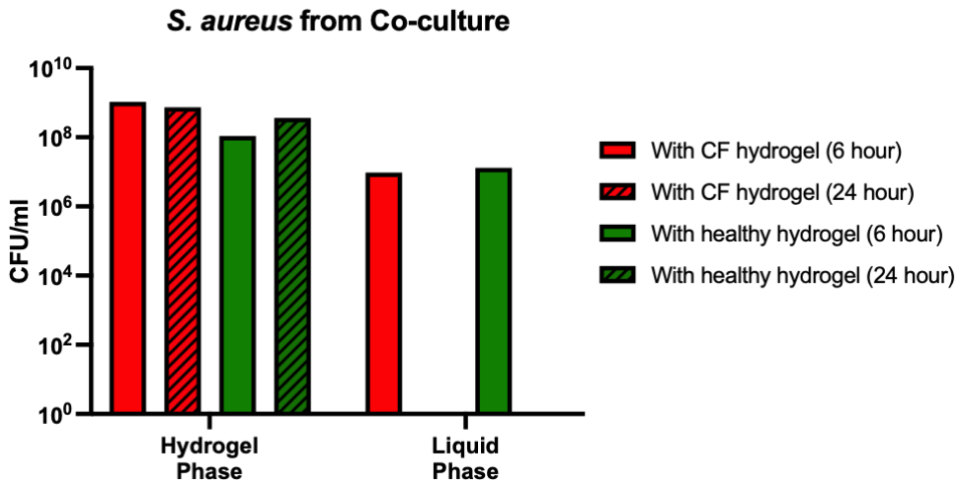

Figure 25: Concentration of viable *S. aureus* (CFU/ml) grown in co-culture with *P. aeruginosa* and with 16-HBE cells and healthy and CF mucus-like hydrogels for a total of 6 and 24 hours. No ciprofloxacin was included within this experiment.

3.7.3 16-HBE cell viability after 6 hours and 24 hours of culture with bacteria and hydrogels without ciprofloxacin

A major difference in 16-HBE cell viability was observed between the 6-hour and 24-hour culture timepoints with the bacteria (Figure 26). After 6 hours, the majority of 16-HBE cells were observed to be viable for all culture conditions. After 24 hours, 16-HBE cell viability was varied between *P. aeruginosa* monocultures, *S. aureus* monocultures, and *P. aeruginosa* and *S. aureus* co-cultures. For the *S. aureus* monoculture conditions after 24 hours of culture, the 16-HBE cells remained adhered to the bottom of the well but cell viability was poor with the majority of cells being non-viable. For *P. aeruginosa* monoculture conditions after 24 hours of culture, there were almost no remaining 16-HBE cells on the bottom of the well. For *P. aeruginosa* and *S. aureus* co-culture conditions after 24 hours of culture, there were no viable 16-HBE cells remaining. While the 16-HBE cells within these conditions did not stain red with the live/dead staining assay, the entire area containing 16-HBE cells (as opposed to only the nuclei of each cell)

stained blue with the Hoechst 33342 stain and there were some localized regions of more intense staining (Figure 27). Additionally, the morphology of the 16-HBE cells after incubation in the co-culture conditions was significantly different from controls with a lack of thickness and very little distinction between individual cells. For each bacteria culture condition, 16-HBE cell viability did not appear different between the healthy mucus-like hydrogel culture and the CF mucus-like hydrogel culture.

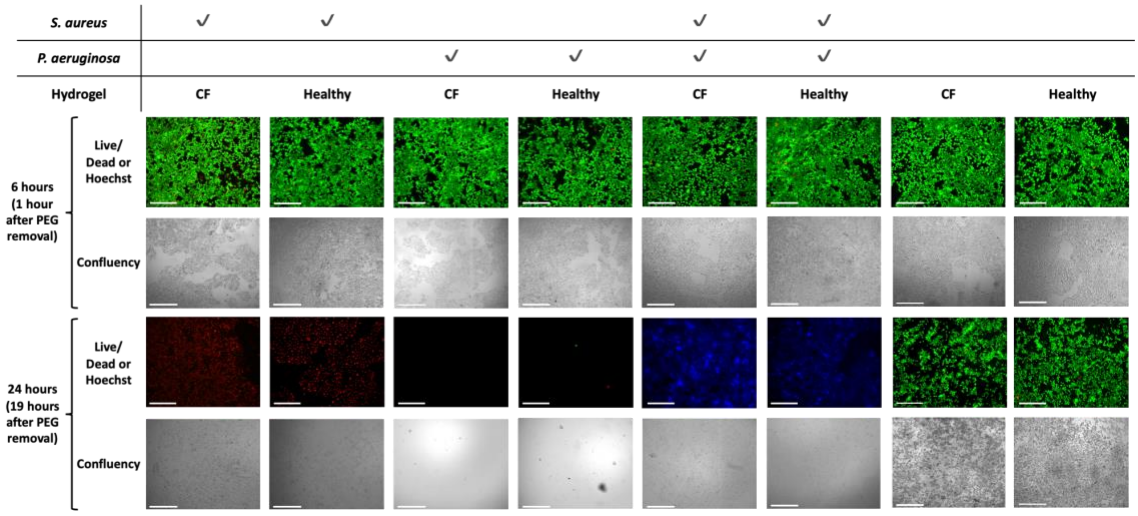

Figure 26: 16-HBE cell viability and overall adherence after 6 and 24 hours culture with *P. aeruginosa* and *S. aureus* in monoculture and in co-culture. No ciprofloxacin was included in this experiment. Live/dead assay with calcein AM and ethidium homodimer-1 and DNA staining with Hoechst 33342 performed after 6 and 24 hours of culture. Green cells are viable and red cells are non-viable. Images captured on EVOS™ FL Auto 2 Imaging System using GFP, RFP, and DAPI channels. Hoechst DNA stain (blue) is presented in conditions where cellular material is remaining but is not staining green or red. Scale bar = 275 μm for fluorescent images (live/dead or Hoechst). Scale bar = 650 μm for cell confluency images.

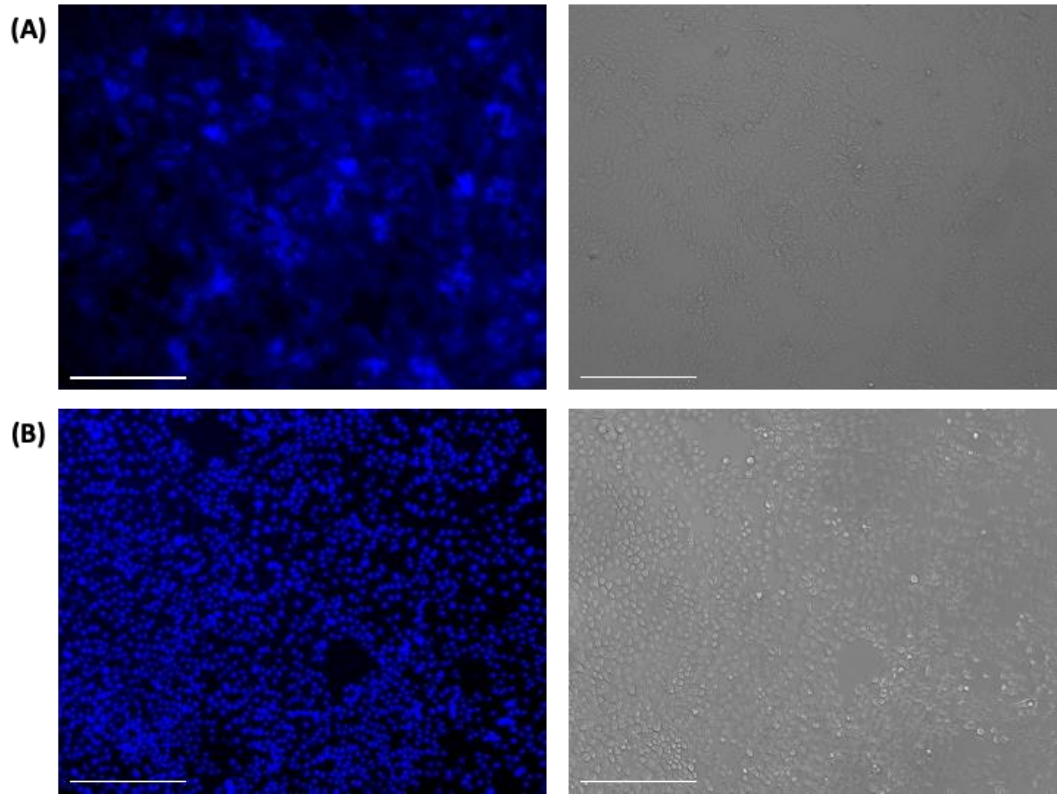

Figure 27: Comparison of Hoechst 33342 stain on 16-HBE cells cultured with *P. aeruginosa*/*S. aureus* for 24 hours and 16-HBE cells cultured with cell culture medium for 24 hours. (A) 16-HBE cells stained with Hoechst 33342 after being cultured with *P. aeruginosa* and *S. aureus* for 24 hours. The Hoechst stain appeared to stain the entire cell-containing surface blue with some areas of concentration. 16-HBE cells cultured under these conditions did not stain green or red with the live/dead assay. **(B)** 16-HBE cells stained with Hoechst 33342 after being cultured with cell culture medium only for 24 hours. For 16-HBE cells cultured under these conditions, individual nuclei were stained with Hoechst and the majority of cells stained green with the live/dead assay. Representative images chosen for each condition.

3.8 Bacteria growth and 16-HBE cell viability within healthy and CF airway models

Bacteria growth and 16-HBE cell viability were also assessed for the healthy and CF airway models. For these models, the healthy and CF mucus-like hydrogels were overlaid on top of a layer of 16-HBE cells. A 5-hour confined monoculture and co-culture of *P. aeruginosa* and *S. aureus* was deposited over top of the mucus-like hydrogels using an

ATPS. Ciprofloxacin was then added to the cultures at a concentration of 0.5 μg/ml and, after 43 additional hours, the concentration of viable bacteria within the liquid and hydrogel phases of the cultures was determined. 16-HBE cell viability was also assessed for each culture condition after the total culture period.

3.8.1 Viable *Pseudomonas aeruginosa* within liquid and hydrogel phases of healthy and CF airway models after 48 hours of culture

After 48 hours of total growth within the healthy and CF airway models, *P. aeruginosa* susceptibility to ciprofloxacin was varied (Figure 28). In monoculture, the concentration of viable *P. aeruginosa* was generally higher within the healthy airway model. This is the opposite trend to what was observed for *P. aeruginosa* grown in the same conditions with no 16-HBE cells. While the average monoculture *P. aeruginosa* concentration within the CF hydrogel was similar with and without 16-HBE cells, the average monoculture *P. aeruginosa* concentration within the healthy hydrogel appeared to increase with the inclusion of 16-HBE cells. In co-culture with *S. aureus*, the concentration of viable *P. aeruginosa* was generally higher within the CF airway model, which was consistent with the trend observed for the same condition with no 16-HBE cells. Additionally, the concentration of viable *P. aeruginosa* within the liquid phase of the co-culture with *S. aureus* was less than all other conditions, with two of the three biological replicates having no viable *P. aeruginosa* within this phase. The concentration of viable *P. aeruginosa* in co-culture with *S. aureus* within both the healthy and the CF hydrogel also appeared to decrease by approximately 10-fold with the addition of 16-HBE cells. The differences in viable *P. aeruginosa* concentration between the CF and healthy conditions were not statistically significant. Results from individual biological

replicates were plotted to demonstrate trends in relative growth between the models despite differences in growth magnitude between replicates.

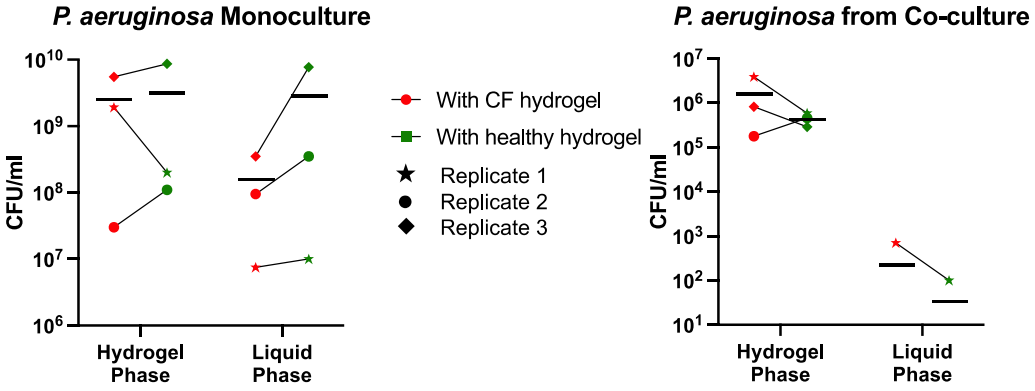

Figure 28: Concentration of viable *P. aeruginosa* (CFU/ml) grown in monoculture and co-culture within the healthy and CF airway models for 48 hours in the presence of 0.5 µg/ml ciprofloxacin. *P. aeruginosa* grown in monoculture on the left and *P. aeruginosa* grown in co-culture with *S. aureus* on the right. The values from each biological replicate are indicated by a different icon and horizontal black bars represent the mean (n = 3). Values from *P. aeruginosa* grown with the CF and healthy hydrogels from the same biological replicate are connected by a line. Any missing icons or lines passing through the x-axis indicate a value of zero.

3.8.2 Viable *Staphylococcus aureus* within liquid and hydrogel phases of healthy and CF airway models after 48 hours of culture

After 48 hours of total growth within the healthy and CF airway models, *S. aureus* appeared to show more resistance to ciprofloxacin within the CF airway model (Figure 29). In monoculture, the concentration of viable *S. aureus* was generally higher within the CF airway model, although one replicate showed the opposite of this trend with a much higher concentration within the healthy airway model. This trend was consistent with the same condition with no 16-HBE cells. In co-culture with *P. aeruginosa*, the concentration of viable *S. aureus* was higher in the CF airway model for all conditions. The differences in viable *S. aureus* concentration between the CF and healthy conditions were not statistically significant. Results from individual biological replicates were plotted to

demonstrate trends in relative growth between the models despite differences in growth magnitude between replicates.

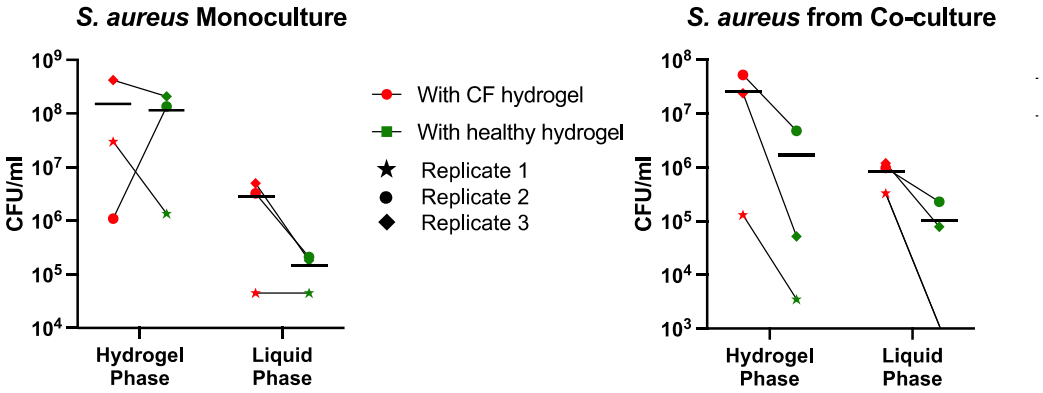

Figure 29: Concentration of viable *S. aureus* (CFU/ml) grown in monoculture and co-culture within the healthy and CF airway models for 48 hours in the presence of 0.5 µg/ml ciprofloxacin. *S. aureus* grown in monoculture on the left and *S. aureus* grown in co-culture with *P. aeruginosa* on the right. The values from each biological replicate are indicated by a different icon and horizontal black bars represent the mean (n = 3). Values from *S. aureus* grown with the CF and healthy hydrogels from the same biological replicate are connected by a line. Any missing icons or lines passing through the x-axis indicate a value of zero.

3.8.3 16-HBE cell viability after culture within healthy and CF airway models for 48 hours

16-HBE cell viability after culture within the healthy and CF airway models for 48 hours was varied between biological replicates (Figure 30). 16-HBE cell viability appeared to be poorest for the *S. aureus* monoculture conditions, with two out of three biological replicates having no viable 16-HBE cells remaining. For the first biological replicate of the *S. aureus* monoculture condition, overall cell coverage was reduced for the CF model relative to the healthy model. For the *P. aeruginosa* monoculture conditions, 16-HBE viability was high and was similar for the CF and healthy models but 16-HBE confluency varied between the two models. 16-HBE cell coverage appeared to be reduced for the CF model for two of the three biological replicates of the *P.*

aeruginosa monoculture. For the *P. aeruginosa* and *S. aureus* co-culture conditions, cell viability was high for two of the three biological replicates with the third replicate showing poor viability with regions of viable cells. Cell viability and coverage was similar for the co-culture CF and healthy models.

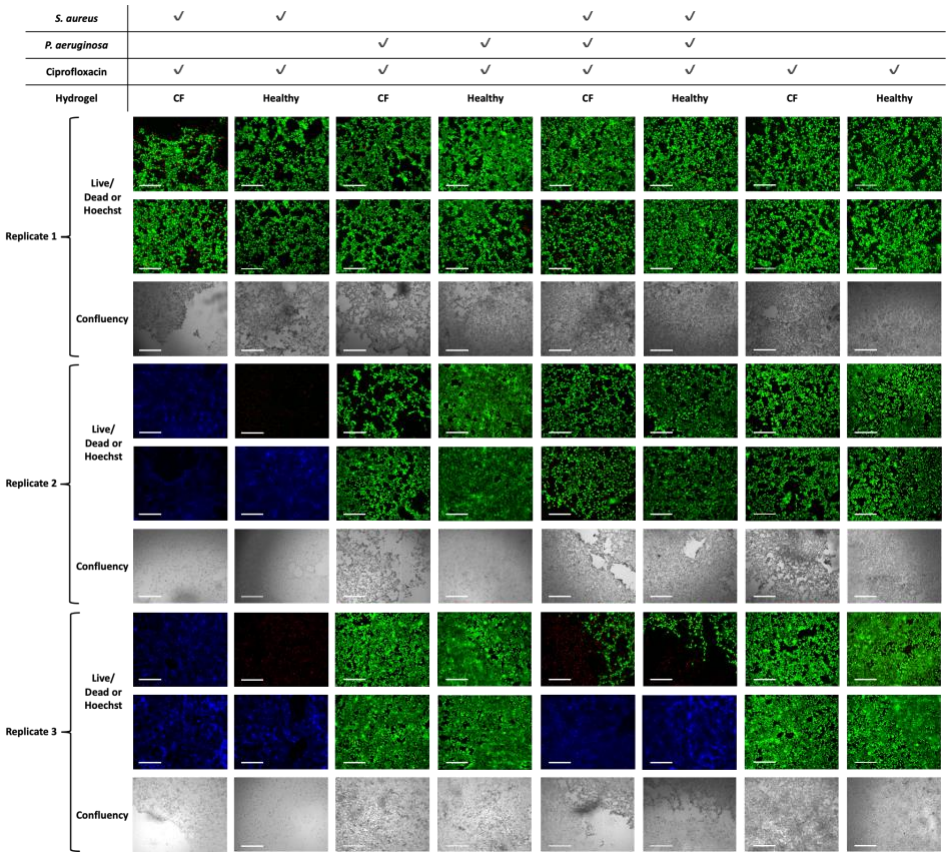

Figure 30: 16-HBE cell viability and overall adherence after culture within the CF and healthy airway models. Conditions included *S. aureus* monoculture, *P. aeruginosa* monoculture, *P. aeruginosa* and *S. aureus* co-culture, and models with no bacteria. All conditions were exposed to 0.5 μg/ml ciprofloxacin. Live/dead assay with calcein AM and ethidium homodimer-1 and DNA staining with Hoechst 33342 performed after 48 hours of culture. Green cells are viable and red cells are non-viable. Images captured on EVOS™ FL Auto 2 Imaging System using GFP, RFP, and DAPI channels. Hoechst DNA stain (blue) presented in conditions where cellular material is remaining but is not staining green or red. Images from three biological replicates presented individually to capture variation between trials. Representative images selected from each replicate. Scale bar = 275 μm for fluorescent images (live/dead or Hoechst). Scale bar = 650 μm for cell confluency images.

CHAPTER 4. Discussion

Airway mucus acts as a protective barrier for the respiratory system by collecting and clearing harmful pathogens from the airways [2], [3]. In CF, the airway epithelial surface is dehydrated which causes airway mucus to become more viscoelastic with increased solids and mucin protein concentrations [7], [8], [18]–[20]. These altered airway mucus properties impair mucus clearance mechanisms such as mucociliary clearance and cough [29]–[32]. Impaired mucus clearance in CF leads to mucus layer thickening and chronic airway infections as opportunistic pathogens, such as *P. aeruginosa* and *S. aureus*, colonize the stagnant airway mucus. Pathogens that infect the airways of CF patients are also prone to developing resistance to antibiotics which makes these infections increasingly difficult to treat [55], [56]. Respiratory function decline due to chronic airway infections is the leading cause of mortality in CF patients [57] which emphasizes the importance of investigating microbe-microbe and host-microbe interactions in these airway infections. Limitations with *in vivo* animal models of CF airway infections create the need for *in vitro* models of the CF airway microenvironment. Current *in vitro* models of the CF airway include only one or two of the main elements of this microenvironment, such as microbes/airway cells or microbes/mucus. These models lack the combined components required to capture complex interactions within the CF airway microenvironment. The research outlined in this thesis involved the development of CF and healthy mucus-like hydrogels which capture the relative differences in viscoelastic properties and component concentrations seen in CF and healthy airway mucus. These mucus-like hydrogels were combined with human bronchial epithelial cells, relevant CF pathogens, and a common CF antibiotic to observe host-microbe and microbe-microbe

interactions in response to some of the key differences between the CF and healthy airway microenvironments.

4.1 Mucus-like hydrogel crosslinking method and gel-forming components impacted 16-HBE cell viability

When developing the mucus-like hydrogels, one of the main components included were mucins as these are one of the major solids components of healthy and CF airway mucus. Although these proteins are known to give airway mucus its characteristic viscoelastic properties, commercially available mucins do not have gel-forming ability on their own [20], [99], [100]. For this reason, a gel-forming component was necessary to achieve these viscoelastic properties. The use of natural materials was explored due to their general compatibility with mammalian cells and microbes. While investigating which gel-forming component should be the base of the mucus-like hydrogels, it was determined that HA-based hydrogels and $CaCO_3$/GDL-crosslinked alginate hydrogels containing mucins were not compatible with 16-HBE cells. Both types of hydrogels yielded particularly poor 16-HBE cell viability when mucins were incorporated into the hydrogels at both high and low mucin concentrations (Figure 6, Figure 7, and Figure 8). A major difference between these hydrogels and the $CaCl_2$-crosslinked alginate hydrogels was their apparent stiffness. The $CaCl_2$-crosslinked alginate hydrogels form a very soft, lightly crosslinked hydrogel while the $CaCO_3$/GDL-crosslinked alginate hydrogels and the HA hydrogels formed much more solid and stiff hydrogels (based on visual assessment and physical assessment with a pipette tip). This greater hydrogel stiffness

may indicate increased crosslinking and a correspondingly decreased hydrogel mesh size which can hinder diffusion through the hydrogel [133].

Both healthy and CF airway mucus have been shown to act as a barrier to diffusion. The diffusion of nanoparticles in airway mucus is restricted, with larger nanoparticles being immobilized within the mucus matrix and smaller nanoparticles diffusing slowly [26]. Diffusion is reduced further in CF airway mucus relative to healthy airway mucus, which is likely due to the increased solids content in CF airway mucus [26], [134]. In addition to airway mucus, mucus-like hydrogels have also been shown to act as a barrier to diffusion of drugs and nanoparticles [7], [103], [104]. Mucin interactions contribute to the barrier properties of mucus and mucus-like hydrogels, both due to physical size filtering and due to adhesive interactions within the mucin network [26], [135], [136]. It is possible that the barrier properties of mucin proteins within the mucus-like hydrogels, in combination with the increased stiffness of the HA-based and $CaCO_3$/GDL-crosslinked alginate hydrogels, created an increased barrier to diffusion. This may have limited diffusion of the nutrients from the cell culture medium above the hydrogels to the 16-HBE cells beneath the hydrogels, resulting in poor 16-HBE cell viability. These 16-HBE cell viability issues were not observed for the $CaCl_2$-crosslinked alginate hydrogels containing mucins. Due to this compatibility with 16-HBE cells, twelve $CaCl_2$-crosslinked alginate hydrogel formulations were considered potential mucus-like hydrogels and were further investigated by measuring their viscoelastic properties.

4.2 Viscoelastic properties of potential mucus-like hydrogels were dependent on component concentrations

Viscoelastic properties, such as the storage and loss moduli, are obtained through oscillatory testing and are commonly used to characterize healthy and pathologic airway mucus samples in literature. The storage (or elastic) modulus describes the elastic response of a material to deformation, which is the deformation energy that is stored within the material structure [137]. The loss (or viscous) modulus describes the viscous response of a material to deformation, which is the energy that is dissipated during material deformation due to molecular motion and internal friction [137]. The storage and loss moduli were measured for each of the twelve potential mucus-like hydrogel formulations, which included combinations of 1% and 1.5% (w/v) alginate, 0.5 and 0.6 mg/ml $CaCl_2$, and 0%, 1%, and 4% (w/v) mucins (Table 1). The 0% mucin formulations were included to compare how the presence of mucins within the hydrogels impacts the hydrogel behavior while the 1% and 4% (w/v) mucin formulations were considered potential healthy and CF mucus-like hydrogels, respectively. These mucin concentrations were chosen to capture the relative difference between healthy and CF airway mucus [8]. They were also chosen to increase the overall solids concentration of the mucus-like hydrogels to better mimic the solids concentration within healthy and CF mucus while maintaining a small number of components within the hydrogels.

The storage and loss moduli of the potential mucus-like hydrogel formulations were influenced by crosslinker, alginate, and mucin concentration. When the concentration of $CaCl_2$ crosslinker was increased, the viscoelastic moduli of the hydrogels tended to increase (Table 2). The relative increase in properties was slightly greater for the storage

modulus of the hydrogels compared to the increase in loss modulus. Larger viscoelastic moduli with increased crosslinker concentration was expected as increasing the crosslinker concentration results in a greater number of calcium ions available to form crosslinks between alginate strands [133]. These crosslinks are formed through the positively charged calcium ions replacing sodium ions within the sodium alginate solution and forming ionic bonds between the negatively charged alginate side groups. The greater amount of crosslinking increases the ability for the hydrogel to resist deformation through storage of the deformation energy which increases the storage modulus of the hydrogel [137]. The observed increase in loss modulus may be due to the larger amount of molecules within the hydrogel which dissipate energy during deformation [137]. This trend has also been observed for other $CaCl_2$-crosslinked alginate systems [133], [138].

An additional trend related to crosslinker concentration that was observed was that the relative increase in viscoelastic moduli with increasing crosslinker concentration was generally lower for hydrogels with higher mucin concentrations. For example, the average storage and loss moduli of hydrogel formulations containing 0% mucins and 1% alginate increased approximately 2.2-fold and 1.9-fold, respectively, with a 0.1 mg/ml increase in $CaCl_2$ concentration. Conversely, the average storage and loss moduli of hydrogel formulations containing 4% mucins and 1% alginate increased 1.6-fold and 1.3-fold, respectively, with a 0.1 mg/ml increase in $CaCl_2$ concentration. This may be explained by interactions between mucins and calcium ions from the $CaCl_2$ crosslinker. In the airway, calcium ions interact with mucin strands by binding to mucins, forming crosslinks between mucin chains, and causing mucin compaction, all due to the

polyanionic nature of mucin proteins [4], [6]. Ca^{2+} has been found to form reversible crosslinks between mucin polymers [139] and the binding of Ca^{2+} to mucins appears to contribute to the aggregation of mucins and mucus gels [140]. These Ca^{2+}-mucin interactions may have occurred in the potential mucus-like hydrogel formulations, particularly in the higher mucin concentration hydrogels. An increase in Ca^{2+}-mucin interactions in these hydrogel formulations would reduce the amount of calcium ions available for alginate crosslinking. Compared to formulations with less mucins or no mucins, this could have reduced the number of crosslinks between the alginate strands and caused an overall lower relative increase in viscoelastic moduli.

When the concentration of alginate within the hydrogels was increased, the storage moduli of the hydrogels were very similar but the loss moduli generally tended to increase (Table 3). This trend was expected as the addition of alginate, with no change in the amount of available $CaCl_2$ crosslinker, leads to more uncrosslinked alginate molecules within the hydrogel. An increase in mobile and uncrosslinked alginate molecule chains can result in a greater dissipation of deformation energy and contribute to an overall greater resistance to deformation, leading to a larger loss modulus [137]. To maintain the viscoelastic moduli with an increase in alginate concentration, the $CaCl_2$ crosslinker concentration must also be increased [138].

The presence of mucins within the mucus-like hydrogels tended to decrease the storage modulus while increasing the loss modulus of the hydrogels (Table 4). The relative decrease in storage modulus was similar when comparing both the 4% and 1% mucin concentration hydrogels to the 0% mucin concentration hydrogels. The relative increase in loss modulus was generally greatest when comparing the 4% mucin

concentration hydrogels to the 0% mucin concentration hydrogels. Taken together, this suggests that the mucin-containing hydrogels have a more viscous response to deformation and that this viscous response is greater when the mucin concentration is increased. These trends could be attributed to the interactions between calcium ions and mucins described above. The decrease in storage modulus with the presence of mucins within the mucus-like hydrogels is likely caused by Ca^{2+} binding to the polyanionic mucin proteins, resulting in a reduction in available Ca^{2+} for alginate crosslinking [4], [6], [141]. The increase in loss modulus with the presence of mucins within the mucus-like hydrogels is likely caused by the increase in mobile mucin chains which result in a greater dissipation of deformation energy and, in turn, a greater loss modulus [137]. Additionally, if there is less Ca^{2+} available for alginate crosslinking, there may be an increase in mobile alginate chains as well which further contributes to the increased loss modulus [137]. Other studies that have looked at the impact of mucins on alginate hydrogel viscoelastic properties have found similar trends [104], [121]. The viscoelastic properties of the twelve potential mucus-like hydrogels, along with the hydrogel compositions, were assessed in combination to choose a healthy and a CF mucus-like hydrogel.

4.3 Chosen healthy and CF mucus-like hydrogels capture important relative differences between healthy and CF airway mucus

The chosen mucus-like hydrogel formulations had differing viscoelastic properties owing to their differing compositions. Gel-E, the healthy mucus-like hydrogel, was composed of 0.5 mg/ml $CaCl_2$ crosslinker, 1.5% alginate, and 1% mucin. Gel-L, the CF

mucus-like hydrogel, was composed of 0.6 mg/ml $CaCl_2$ crosslinker, 1.5% alginate, and 4% mucin. The CF mucus-like hydrogel has both an increased mucin concentration and an increased $CaCl_2$ crosslinker concentration relative to the healthy mucus-like hydrogel. While the increased mucin concentration was desirable to mimic the relative increase in mucin concentration seen in CF airway mucus, the increased $CaCl_2$ crosslinker concentration was necessary to increase the viscoelastic properties of the CF mucus-like hydrogel.

Both of the chosen mucus-like hydrogels showed elastically dominant behavior with storage moduli larger than their respective loss moduli, which is characteristic of airway mucus [24]–[27]. The CF mucus-like hydrogel, Gel-L, also had greater viscoelastic properties than the healthy mucus-like hydrogel, Gel-E, with the average storage and loss moduli of Gel-L at each frequency (between 0.1 and 20 rad/s) being at least 1.6 times greater than Gel-E (Figure 15). While the relative difference varies, CF airway mucus has been found to have greater viscoelastic moduli than healthy airway mucus [19], [20]. Additionally, the viscoelastic properties of the CF and healthy mucus-like hydrogels were within the same order of magnitude as the viscoelastic properties of CF and healthy airway mucus that has been analyzed and reported in literature (Figure 16). The storage and loss moduli of CF and healthy airway mucus were found to be generally within the 0.1 to 100 Pa range with some values exceeding 100 Pa for the storage modulus of CF airway mucus. The average viscoelastic moduli of the CF and healthy mucus-like hydrogels ranged from 4.2 to 36.2 Pa (when measured at angular frequencies of 0.1 to 20 rad/s). There is a large amount of variation in the reported values of airway mucus viscoelastic properties in literature, particularly for CF airway mucus. This is due to a

number of reasons, including differences in disease severity and progression, sample collection techniques, sample preparation and measurement, and data reporting as well as challenges with accessing CF airway mucus samples [18]–[20], [28]. In addition to the viscoelastic properties and mucin concentrations capturing differences between healthy and CF airway mucus, the difference in total solids concentrations of healthy and CF airway mucus was also captured. The total solids concentrations of the healthy and CF mucus-like hydrogels were 2.6% and 5.6% (w/v) respectively, which are comparable to the solids concentrations of healthy and CF airway mucus [7], [8]. The differences in viscoelastic properties, mucin concentration, and solids concentration between the CF and healthy mucus-like hydrogels represent key differences observed between CF and healthy airway mucus. For future validation of the mucus-like hydrogels, the properties of the CF mucus-like hydrogel can be tuned to represent a more specific state of CF airway mucus and the properties can be compared to collected patient samples.

4.4 Bacteria growth is mainly on top of or within the hydrogel phase when cultured short-term using an ATPS

Prior to incorporating ciprofloxacin into the airway models, it was desirable to first establish a confined bacteria culture over top of and within the mucus-like hydrogels. This was to discourage initial planktonic bacteria growth and to encourage the bacteria to colonize the mucus-like hydrogels. An ATPS was used for the short-term (5-hour) bacteria culture establishment by suspending the bacteria in the DEX-rich phase of the ATPS and then depositing a small droplet of this bacteria-containing DEX-rich phase into the PEG-rich phase of the ATPS over top of the mucus-like hydrogels. As the DEX-rich

phase is denser than the PEG-rich phase, the DEX-rich phase droplet containing bacteria was expected to settle onto the mucus-like hydrogels, providing a surface for bacteria growth establishment [142], [143]. The mammalian cell compatibility of PEG/DEX ATPS and the ability for a PEG/DEX ATPS to confine bacteria growth for prolonged timepoints has previously been demonstrated [121], [144], [145].

It was expected that the use of an ATPS for bacteria deposition would confine the bacteria to grow on top of or within the hydrogel for the short-term (5-hour) culture. Preliminary experiments without hydrogels had shown the ability for *P. aeruginosa* CF18 at the same seeding density to remain contained within an ATPS for at least 6 hours (Figure 17). The containment of *S. aureus* ATCC 6538 within an ATPS at the same seeding density had also been previously investigated by another student and confirmed for longer timepoints. While these preliminary investigations did not include a hydrogel component, the addition of a hydrogel did not appear to impact bacteria containment for the short-term culture. Bacteria containment could not be confirmed visually after 5 hours as the mucins within the mucus-like hydrogels caused the hydrogels to be opaque, preventing the use of microscopy imaging. Containment was instead confirmed by measuring the concentration of viable bacteria within the liquid PEG-rich phase and the hydrogel phase of the culture after 5 hours. For all growth conditions, including *P. aeruginosa* and *S. aureus* in both monoculture and co-culture, the majority of viable bacteria was found to be collected with the hydrogel phase (Figure 18 and Figure 19). This suggests that either the bacteria remained confined within the DEX-rich phase of the ATPS and grew on top of the hydrogel, or that the bacteria grew into the hydrogel phase. Confirming that the upper liquid PEG-rich phase of the ATPS could be removed without

removing the majority of the bacteria from the system was an important step prior to incorporating cell culture medium containing ciprofloxacin into the system.

4.5 16-HBE cell viability is impacted by bacteria growth behavior within the airway models in the absence and presence of ciprofloxacin

The viability of 16-HBE cells was assessed for multiple culture conditions, including within the healthy and CF airway models with and without ciprofloxacin. This involved the 5-hour bacteria culture establishment over the hydrogels, as described above, and then the removal of the upper liquid PEG-rich phase of the ATPS which was replaced with either cell culture medium alone or with cell culture medium that was supplemented with 0.5 μg/ml ciprofloxacin.

When the 16-HBE cells were cultured within the healthy and CF airway models without ciprofloxacin, their viability was assessed after 6 hours and 24 hours (1 hour and 19 hours, respectively, after removal of the upper liquid PEG-rich phase of the ATPS). After 6 hours of culture, the majority of 16-HBE cells were observed to be viable for *P. aeruginosa* and *S. aureus* monoculture and co-culture conditions in both the healthy and CF airway models (Figure 26). This is possibly due to bacteria growth being partially confined to the DEX-rich phase of the ATPS and on top of the hydrogels for the first 5 hours of culture. After the ATPS was disassembled by removing the PEG-rich phase and adding cell culture medium in its place, there were no longer two immiscible liquid phases due to the lack of PEG [143]. It is then likely that the DEX-rich phase of the ATPS became incorporated into the cell culture medium and that bacteria growth was no longer confined. At the 6-hour culture timepoint, it appears that the 1 hour of growth after

removal of the upper liquid PEG-rich phase of the ATPS was not enough time for the bacteria to affect 16-HBE cell viability. Conversely, 16-HBE cell viability was significantly impacted at the 24-hour culture timepoint for all conditions, although no differences were observed between the healthy and CF models for each condition (Figure 26). There were almost no viable 16-HBE cells remaining for any culture conditions at this timepoint, possibly due to the large increase in concentrations of viable bacteria. Between the 6-hour and 24-hour timepoints, the concentration of monoculture and co-culture *P. aeruginosa* increased at least 1700-fold for all culture conditions (Figure 22 and Figure 23). The concentration of *S. aureus* in monoculture was less extreme, with increases of at least 10-fold in the hydrogel phase and at least 2-fold in the liquid phase (Figure 24 and Figure 25). Interestingly, *S. aureus* in co-culture had very similar hydrogel-phase concentrations at the 6-hour and 24-hour timepoints, and after 24 hours of culture, there was no viable *S. aureus* detected in the liquid phases. For the co-culture, it appears as though *P. aeruginosa* inhibited the growth of *S. aureus* in the hydrogel phase and may have outcompeted *S. aureus* in the liquid phase. A decrease in planktonic *S. aureus* has been seen for other co-cultures of *S. aureus* and *P. aeruginosa*, although these studies have also observed a decrease in *S. aureus* biofilm [81], [83]. As these studies were conducted with no mucus-like component within their co-culture systems, their observed reduction in *S. aureus* biofilm formation may not be predictive of the co-culture behavior within the mucus-like hydrogels. The survival of *S. aureus* within the hydrogel phases of the co-cultures could have been due to the mucus-like hydrogel providing a network for spatially organized growth, which has been observed for the two species coexisting in an *in vitro* CF model containing SCFM [146] as well as for the two

species in chronic wounds [147]. Additionally, some *P. aeruginosa* isolates have been shown to better co-exist with *S. aureus* in reduced oxygen concentrations, like that of the mucus-like hydrogel [87]. It is also possible that the *P. aeruginosa* and *S. aureus* formed dual-species biofilms within the mucus-like hydrogels, which is known to occur within CF airway mucus and has been observed *in vitro* [84], [148].

Although 16-HBE cells were non-viable for all of the culture conditions at the 24-hour timepoint with no ciprofloxacin, cell morphology and staining differed between *P. aeruginosa* monoculture, *S. aureus* monoculture, and *P. aeruginosa* and *S. aureus* co-culture conditions at this timepoint. For the *P. aeruginosa* monoculture conditions, all 16-HBE cells had detached from the surface of the wells. Other *in vitro* studies have found that *P. aeruginosa* causes epithelial cell detachment in as short as 3 hours of culture [113], [149]–[151]. The type II and type III secretion systems have both been implicated in *P. aeruginosa* virulence and host cell cytotoxicity [151]–[153] and 16-HBE cell detachment observed in the 24-hour *P. aeruginosa* monoculture was likely due to toxins secreted by these systems. For *S. aureus* monoculture conditions, the 16-HBE cells remained adhered but were non-viable. This could have been due to potential epithelial cell internalization and subsequent intracellular replication of *S. aureus*, which have been found to cause host cell cytotoxicity including the induction of apoptosis [154]–[156]. For the *P. aeruginosa* and *S. aureus* co-culture conditions, 16-HBE cells remained adhered but did not stain red or green in the live/dead assay. They did, however, stain blue with the Hoechst 33342 DNA stain over the entire surface of cell coverage (Figure 27). As bacteria can also be stained with Hoechst 33342 [157], it is possible that this is indicative of mass cell destruction and that a portion of the excessive DNA staining from

the *P. aeruginosa* and *S. aureus* co-culture conditions could be stained adherent bacteria. Research has not yet elucidated the mechanisms of host cell death when co-infected with *P. aeruginosa* and *S. aureus*, but based on the difference in 16-HBE morphology and staining observed in the co-culture conditions compared to the monoculture conditions, it appears as though interactions between the two species alters their virulence and behavior. For example, internalization of *S. aureus* into cells from an alveolar epithelial cell line (A549) has been found to increase almost 3-fold when *S. aureus* was co-cultured with *P. aeruginosa* relative to when it was grown in monoculture [158]. Overall, 16-HBE cells did not survive in any of the culture conditions after 24 hours with no ciprofloxacin, likely due to the uninhibited growth of the bacteria.

When the 16-HBE cells were grown within the airway models in the presence of 0.5 μg/ml ciprofloxacin, their viability was assessed after 48 hours of culture (Figure 30). The incorporation of ciprofloxacin into the airway models altered both bacteria growth behavior (which will be discussed in the following section) and 16-HBE cell viability. While 16-HBE cell viability was observed to be very poor after 24 hours within all culture conditions with no ciprofloxacin, the inclusion of 0.5 μg/ml ciprofloxacin resulted in varied 16-HBE cell viability and increased cell survival after 48 hours. 16-HBE cell viability did not appear to differ significantly between the healthy and CF models but did differ between bacteria culture conditions. For the *S. aureus* monoculture conditions there were no viable 16-HBE cells remaining for two of the three biological replicates, and for the *P. aeruginosa* and *S. aureus* co-culture conditions, there were no viable 16-HBE cells remaining for one of the three biological replicates. For these conditions with no viable 16-HBE cells remaining, portions of the 16-HBE cells stained red to indicate that they

were non-viable, but the majority of the 16-HBE cells stained blue with the Hoechst 33342 stain over the entire surface of the cells (rather than just the nuclei). This was also observed for the 24-hour *P. aeruginosa* and *S. aureus* co-culture conditions with no ciprofloxacin, as discussed above, and may partially be due to staining of adherent bacteria on the surface of the cells. The similar Hoechst staining in these conditions may indicate that ciprofloxacin induces altered behavior in *S. aureus* that is comparable to the altered behavior of *S. aureus* when co-cultured with *P. aeruginosa* in these models. This may be due to the concentration of ciprofloxacin that was used. While 0.5 μg/ml ciprofloxacin reduces *S. aureus* growth relative to without ciprofloxacin, this concentration appears to be subinhibitory within the airway models (despite being greater than the MIC when tested in conditions without the mucus-like hydrogels). This subinhibitory concentration could have induced changes in *S. aureus*, such as increased virulence and toxin secretion, which has been found to occur with *S. aureus* and other antibiotics [159]. *S. aureus* virulence genes related to biofilm formation, cytotoxicity, and stress response have also been found to be more expressed in co-culture with *P. aeruginosa* [84], which may explain why similar modes of 16-HBE killing were observed when *S. aureus* was cultured with *P. aeruginosa* or exposed to a subinhibitory concentration of ciprofloxacin. The subinhibitory concentration of ciprofloxacin could also be causing the variation and inconsistency observed for 16-HBE cell viability between biological replicates of *S. aureus* culture conditions, as 16-HBE cell viability was observed to be high for some biological replicates of *S. aureus* monoculture and co-culture conditions within the airway models. For the *P. aeruginosa* monoculture, 16-HBE cell viability was much more consistent and appeared to be relatively high for all three

biological replicates, although 16-HBE cell attachment was generally reduced within the CF airway model. This cell detachment indicates that there was likely some 16-HBE killing by *P. aeruginosa* [113], [149]–[151] but to a lesser extent than what was observed in the airway models with no ciprofloxacin. The inclusion of 0.5 μg/ml ciprofloxacin within the airway models provided some control of bacteria growth which resulted in variable cell viability depending on bacteria species.

4.6 Bacteria grown in monoculture show differential responses to ciprofloxacin in the healthy and CF airway models

The growth of *P. aeruginosa* and *S. aureus* in monoculture in the presence of ciprofloxacin was assessed within the healthy and CF airway models with and without 16-HBE cells. This involved the 5-hour bacteria culture establishment over the hydrogels, followed by the removal of the upper liquid PEG-rich phase of the ATPS which was replaced with cell culture medium that was supplemented with 0.5 μg/ml ciprofloxacin and cultured for 43 hours. Although differences in bacteria viability between the CF and healthy model were not found to be statistically significant, trends in relative growth between the two models were observed.

When there were no 16-HBE cells included within the airway models, *P. aeruginosa* in monoculture tended to have a greater resistance to ciprofloxacin within the CF model (Figure 20). *P. aeruginosa* cultured within mucus-mimetic hydrogels *in vitro* has been found to form aggregates that behave similarly to biofilms and are capable of attaching to mucins and other hydrogel matrix surfaces, rather than to a solid surface, and these aggregates have shown an increased resistance to antibiotics [101], [160]. *P. aeruginosa*

biofilms and aggregates are also known to form within CF airways *in vivo* [42]. As mucus-like hydrogels with a higher mucin concentration have been found to promote the formation of *P. aeruginosa* aggregates [116], [161], it is possible that aggregates formed more readily within the CF airway model, leading to a greater ciprofloxacin tolerance. A number of studies have found that mucins inhibit *P. aeruginosa* biofilm formation and surface attachment [72], [73], [95], [162] but this may be due to *P. aeruginosa* cells and cellular aggregates binding to mucins rather than the underlying culture surface [17], [50], [101]. In contrast to the findings that mucins inhibit *P. aeruginosa* biofilm formation, *P. aeruginosa* biofilms have been formed within HBE derived mucus *in vitro* and mucus with greater solids content resulted in stronger, more robust biofilms [48].

When 16-HBE cells were included within the airway models, *P. aeruginosa* in monoculture tended to show greater resistance to ciprofloxacin when grown within the healthy airway model, although the average concentration of viable *P. aeruginosa* within the hydrogels was very similar for the healthy and CF models (Figure 28). Along with this trend, the average growth of *P. aeruginosa* within the healthy model appeared to increase with the addition of 16-HBE cells while the average growth of *P. aeruginosa* within the CF model was similar with and without 16-HBE cells. Other airway model studies have also reported changes in *P. aeruginosa* behavior when grown on lung epithelial cells or an abiotic surface, such as altered gene expression or an increase in antibiotic tolerance [150], [151]. A potential cause of observed increased *P. aeruginosa* growth in the healthy model in the presence of 16-HBE cells could be the influence of epithelial cell metabolites [163], [164]. While host-microbe metabolic interactions in CF airway infections have yet to be fully understood due to the complex and polymicrobial

nature of these infections, there is evidence that the effectiveness of antibiotics can be modulated by host metabolites [165]. Some host metabolites, such as lactate, have also been found to act as potential carbon sources for *P. aeruginosa* [166]. As the healthy mucus-like hydrogel has a lower protein content, it is possible that *P. aeruginosa* could better access these metabolites within the healthy mucus-like hydrogels due to a reduction in protein-protein interactions. It may have been more difficult for host metabolites to diffuse through the higher mucin concentration CF mucus-like hydrogel, which has been seen for other molecules [136].

S. aureus grown in monoculture tended to show greater resistance to ciprofloxacin within the CF airway model, both with and without the inclusion of 16-HBE cells, although the average concentration of viable *S. aureus* within the hydrogels was very similar for the healthy and CF models containing 16-HBE cells (Figure 21 and Figure 29). It has been established that *S. aureus* adheres to mucins through surface protein interactions between *S. aureus* adhesins and mucin receptors [167]–[170]. Surface attachment is known to be the first step of *S. aureus* biofilm formation, which is then followed by the production of a protective biofilm matrix and microcolony growth, and ultimately the release of bacterial cells to further colonize the microenvironment [171]. As there is a greater concentration of mucins within the CF mucus-like hydrogel, this may have resulted in greater *S. aureus* biofilm formation within the CF airway model due to the increased number of attachment sites. As with other species of bacteria, the antibiotic resistance of *S. aureus* is increased when grown in biofilms relative to planktonically grown cells [62]. Additionally, *S. aureus* has been found to grow in aggregates with increased antibiotic tolerance within the mucus-like layer of an *ex vivo*

porcine CF model [118]. These results indicate that *S. aureus* grown within the CF airway model may have had a greater potential for biofilm or aggregate growth compared to the healthy airway model, leading to a greater resistance to ciprofloxacin. While the overall trend in the majority of biological replicates was greater ciprofloxacin resistance for *S. aureus* grown within the CF airway model, there was variation in the relative growth within the two models. This variation may be due to the potentially subinhibitory concentration of ciprofloxacin used, as discussed in the previous section.

4.7 Bacteria grown in co-culture show differential responses to ciprofloxacin in the healthy and CF airway models

The growth of *P. aeruginosa* and *S. aureus* was also assessed in co-culture in the presence of ciprofloxacin within the healthy and CF airway models with and without 16-HBE cells. Similarly to above, this involved the 5-hour bacteria culture establishment over the hydrogels, followed by the removal of the upper liquid PEG-rich phase of the ATPS which was replaced with cell culture medium supplemented with 0.5 μg/ml ciprofloxacin and cultured for 43 hours. Although differences in bacteria viability between the CF and healthy model were not found to be statistically significant, trends in relative growth between the two models were observed.

When *P. aeruginosa* was grown in co-culture with *S. aureus*, it tended to have a greater resistance to ciprofloxacin within the CF airway model, both with and without 16-HBE cells (Figure 20 and Figure 28). This trend was also observed between the healthy and CF conditions of *P. aeruginosa* in monoculture without 16-HBE cells and could similarly be attributed to possible *P. aeruginosa* aggregate formation. Additionally, the

presence of *S. aureus* in co-culture may have enhanced the ability for *P. aeruginosa* to form antibiotic tolerant aggregates or biofilms, as seen in other studies with *P. aeruginosa* co-cultured with *S. aureus* or with *S. aureus* exoproducts [78], [148]. As discussed above, these aggregates or biofilms are also likely to form in structured, mucin-rich microenvironments [101], [160]. An additional observation of *P. aeruginosa* growth within the co-culture airway model conditions was the lack of viable *P. aeruginosa* within the majority of the liquid phases of the models. The liquid phases of the co-culture healthy airway model with no 16-HBE cells and of the co-culture CF and healthy airway models with 16-HBE cells contained very little viable *P. aeruginosa*. This lack of viable *P. aeruginosa* within the co-culture condition liquid phases may be related to the oxygen availability within the models. Decreased oxygen availability has been observed for *P. aeruginosa* and *S. aureus* in co-culture relative to the two species in monoculture [172]. As previously discussed, reduced oxygen levels can lead to phenotypic changes in *P. aeruginosa* that are also observed in biofilm formation, such as increased alginate production [17]. In addition, ciprofloxacin diffusion through airway mucus has been found to be significantly decreased compared to a liquid control (PBS) [101]. Potential changes to *P. aeruginosa* due to oxygen availability within the *P. aeruginosa* and *S. aureus* co-culture conditions, combined with a possible reduction in diffusion of ciprofloxacin into the hydrogel phase, may have driven *P. aeruginosa* to preferentially colonize the hydrogel phases of the co-culture conditions.

The presence of 16-HBE cells within the co-culture also appeared to cause a reduction in *P. aeruginosa* viability. When co-cultured with *S. aureus*, the concentration of viable *P. aeruginosa* in the healthy and CF hydrogel phases was reduced

approximately 10-fold when 16-HBE cells were included within the model. This observation could be attributed to the presence of antimicrobial peptides (AMPs) produced by epithelial cells, such as human β-defensins (hBDs), The expression of hBDs by epithelial cells can be induced by a number of factors including bacteria and bacteria endotoxins [173]. Some hBDs have shown greater activity against Gram-negative bacteria while others have been found to be active against both Gram-positive and Gram-negative bacteria [174], [175]. 16-HBE cells have shown the ability to produce hBDs and have been found to increase expression of hBDs in the presence of *Aspergillus fumigatus*, a respiratory infection-causing fungus [176]. This reduction in *P. aeruginosa* viability with the addition of 16-HBE cells was not observed for *P. aeruginosa* in monoculture. The presence of *S. aureus* within the co-culture may have resulted in greater expression of hBDs, as *S. aureus* has been found to increase expression of epithelial hBD-2 *in vitro* [177]. hBD-2 has been implicated in a reduction in *P. aeruginosa* biofilm formation [178]. These AMPs may have also had a role in the decrease in liquid phase *P. aeruginosa* observed for the co-culture condition of the CF model.

When *S. aureus* was grown in co-culture with *P. aeruginosa*, its response to ciprofloxacin within the airway models was altered by the presence of 16-HBE cells. When no 16-HBE cells were included within the models, *S. aureus* tended to show a greater resistance to ciprofloxacin within the healthy airway model, although this response showed notable inconsistency between biological replicates (Figure 21). This may be a further indication that 0.5 μg/ml of ciprofloxacin is subinhibitory for *S. aureus* when grown within the airway models, leading to changes in *S. aureus* behavior that appear to vary for each biological replicate. When 16-HBE cells were included within the

co-culture models, *S. aureus* tended to show a greater resistance to ciprofloxacin within the CF airway model, and this trend was more consistent than what was observed with no 16-HBE cells (Figure 29). *S. aureus* surface proteins have been shown to be more expressed in co-culture with *P. aeruginosa*, resulting in greater binding to surfaces [79]. There could have been a greater prevalence of *S. aureus* biofilm formation within the CF airway model due to the increased amount of hydrogel matrix and component surfaces for attachment. The increased resistance of *S. aureus* to ciprofloxacin within the co-culture CF airway model could also be attributed to the possible formation of dual-species biofilms with *P. aeruginosa*. Studies have found that *S. aureus* is capable of forming dual-species biofilms with *P. aeruginosa in vitro* [148], [179]. Magalhães et al. showed that *S. aureus* was less susceptible to ciprofloxacin within these dual-species biofilms with *P. aeruginosa* [179].

An additional trend observed for the co-culture model conditions was that *P. aeruginosa* CF18 and *S. aureus* ATCC 6538 appeared to coexist within the airway models with neither species being eradicated in co-culture. The complex relationship between *P. aeruginosa* and *S. aureus* has been found to be simultaneously mutually beneficial and antagonistic, and this relationship has also been found to vary between strains [180]. While *P. aeruginosa* is known to secrete anti-staphylococcal proteins *in vitro* which cause a reduction in *S. aureus* viability, the influence of these products on *S. aureus* is typically assessed without the presence of a mucus-like component [81], [180]. The mucus-like hydrogels within the airway models may have interacted with these products or influenced altered bacteria gene expression and, therefore, promoted coexistence between the two species. Similar interactions have been seen in other studies,

where mucus and mucins have been found to decrease the activity of antibiotics [181] and the presence of exogenous alginate has been found to protect *S. aureus* from *P. aeruginosa* due to the downregulation of virulence factors [182]. Another possible interaction between the mucus-like hydrogels and products secreted by *P. aeruginosa* is the iron content within porcine gastric mucins (PGM), one of the primary components of the mucus-like hydrogels [183]. The high iron content within PGM has been found to contribute to a decrease in *P. aeruginosa* production of rhamnolipids and siderophores, both of which are virulence factors [183]. This may have been implicated in the coexistence of *P. aeruginosa* and *S. aureus* observed within the airway models.

Despite their coexistence, the magnitudes of mean viable *P. aeruginosa* and *S. aureus* concentrations within the airway models tended to be lower in co-culture relative to monoculture for both species with the same concentration of ciprofloxacin. Magalhães et al. found the opposite trend, with an increased or similar concentration of viable *P. aeruginosa* and *S. aureus* in co-culture in the presence of ciprofloxacin with no mucus-like component [179]. While they assessed the impact of ciprofloxacin on mono- and dual-species biofilms that were grown on tissue culture plastic for 48 hours prior to exposure, the airway models within this project had a much shorter 5-hour colony establishment period with the hydrogels prior to ciprofloxacin exposure. Based on this comparison, the reduced growth within the co-culture airway models relative to the monoculture airway models may indicate that *P. aeruginosa* and *S. aureus* in co-culture were less established within the mucus-like hydrogels during the 5-hour colony establishment period, making them more vulnerable to ciprofloxacin. Tognon et al. found that genetic adaptations of *P. aeruginosa* and *S. aureus* have been observed as early as 3

hours after co-culture, with up-regulation in genes related to nutrient competition and shifts in metabolism and down-regulation in many virulence factors [172]. It is possible that, during the 5-hour colony establishment period within the airway models, *P. aeruginosa* and *S. aureus* may have been adapting genetically to the co-culture microenvironment as observed by Tognon et al., while in monoculture they may have had increased virulence with the ability to better colonize the hydrogel during this time period.

4.8 CF airway model exhibits features characteristic of chronic CF airway infection

Despite the varied ciprofloxacin resistance observed between the healthy and CF airway models, the CF airway model demonstrated multiple features characteristic of chronic CF airway infections. One of the features of chronic CF airway infections is an increased tolerance to antibiotics. The ciprofloxacin MIC was determined to be 0.125 μg/ml for *P. aeruginosa* and *S. aureus* monoculture and co-culture without the presence of a mucus-like hydrogel or mammalian cells. *P. aeruginosa* and *S. aureus*, in monoculture and co-culture, remained viable for 48 hours within the CF airway model in the presence of 0.5 μg/ml ciprofloxacin, a concentration 4-fold greater than the MIC. An additional feature of chronic CF airway infections is altered or reduced virulence of *P. aeruginosa* which influences interactions between *P. aeruginosa* and *S. aureus*. *P. aeruginosa* strains isolated from long-term chronically infected patients have been shown to have a greater ability to co-exist with *S. aureus in vitro* relative to reference strains or early-adapted strains [80], [83]. Many models lack the ability to capture the coexistence of *P. aeruginosa* and *S. aureus in vitro* while the two are known to co-infect CF patient

airways *in vivo* [34], [106]. In contrast, the CF airway model was able to sustain *P. aeruginosa* and *S. aureus* in co-culture for 48 hours and mammalian cells within the co-culture model remained viable for two out of three biological replicates.

The longevity of the CF airway model is also a feature of its chronicity, as the 48-hour culture period demonstrated with the model surpasses the culture periods achieved in other *in vitro* CF airway infection models. Current *in vitro* CF airway infection models only demonstrate microbe-mammalian culture for short time periods, generally ranging from 2 up to 24 hours [114], [151], [158], [184], [185]. In addition to sustained monoculture and co-culture bacteria growth over 48 hours, this model also has the ability to maintain 16-HBE cell viability over this culture period, as demonstrated for culture conditions with *P. aeruginosa* in monoculture as well as for some biological replicates of *S. aureus* in monoculture and *P. aeruginosa* and *S. aureus* in co-culture. Biological variation appeared to supersede the inhibition ability of this concentration of ciprofloxacin for some biological replicates. With increased ciprofloxacin concentrations, it is possible that more consistent 16-HBE cell survival could be achieved. Nonetheless, the increased culture period achieved for the CF airway model in this study is beneficial to its use for studying longer term growth behavior of CF pathogens.

It is also notable that alginate, one of the main components of the mucus-like hydrogels, is a major exopolysaccharide produced by mucoid *P. aeruginosa* during CF chronic infections [186], [187]. The presence of alginate within the mucus-like hydrogels may have enhanced the chronicity of the model by protecting the bacteria. For example, an alginate-overproducing strain of *P. aeruginosa* has been found to form biofilms with increased antibiotic tolerance relative to biofilms formed by a nonmucoid strain of *P.*

aeruginosa [66]. Additionally, the presence of alginate has been found to mitigate *P. aeruginosa* killing of *S. aureus in vitro*, implying that alginate may have a role in the coexistence of the two species [182].

CHAPTER 5. Conclusions

5.1 Limitations and Future Directions

The mucus-like hydrogels developed in this research have relative differences representative of some of the key differences between CF and healthy airway mucus, and these hydrogels have been shown to influence the growth behavior of relevant CF pathogens in the presence of an antibiotic, both with and without the incorporation of human bronchial epithelial cells. This research also has limitations, some of which have prompted future directions for the project. One of the limitations of the airway models is their lack of imageability due to the mucin component within the mucus-like hydrogels. The mucins cause the mucus-like hydrogels to be opaque, resulting in the inability to use transmission light microscopy to visualize bacteria or mammalian cell growth throughout the culture period. For this reason, all mammalian cell microscopy imaging was performed at experiment endpoints, once the mucus-like hydrogels were removed from the system. In future investigations, bacteria could be labelled with fluorescent proteins and fluorescence imaging techniques could be performed to visualize bacteria within the mucus-like hydrogels during culture. This could provide information about their spatial organization and aggregate formation within the mucus-like hydrogels, which has been found to differ in co-culture [97], [146]. Visualization of the bacteria within the models could also provide more information on the variation observed between biological replicates, as their spatial organization may differ between the healthy and CF mucus-like hydrogels.

An additional limitation of this research was the use of only one strain of each species of bacteria. Literature has shown that there is variation in gene expression and behavior

between different strains of *P. aeruginosa* and *S. aureus* [62], [188]. *P. aeruginosa* and *S. aureus* co-culture interactions, including their ability to compete or coexist, have also been shown to be strain dependent [83], [158], [180]. In the future, additional strains of *P. aeruginosa* and *S. aureus* with well-defined behavior should also be grown within the airway models to assess whether the results from this research are unique to the strains used. Additionally, differences between colony phenotypes were not discerned for this study but future work should focus on confirming the existence of phenotypic changes within the models, such as the presence of small colony variants.

Another limitation of this research is that the simplified composition of the mucus-like hydrogels lack a number of the components found in CF airway mucus, such as DNA and lipids [92]. For this research, the focus was not on recapitulating the composition of CF airway mucus but was instead on observing how changes in the mucus-like hydrogels (that are reflective of relative differences found between CF and healthy airway mucus) would impact bacteria growth in the presence of a CF antibiotic. Future studies with these models should consider incorporating an additional component into the mucus-like hydrogels while maintaining the total solids concentrations of each hydrogel. This could be achieved by reducing the mucin concentration within the healthy and CF mucus-like hydrogels but keeping the same relative difference in mucin concentration between the two hydrogels. A reduction in mucin concentrations within the hydrogels, without compromising the overall solids concentrations, could also be beneficial as commercially available PGM has been found to have an influence on *P. aeruginosa* virulence [183]. Despite this potential influence, the use of commercially available PGM within the models is still recommended for future work as the collection and purification of native

mucins (typically obtained from pig stomachs) is both cost- and labour-prohibitive [183]. Additionally, the growth behavior of bacteria in the presence of an antibiotic within these models was limited to ciprofloxacin at one concentration. Future studies investigating the growth behavior and antibiotic resistance of bacteria within these models should investigate the effects of a range of ciprofloxacin concentrations. *P. aeruginosa* and *S. aureus* exposed to increased concentrations of ciprofloxacin have been found to have differing susceptibilities when in monoculture or co-culture depending on the culture conditions and model [189], [190]. Testing a range of ciprofloxacin concentrations would provide more information on antibiotic resistance of the bacteria grown within the models and could potentially reduce variation between biological replicates due to growth inhibition. Relevant CF antibiotics from other antibiotic classes, such as aminoglycosides like gentamicin and tobramycin, should also be tested within the airway models, as *P. aeruginosa* and *S. aureus* would likely respond differently to antibiotics with differing mechanisms of action. For example, gentamicin has been found to be more effective than ciprofloxacin against co-culture biofilms formed by *P. aeruginosa* and *S. aureus* [190].

Finally, the relative nature of this study also imposes limits on the model. The healthy and CF mucus-like hydrogels lack many of the components and biochemical characteristics of physiological airway mucus. The healthy and CF mucus-like hydrogels do, however, possess relative differences representing some of the altered properties between healthy and CF airway mucus. This approach allows for observation of how specific changes in mucus-like hydrogel properties impact bacteria response to antibiotics. Future validation of the CF airway model will require identification of model limits, including clear definitions of patient state of disease being modeled. For example,

whether the CF mucus-like hydrogel within the model is representing a completely plugged airway or a thickened airway mucus layer. Result reproducibility will also need to be improved prior to model validation. This will require greater characterization of the CF mucus-like hydrogel to assess for hydrogel homogeneity as well as batch-to-batch variation. This will also require the assessment of bacteria responses to ranges of antibiotic concentrations and antibiotics of different classes within the model, as previously mentioned. A potential validation strategy for potential use in antimicrobial drug discovery is that the drug diffusion properties of the mucus-like hydrogels could be measured and validated against collected patient samples.

5.2 Conclusions

In this research project, mucus-like hydrogels were developed which capture key relative differences between CF and healthy airway mucus, including increased mucin and solids concentrations as well as increased viscoelastic properties. This research showed that the altered properties of these mucus-like hydrogels can influence the growth behavior and antibiotic tolerance of *P. aeruginosa* and *S. aureus* in monoculture and co-culture *in vitro* systems. As the CF mucus-like hydrogel did not always result in a greater bacterial resistance to antibiotics compared to the healthy mucus-like hydrogel, the relative differences in select properties between the CF and healthy mucus-like hydrogels may not have been enough to consistently elicit this behavior. Other features of the complex CF airway microenvironment that were not included within the airway models, such as an immune component, also likely have a contribution to the behavior of *P. aeruginosa* and *S. aureus in vivo*. Nonetheless, the mucus-like hydrogels developed in

this research project can serve as a base for investigating the influence of altered CF airway mucus properties on bacteria antibiotic tolerance. In addition, the CF mucus-like hydrogel showed the ability to capture aspects of chronic infection behavior in the CF airway model.

The results of this research demonstrate that the growth and behavior of *P. aeruginosa* and *S. aureus* within an *in vitro* airway model can be influenced by changes in composition and physical properties, as well as by the presence of mammalian cells. The inclusion of mucus-like hydrogels within *in vitro* CF airway models represents an important step towards better understanding the complex microbe-microbe and host-microbe interactions in the CF airway microenvironment. Additionally, the ability for these models to support co-culture growth of *P. aeruginosa* and *S. aureus* is an important feature as they are commonly known to coexist within CF patient airways *in vivo*. The hydrogels developed in this project can also be adapted to observe how altered mucus properties and composition in other states of disease impact bacteria growth behavior and antibiotic tolerance. Overall, this study demonstrates that mucus-like hydrogels can be incorporated into microbe-mammalian co-culture systems and that the properties and composition of the hydrogel have an influence on bacteria behavior and antibiotic resistance. This study also shows that an *in vitro* CF airway model, with the inclusion of a CF mucus-like hydrogel, is able to capture a number of characteristics of chronic CF airway infection such as antibiotic tolerance and sustained polymicrobial growth.

References

[1] S. K. Lai, Y. Y. Wang, D. Wirtz, and J. Hanes, "Micro- and macrorheology of mucus," *Adv. Drug Deliv. Rev.*, vol. 61, no. 2, pp. 86–100, 2009, doi: 10.1016/j.addr.2008.09.012.

[2] C. E. Wagner, K. M. Wheeler, and K. Ribbeck, "Mucins and their role in shaping the functions of mucus barriers," *Annu. Rev. Cell Dev. Biol.*, vol. 34, pp. 189–215, 2018, doi: 10.1146/annurev-cellbio-100617-0628181.

[3] J. V. Fahy and B. F. Dickey, "Airway mucus function and dysfunction," *N. Engl. J. Med.*, vol. 363, no. 23, pp. 2233–2247, 2010, doi: 10.1056/nejmra0910061.

[4] D. J. Thornton, K. Rousseau, and M. A. McGuckin, "Structure and function of the polymeric mucins in airways mucus," *Annu. Rev. Physiol.*, vol. 70, pp. 459–486, 2008, doi: 10.1146/annurev.physiol.70.113006.100702.

[5] M. R. Knowles and R. C. Boucher, "Mucus clearance as a primary innate defense mechanism for mammalian airways," *J. Clin. Invest.*, vol. 109, no. 5, pp. 571–577, 2002, doi: 10.1172/JCI0215217.

[6] C. B. Morrison, M. R. Markovetz, and C. Ehre, "Mucus, mucins, and cystic fibrosis," *Pediatr. Pulmonol.*, vol. 54, no. S3, pp. S84–S96, 2019, doi: 10.1002/ppul.24530.

[7] D. B. Hill *et al.*, "A biophysical basis for mucus solids concentration as a candidate biomarker for airways disease," *PLoS One*, vol. 9, no. 2, pp. 1–11, 2014, doi: 10.1371/journal.pone.0087681.

[8] A. G. Henderson *et al.*, "Cystic fibrosis airway secretions exhibit mucin hyperconcentration and increased osmotic pressure," *J. Clin. Invest.*, vol. 124, no. 7, pp. 3047–3060, 2014, doi: 10.1172/JCI73469.

[9] R. Bansil and B. S. Turner, "Mucin structure, aggregation, physiological functions and biomedical applications," *Curr. Opin. Colloid Interface Sci.*, vol. 11, no. 2–3, pp. 164–170, 2006, doi: 10.1016/j.cocis.2005.11.001.

[10] C. Werlang, G. Cárcarmo-Oyarce, and K. Ribbeck, "Engineering mucus to study and influence the microbiome," *Nat. Rev. Mater.*, vol. 4, no. 2, pp. 134–145, 2019, doi: 10.1038/s41578-018-0079-7.

[11] R. Bansil and B. S. Turner, "The biology of mucus: Composition, synthesis and organization," *Adv. Drug Deliv. Rev.*, vol. 124, pp. 3–15, 2018, doi: 10.1016/j.addr.2017.09.023.

[12] D. Song, D. Cahn, and G. A. Duncan, “Mucin biopolymers and their barrier function at airway surfaces,” *Langmuir*, vol. 36, no. 43, pp. 12773–12783, 2020, doi: 10.1021/acs.langmuir.0c02410.

[13] T. Crouzier *et al.*, “Modulating mucin hydration and lubrication by deglycosylation and polyethylene glycol binding,” *Adv. Mater. Interfaces*, vol. 2, no. 18, pp. 1–7, 2015, doi: 10.1002/admi.201500308.

[14] S. Kirkham, J. K. Sheehan, D. Knight, P. S. Richardson, and D. J. Thornton, “Heterogeneity of airways mucus: Variations in the amounts and glycoforms of the major oligomeric mucins MUC5AC and MUC5B,” *Biochem. J.*, vol. 361, no. 3, pp. 537–546, 2002, doi: 10.1042/0264-6021:3610537.

[15] R. A. Cone, “Barrier properties of mucus,” *Adv. Drug Deliv. Rev.*, vol. 61, no. 2, pp. 75–85, 2009, doi: 10.1016/j.addr.2008.09.008.

[16] S. Kotnala, A. Dhasmana, V. K. Kashyap, S. C. Chauhan, M. M. Yallapu, and M. Jaggi, “A bird eye view on cystic fibrosis: An underestimated multifaceted chronic disorder,” *Life Sci.*, vol. 268, no. December 2020, p. 118959, 2021, doi: 10.1016/j.lfs.2020.118959.

[17] D. Worlitzsch *et al.*, “Effects of reduced mucus oxygen concentration in airway Pseudomonas infections of cystic fibrosis patients,” *J. Clin. Invest.*, vol. 109, no. 3, pp. 317–325, 2002, doi: 10.1172/JCI0213870.

[18] P. R. Burgel, D. Montani, C. Danel, D. J. Dusser, and J. A. Nadel, “A morphometric study of mucins and small airway plugging in cystic fibrosis,” *Thorax*, vol. 62, no. 2, pp. 153–161, 2007, doi: 10.1136/thx.2006.062190.

[19] R. Ghanem *et al.*, “Apparent yield stress of sputum as a relevant biomarker in cystic fibrosis,” *Cells*, vol. 10, no. 11, 2021, doi: 10.3390/cells10113107.

[20] M. Völler *et al.*, “An optimized protocol for assessment of sputum macrorheology in health and muco-obstructive lung disease,” *Front. Physiol.*, no. August, pp. 1–11, 2022, doi: 10.3389/fphys.2022.912049.

[21] N. N. Sanders, S. C. De Smedt, E. Van Rompaey, P. Simoens, F. De Baets, and J. Demeester, “Cystic fibrosis sputum: A barrier to the transport of nanospheres,” *Am. J. Respir. Crit. Care Med.*, vol. 162, no. 5, pp. 1905–1911, 2000, doi: 10.1164/ajrccm.162.5.9909009.

[22] K. A. Ramsey *et al.*, “Airway mucus hyperconcentration in non–cystic fibrosis bronchiectasis,” *Am. J. Respir. Crit. Care Med.*, vol. 201, no. 6, pp. 661–670, 2020, doi: 10.1164/rccm.201906-1219OC.

[23] A. A. Pezzulo *et al.*, "Reduced airway surface pH impairs bacterial killing in the porcine cystic fibrosis lung," *Nature*, vol. 487, no. 7405, pp. 109–113, 2012, doi: 10.1038/nature11130.

[24] H. Nielsen, S. Hvidt, C. A. Sheils, and P. A. Janmey, "Elastic contributions dominate the viscoelastic properties of sputum from cystic fibrosis patients," *Biophys. Chem.*, vol. 112, no. 2-3 SPEC. ISS., pp. 193–200, 2004, doi: 10.1016/j.bpc.2004.07.019.

[25] M. Dawson, D. Wirtz, and J. Hanes, "Enhanced viscoelasticity of human cystic fibrotic sputum correlates with increasing microheterogeneity in particle transport," *J. Biol. Chem.*, vol. 278, no. 50, pp. 50393–50401, 2003, doi: 10.1074/jbc.M309026200.

[26] B. S. Schuster, J. Soo, G. F. Woodworth, and J. Hanes, "Nanoparticle diffusion in respiratory mucus from humans without lung disease," *Biomaterials*, vol. 34, no. 13, pp. 3439–3446, 2013, doi: 10.1016/j.biomaterials.2013.01.064.

[27] M. R. Markovetz *et al.*, "Endotracheal tube mucus as a source of airway mucus for rheological study," *Am. J. Physiol. Lung Cell. Mol. Physiol.*, vol. 317, no. 4, pp. L498–L509, 2019, doi: 10.1152/ajplung.00238.2019.

[28] T. Radtke, L. Böni, P. Bohnacker, P. Fischer, C. Benden, and H. Dressel, "The many ways sputum flows – Dealing with high within-subject variability in cystic fibrosis sputum rheology," *Respir. Physiol. Neurobiol.*, vol. 254, no. February, pp. 36–39, 2018, doi: 10.1016/j.resp.2018.04.006.

[29] H. Matsui *et al.*, "Evidence for periciliary liquid layer depletion, not abnormal ion composition, in the pathogenesis of cystic fibrosis airways disease," *Cell*, vol. 95, no. 7, pp. 1005–1015, 1998, doi: 10.1016/S0092-8674(00)81724-9.

[30] B. Button *et al.*, "A periciliary brush promotes the lung health by separating the mucus layer from airway epithelia," *Science (80-.).*, vol. 337, no. 6097, pp. 937–941, 2012, doi: 10.1126/science.1223012.

[31] R. C. Boucher, "Evidence for airway surface dehydration as the initiating event in CF airway disease," *J. Intern. Med.*, vol. 261, no. 1, pp. 5–16, 2007, doi: 10.1111/j.1365-2796.2006.01744.x.

[32] B. Button *et al.*, "Roles of mucus adhesion and cohesion in cough clearance," *Proc. Natl. Acad. Sci. U. S. A.*, vol. 115, no. 49, pp. 12501–12506, 2018, doi: 10.1073/pnas.1811787115.

[33] J. M. Flynn, D. Niccum, J. M. Dunitz, and R. C. Hunter, "Evidence and role for bacterial mucin degradation in cystic fibrosis airway disease," *PLoS Pathog.*, vol. 12, no. 8, pp. 1–21, 2016, doi: 10.1371/journal.ppat.1005846.

[34] Cystic Fibrosis Foundation, “2019 Patient Registry Annual Data Report,” 2020, [Online]. Available: http://www.cff.org/UploadedFiles/research/ClinicalResearch/Patient-Registry-Report-2009.pdf.

[35] S. P. Lopes, N. F. Azevedo, and M. O. Pereira, “Microbiome in cystic fibrosis: Shaping polymicrobial interactions for advances in antibiotic therapy,” *Crit. Rev. Microbiol.*, vol. 41, no. 3, pp. 353–365, 2015, doi: 10.3109/1040841X.2013.847898.

[36] G. B. Rogers, M. P. Carroll, D. J. Serisier, P. M. Hockey, G. Jones, and K. D. Bruce, “Characterization of bacterial community diversity in cystic fibrosis lung infections by use of 16S ribosomal DNA terminal restriction fragment length polymorphism profiling,” *J. Clin. Microbiol.*, vol. 42, no. 11, pp. 5176–5183, 2004, doi: 10.1128/JCM.42.11.5176.

[37] V. Klepac-Ceraj *et al.*, “Relationship between cystic fibrosis respiratory tract bacterial communities and age, genotype, antibiotics and *Pseudomonas aeruginosa*,” *Environ. Microbiol.*, vol. 12, no. 5, pp. 1293–1303, 2010, doi: 10.1111/j.1462-2920.2010.02173.x.

[38] L.-A. J. Ghuneim *et al.*, “Complex and unexpected outcomes of antibiotic therapy against a polymicrobial infection,” *ISME J.*, vol. 16, pp. 2065–2075, 2022, doi: 10.1038/s41396-022-01252-5.

[39] M. J. Cox *et al.*, “Airway microbiota and pathogen abundance in age-stratified cystic fibrosis patients,” *PLoS One*, vol. 5, no. 6, 2010, doi: 10.1371/journal.pone.0011044.

[40] J. Zhao *et al.*, “Decade-long bacterial community dynamics in cystic fibrosis airways,” *Proc. Natl. Acad. Sci. U. S. A.*, vol. 109, no. 15, pp. 5809–5814, 2012, doi: 10.1073/pnas.1120577109.

[41] J. Lam, R. Chan, K. Lam, and J. W. Costerton, “Production of mucoid microcolonies by *Pseudomonas aeruginosa* within infected lungs in cystic fibrosis,” *Infect. Immun.*, vol. 28, no. 2, pp. 546–556, 1980, doi: 10.1128/iai.28.2.546-556.1980.

[42] T. Bjarnsholt *et al.*, “*Pseudomonas aeruginosa* biofilms in the respiratory tract of cystic fibrosis patients,” *Pediatr. Pulmonol.*, vol. 44, no. 6, pp. 547–558, 2009, doi: 10.1002/ppul.21011.

[43] S. J. Gabryszewski *et al.*, “Metabolic Adaptation in Methicillin-Resistant Staphylococcus aureus Pneumonia,” *Am. J. Respir. Cell Mol. Biol.*, vol. 61, no. 2, pp. 185–197, 2019, doi: 10.1165/rcmb.2018-0389OC.

[44] S. Moreau-Marquis, B. A. Stanton, and G. A. O'Toole, "*Pseudomonas aeruginosa* biofilm formation in the cystic fibrosis airway," *Pulm. Pharmacol. Ther.*, vol. 21, no. 4, pp. 595–599, 2008, doi: 10.1016/j.pupt.2007.12.001.

[45] D. E. Moormeier and K. W. Bayles, "*Staphylococcus aureus* biofilm: a complex developmental organism," *Mol. Microbiol.*, vol. 104, no. 3, pp. 365–376, 2017, doi: 10.1111/mmi.13634.

[46] J. W. Costerton, P. S. Stewart, and E. P. Greenberg, "Bacterial biofilms: A common cause of persistent infections," *Science (80-.).*, vol. 284, no. 5418, pp. 1318–1322, 1999, doi: 10.1126/science.284.5418.1318.

[47] J. C. Nickel, I. Ruseska, J. B. Wright, and J. W. Costerton, "Tobramycin resistance of *Pseudomonas aeruginosa* cells growing as a biofilm on urinary catheter material," *Antimicrob. Agents Chemother.*, vol. 27, no. 4, pp. 619–624, 1985, doi: 10.1128/AAC.27.4.619.

[48] K. Rouillard, S. Maloney, W. Kissner, M. Markovetz, M. Schoenfisch, and D. Hill, "Effects of mucin and DNA concentrations in mucus on *Pseudomonas aeruginosa* biofilm recalcitrance," *J. Cyst. Fibros.*, vol. 20, p. S239, 2021, doi: 10.1016/s1569-1993(21)01930-5.

[49] R. T. Rozenbaum, H. C. van der Mei, W. Woudstra, E. D. de Jong, H. J. Busscher, and P. K. Sharma, "Role of viscoelasticity in bacterial killing by antimicrobials in differently grown *Pseudomonas aeruginosa* biofilms," *Am. Soc. Microbiol.*, no. December 2018, pp. 1–11, 2019.

[50] R. M. Landry, D. An, J. T. Hupp, P. K. Singh, and M. R. Parsek, "Mucin-*Pseudomonas aeruginosa* interactions promote biofilm formation and antibiotic resistance," *Mol. Microbiol.*, vol. 59, no. 1, pp. 142–151, 2006, doi: 10.1111/j.1365-2958.2005.04941.x.

[51] K. W. K. Lee, S. Periasamy, M. Mukherjee, C. Xie, S. Kjelleberg, and S. A. Rice, "Biofilm development and enhanced stress resistance of a model, mixed-species community biofilm," *ISME J.*, vol. 8, no. 4, pp. 894–907, 2014, doi: 10.1038/ismej.2013.194.

[52] R. A. Proctor *et al.*, "Small colony variants: A pathogenic form of bacteria that facilitates persistent and recurrent infections," *Nat. Rev. Microbiol.*, vol. 4, no. 4, pp. 295–305, 2006, doi: 10.1038/nrmicro1384.

[53] B. E. Johns, K. J. Purdy, N. P. Tucker, and S. E. Maddocks, "Phenotypic and genotypic characteristics of small colony variants and their role in chronic infection," *Microbiol. Insights*, vol. 8, p. MBI.S25800, 2015, doi: 10.4137/mbi.s25800.

[54] H. Matsui *et al.*, "Reduced three-dimensional motility in dehydrated airway mucus prevents neutrophil dapture and killing bacteria on airway epithelial surfaces," *J. Immunol.*, vol. 175, no. 2, pp. 1090–1099, 2005, doi: 10.4049/jimmunol.175.2.1090.

[55] T. J. Kidd *et al.*, "Defining antimicrobial resistance in cystic fibrosis," *J. Cyst. Fibros.*, vol. 17, no. 6, pp. 696–704, 2018, doi: 10.1016/j.jcf.2018.08.014.

[56] J. F. Chmiel *et al.*, "Antibiotic management of lung infections in cystic fibrosis: I. The microbiome, methicillin-resistant *Staphylococcus aureus*, gram-negative bacteria, and multiple infections," *Ann. Am. Thorac. Soc.*, vol. 11, no. 7, pp. 1120–1129, 2014, doi: 10.1513/AnnalsATS.201402-050AS.

[57] J. M. Beck, V. B. Young, and G. B. Huffnagle, "The microbiome of the lung," *Transl. Res.*, vol. 160, no. 4, pp. 258–266, 2012, doi: 10.1016/j.trsl.2012.02.005.

[58] M. Schwerdt *et al.*, "*Staphylococcus aureus* in the airways of cystic fibrosis patients - A retrospective long-term study," *Int. J. Med. Microbiol.*, vol. 308, no. 6, pp. 631–639, 2018, doi: 10.1016/j.ijmm.2018.02.003.

[59] Cystic Fibrosis Canada, "CCFR 2018 Annual Data Report," pp. 1–30, 2018, [Online]. Available: https://www.cysticfibrosis.ca/de/action/download?downloads=14&file=dl_en-annual-report-web.pdf.

[60] H. Anwar, J. L. Strap, and J. W. Costerton, "Eradication of biofilm cells of *Staphylococcus aureus* with tobramycin and cephalexin," *Can. J. Microbiol.*, vol. 38, no. 7, pp. 618–925, 1992, doi: 10.1139/m92-102.

[61] G. A. Tramper-Stranders, T. F. W. Wolfs, A. Fleer, J. L. L. Kimpen, and C. K. Van Der Ent, "Maintenance azithromycin treatment in pediatric patients with cystic fibrosis: Long-term outcomes related to macrolide resistance and pulmonary function," *Pediatr. Infect. Dis. J.*, vol. 26, no. 1, pp. 8–12, 2007, doi: 10.1097/01.inf.0000247109.44249.ac.

[62] E. Kamble and K. Pardesi, "Antibiotic tolerance in biofilm and stationary-phase planktonic cells of *Staphylococcus aureus*," *Microb. Drug Resist.*, vol. 27, no. 1, pp. 3–12, 2021, doi: 10.1089/mdr.2019.0425.

[63] H. Moisan, E. Brouillette, C. L. Jacob, P. Langlois-Bégin, S. Michaud, and F. Malouin, "Transcription of virulence factors in *Staphylococcus aureus* small-colony variants isolated from cystic fibrosis patients is influenced by SigB," *J. Bacteriol.*, vol. 188, no. 1, pp. 64–76, 2006, doi: 10.1128/JB.188.1.64-76.2006.

[64] E. Kamali, A. Jamali, A. Ardebili, F. Ezadi, and A. Mohebbi, “Evaluation of antimicrobial resistance, biofilm forming potential, and the presence of biofilm-related genes among clinical isolates of *Pseudomonas aeruginosa*,” *BMC Res. Notes*, vol. 13, no. 1, pp. 4–9, 2020, doi: 10.1186/s13104-020-4890-z.

[65] D. Hill *et al.*, “Antibiotic susceptibilities of *Pseudomonas aeruginosa* isolates derived from patients with cystic fibrosis under aerobic, anaerobic, and biofilm conditions,” *J. Clin. Microbiol.*, vol. 43, no. 10, pp. 5085–5090, 2005, doi: 10.1128/JCM.43.10.5085-5090.2005.

[66] M. Hentzer *et al.*, “Alginate overproduction affects *Pseudomonas aeruginosa* biofilm structure and function,” *J. Bacteriol.*, vol. 183, no. 18, pp. 5395–5401, 2001, doi: 10.1128/JB.183.18.5395-5401.2001.

[67] N. Mayer-Hamblett *et al.*, “*Pseudomonas aeruginosa* in vitro phenotypes distinguish cystic fibrosis infection stages and outcomes,” *Am. J. Respir. Crit. Care Med.*, vol. 190, no. 3, pp. 289–297, 2014, doi: 10.1164/rccm.201404-0681OC.

[68] I. Bianconi *et al.*, “Persistence and microevolution of *Pseudomonas aeruginosa* in the cystic fibrosis lung: A single-patient longitudinal genomic study,” *Front. Microbiol.*, vol. 9, p. 3242, 2019, doi: 10.3389/fmicb.2018.03242.

[69] A. M. Sousa, R. Monteiro, and M. O. Pereira, “Unveiling the early events of *Pseudomonas aeruginosa* adaptation in cystic fibrosis airway environment using a long-term *in vitro* maintenance,” *Int. J. Med. Microbiol.*, vol. 308, no. 8, pp. 1053–1064, 2018, doi: 10.1016/j.ijmm.2018.10.003.

[70] S. Häußler, B. Tümmler, H. Weissbrodt, M. Rohde, and I. Steinmetz, “Small-colony variants of *Pseudomonas aeruginosa* in cystic fibrosis,” *Clin. Infect. Dis.*, vol. 29, pp. 621–5, 1999.

[71] S. Häußler *et al.*, “Highly adherent small-colony variants of *Pseudomonas aeruginosa* in cystic fibrosis lung infection,” *J. Med. Microbiol.*, vol. 52, no. 4, pp. 295–301, 2003, doi: 10.1099/jmm.0.05069-0.

[72] J. Y. Co *et al.*, “Mucins trigger dispersal of *Pseudomonas aeruginosa* biofilms,” *npj Biofilms Microbiomes*, vol. 4, no. 1, pp. 1–8, 2018, doi: 10.1038/s41522-018-0067-0.

[73] C. L. Haley, C. Kruczek, U. Qaisar, J. A. Colmer-Hamood, and A. N. Hamood, “Mucin inhibits *Pseudomonas aeruginosa* biofilm formation by significantly enhancing twitching motility,” *Can. J. Microbiol.*, vol. 60, no. 3, pp. 155–166, 2014, doi: 10.1139/cjm-2013-0570.

[74] C. Carnoy, A. Scharfman, E. Van Brussel, G. Lamblin, R. Ramphal, and P. Roussel, "*Pseudomonas aeruginosa* outer membrane adhesins for human respiratory mucus glycoproteins," *Infect. Immun.*, vol. 62, no. 5, pp. 1896–1900, 1994, doi: 10.1128/iai.62.5.1896-1900.1994.

[75] J. Emerson, M. Rosenfeld, S. McNamara, B. Ramsey, and R. L. Gibson, "*Pseudomonas aeruginosa* and other predictors of mortality and morbidity in young children with cystic fibrosis," *Pediatr. Pulmonol.*, vol. 34, no. 2, pp. 91–100, 2002, doi: 10.1002/ppul.10127.

[76] M. R. Kosorok *et al.*, "Acceleration of lung disease in children with cystic fibrosis after *Pseudomonas aeruginosa* acquisition," *Pediatr. Pulmonol.*, vol. 32, no. 4, pp. 277–287, 2001, doi: 10.1002/ppul.2009.abs.

[77] A. J. Fischer *et al.*, "Sustained Coinfections with *Staphylococcus aureus* and *Pseudomonas aeruginosa* in Cystic Fibrosis," *Am. J. Respir. Crit. Care Med.*, vol. 203, no. 3, pp. 328–338, 2021, doi: 10.1164/rccm.202004-1322OC.

[78] T. Beaudoin *et al.*, "*Staphylococcus aureus* interaction with *Pseudomonas aeruginosa* biofilm enhances tobramycin resistance," *npj Biofilms Microbiomes*, vol. 3, no. 1, pp. 1–8, 2017, doi: 10.1038/s41522-017-0035-0.

[79] A. Kumar and Y. P. Ting, "Presence of *Pseudomonas aeruginosa* influences biofilm formation and surface protein expression of *Staphylococcus aureus*," *Environ. Microbiol.*, vol. 17, no. 11, pp. 4459–4468, 2015, doi: 10.1111/1462-2920.12890.

[80] C. F. Michelsen, A. M. J. Christensen, M. S. Bojer, N. Høiby, H. Ingmer, and L. Jelsbak, "*Staphylococcus aureus* alters growth activity, autolysis, and antibiotic tolerance in a human host-adapted *Pseudomonas aeruginosa* lineage," *J. Bacteriol.*, vol. 196, no. 22, pp. 3903–3911, 2014, doi: 10.1128/JB.02006-14.

[81] L. M. Filkins *et al.*, "Coculture of *Staphylococcus aureus* with *Pseudomonas aeruginosa* drives *S. aureus* towards fermentative metabolism and reduced viability in a cystic fibrosis model," *J. Bacteriol.*, vol. 197, no. 14, pp. 2252–2264, 2015, doi: 10.1128/JB.00059-15.

[82] M. K. Wieneke *et al.*, "Association of diverse *Staphylococcus aureus* populations with *Pseudomonas aeruginosa* coinfection and inflammation incystic fibrosis airway infection," *Am. Soc. Microbiol.*, vol. 6, no. 3, pp. e00358-21, 2021, doi: 10.1128/ mSphere.00358-21.

[83] R. Baldan *et al.*, "Adaptation of *Pseudomonas aeruginosa* in cystic fibrosis airways influences virulence of *Staphylococcus aureus in vitro* and murine models of co-infection," *PLoS One*, vol. 9, no. 3, 2014, doi: 10.1371/journal.pone.0089614.

[84] A. P. Magalhães, T. Grainha, A. M. Sousa, Â. França, N. Cerca, and M. O. Pereira, "Viable but non-cultivable state: a strategy for *Staphylococcus aureus* survivable in dual-species biofilms with *Pseudomonas aeruginosa*?," *Environ. Microbiol.*, vol. 23, no. 9, pp. 5639–5649, 2021, doi: 10.1111/1462-2920.15734.

[85] L. Camus *et al.*, "Trophic cooperation promotes bacterial survival of *Staphylococcus aureus* and *Pseudomonas aeruginosa*," *ISME J.*, vol. 14, no. 12, pp. 3093–3105, 2020, doi: 10.1038/s41396-020-00741-9.

[86] P. W. Woods, Z. M. Haynes, E. G. Mina, and C. N. H. Marques, "Maintenance of *S. aureus* in co-culture with *P. aeruginosa* while growing as biofilms," *Front. Microbiol.*, vol. 9, p. 3291, 2019, doi: 10.3389/fmicb.2018.03291.

[87] R. Pallett, L. J. Leslie, P. A. Lambert, I. Milic, A. Devitt, and L. J. Marshall, "Anaerobiosis influences virulence properties of *Pseudomonas aeruginosa* cystic fibrosis isolates and the interaction with *Staphylococcus aureus*," *Sci. Rep.*, vol. 9, p. 6748, 2019, doi: 10.1038/s41598-019-42952-x.

[88] D. D. Sriramulu, H. Lünsdorf, J. S. Lam, and U. Römling, "Microcolony formation: A novel biofilm model of *Pseudomonas aeruginosa* for the cystic fibrosis lung," *J. Med. Microbiol.*, vol. 54, no. 7, pp. 667–676, 2005, doi: 10.1099/jmm.0.45969-0.

[89] C. L. Haley, J. A. Colmer-Hamood, and A. N. Hamood, "Characterization of biofilm-like structures formed by *Pseudomonas aeruginosa* in a synthetic mucus medium," *BMC Microbiol.*, vol. 12, p. 181, 2012, doi: 10.1186/1471-2180-12-181.

[90] P. Jaikumpun, K. Ruksakiet, and É. P, "Antibacterial effects of bicarbonate in media modified to mimic cystic fibrosis sputum," *Int. J. Mol. Sci.*, vol. 21, p. 8614, 2020, doi: doi:10.3390/ijms21228614.

[91] K. L. Palmer, L. M. Aye, and M. Whiteley, "Nutritional cues control *Pseudomonas aeruginosa* multicellular behavior in cystic fibrosis sputum," *J. Bacteriol.*, vol. 189, no. 22, pp. 8079–8087, 2007, doi: 10.1128/JB.01138-07.

[92] K. H. Turner, A. K. Wessel, G. C. Palmer, J. L. Murray, and M. Whiteley, "Essential genome of *Pseudomonas aeruginosa* in cystic fibrosis sputum," *Proc. Natl. Acad. Sci. U. S. A.*, vol. 112, no. 13, pp. 4110–4115, 2015, doi: 10.1073/pnas.1419677112.

[93] A. Schick and R. Kassen, "Rapid diversification of *Pseudomonas aeruginosa* in cystic fibrosis lung-like conditions," *Proc. Natl. Acad. Sci. U. S. A.*, vol. 115, no. 42, pp. 10714–10719, 2018, doi: 10.1073/pnas.1721270115.

[94] N. E. Harrington, E. Sweeney, and F. Harrison, “Building a better biofilm - Formation of in vivo-like biofilm structures by *Pseudomonas aeruginosa* in a porcine model of cystic fibrosis lung infection,” *Biofilm*, vol. 2, no. June, p. 100024, 2020, doi: 10.1016/j.bioflm.2020.100024.

[95] A. T. Y. Yeung, A. Parayno, and R. E. W. Hancock, “Mucin promotes rapid surface motility in *Pseudomonas aeruginosa*,” *MBio*, vol. 3, no. 3, 2012, doi: 10.1128/mBio.00073-12.

[96] B. C. Huck *et al.*, “Macro- And microrheological properties of mucus surrogates in comparison to native intestinal and pulmonary mucus,” *Biomacromolecules*, vol. 20, no. 9, pp. 3504–3512, 2019, doi: 10.1021/acs.biomac.9b00780.

[97] S. E. Darch *et al.*, “Spatial determinants of quorum signaling in a *Pseudomonas aeruginosa* infection model,” *Proc. Natl. Acad. Sci. U. S. A.*, vol. 115, no. 18, pp. 4779–4784, 2018, doi: 10.1073/pnas.1719317115.

[98] J. Kočevar-Nared, J. Kristl, and J. Šmid-Korbar, “Comparative rheological investigation of crude gastric mucin and natural gastric mucus,” *Biomaterials*, vol. 18, no. 9, pp. 677–681, 1997, doi: 10.1016/S0142-9612(96)00180-9.

[99] A. W. Larhed, P. Artursson, and E. Björk, “The influence of gastrointestinal mucus components on the diffusion of drugs,” *Pharm. Res.*, vol. 15, no. 1, pp. 66–71, 1998, doi: 10.1023/A:1011948703571.

[100] J. S. Crater and R. L. Carrier, “Barrier properties of gastrointestinal mucus to nanoparticle transport,” *Macromol. Biosci.*, vol. 10, no. 12, pp. 1473–1483, 2010, doi: 10.1002/mabi.201000137.

[101] S. Frisch *et al.*, “A pulmonary mucus surrogate for investigating antibiotic permeation and activity against *Pseudomonas aeruginosa* biofilms,” *J. Antimicrob. Chemother.*, vol. 76, pp. 1472–1479, 2021, doi: 10.1093/jac/dkab068.

[102] R. Hamed and J. Fiegel, “Synthetic tracheal mucus with native rheological and surface tension properties,” *Soc. Biomater.*, vol. 102A, no. 6, pp. 1788–1798, 2013, doi: 10.1002/jbm.a.34851.

[103] I. M. Hansen *et al.*, “Hyaluronic acid molecular weight-dependent modulation of mucin nanostructure for potential mucosal therapeutic applications,” *Mol. Pharm.*, vol. 14, no. 7, pp. 2359–2367, 2017, doi: 10.1021/acs.molpharmaceut.7b00236.

[104] D. P. Pacheco *et al.*, “Disassembling the complexity of mucus barriers to develop a fast screening tool for early drug discovery,” *J. Mater. Chem. B*, vol. 7, no. 32, pp. 4940–4952, 2019, doi: 10.1039/c9tb00957d.

[105] C. Butnarasu, G. Caron, D. P. Pacheco, P. Petrini, and S. Visentin, "Cystic Fibrosis mucus model to design more efficient drug therapies," *Mol. Pharm.*, vol. 19, no. 2, pp. 520–531, 2022, doi: 10.1021/acs.molpharmaceut.1c00644.

[106] G. Millette, J. P. Langlois, E. Brouillette, E. H. Frost, A. M. Cantin, and F. Malouin, "Despite antagonism *in vitro*, *Pseudomonas aeruginosa* enhances *Staphylococcus aureus* colonization in a murine lung infection model," *Front. Microbiol.*, vol. 10, no. December, p. 2880, 2019, doi: 10.3389/fmicb.2019.02880.

[107] N. Hoffmann *et al.*, "Novel mouse model of chronic *Pseudomonas aeruginosa* lung infection mimicking cystic fibrosis," *Infect. Immun.*, vol. 73, no. 8, p. 5290, 2005, doi: 10.1128/IAI.73.8.5290.2005.

[108] D. A. Stoltz *et al.*, "Cystic fibrosis pigs develop lung disease and exhibit defective bacterial eradication at birth," *Sci. Transl. Med.*, vol. 2, no. 29, 2010, doi: 10.1126/scitranslmed.3000928.

[109] B. R. Grubb and R. C. Boucher, "Pathophysiology of gene-targeted mouse models for cystic fibrosis," *Physiol. Rev.*, vol. 79, no. 1 SUPPL. 1, pp. 193–214, 1999, doi: 10.1152/physrev.1999.79.1.S193.

[110] D. K. Meyerholz, D. A. Stoltz, A. A. Pezzulo, and M. J. Welsh, "Pathology of gastrointestinal organs in a porcine model of cystic fibrosis," *Am. J. Pathol.*, vol. 176, no. 3, pp. 1377–1389, 2010, doi: 10.2353/ajpath.2010.090849.

[111] D. A. Stoltz *et al.*, "Intestinal CFTR expression alleviates meconium ileus in cystic fibrosis pigs," *J. Clin. Invest.*, vol. 123, no. 6, pp. 2685–2693, 2013, doi: 10.1172/JCI68867.

[112] C. S. Rogers *et al.*, "Disruption of the CFTR gene produces a model of cystic fibrosis in newborn pigs," *Science (80-.).*, vol. 321, no. September, pp. 1837–1841, 2008.

[113] A. J. Carterson *et al.*, "A549 lung epithelial cells grown as three-dimensional aggregates: Alternative tissue culture model for *Pseudomonas aeruginosa* pathogenesis," *Infect. Immun.*, vol. 73, no. 2, pp. 1129–1140, 2005, doi: 10.1128/IAI.73.2.1129-1140.2005.

[114] G. Orazi and G. A. O'Toole, "*Pseudomonas aeruginosa* alters *Staphylococcus aureus* sensitivity to vancomycin in a biofilm model of cystic fibrosis infection," *MBio*, vol. 8, no. 4, pp. e00873-17, 2017, doi: 10.1128/mBio.00873-17.

[115] D. H. Limoli *et al.*, "*Pseudomonas aeruginosa* alginate overproduction promotes coexistance with *Staphylococcus aureus* in a model of cystic fibrosis respiratory infection," *Am. Soc. Microbiol.*, vol. 8, no. 2, pp. e00186-17, 2017.

[116] H. Matsui *et al.*, “A physical linkage between cystic fibrosis airway surface dehydration and *Pseudomonas aeruginosa* biofilms,” *Proc. Natl. Acad. Sci. U. S. A.*, vol. 103, no. 48, pp. 18131–18136, 2006, doi: 10.1073/pnas.0606428103.

[117] E. Deschamps *et al.*, “Membrane phospholipid composition of *Pseudomonas aeruginosa* grown in a cystic fibrosis mucus-mimicking medium,” *Biochim. Biophys. Acta - Biomembr.*, vol. 1863, no. 1, 2021, doi: 10.1016/j.bbamem.2020.183482.

[118] E. Sweeney *et al.*, “An *ex vivo* cystic fibrosis model recapitulates key clinical aspects of chronic *Staphylococcus aureus* infection,” *Microbiol. (United Kingdom)*, vol. 167, no. 1, pp. 1–15, 2021, doi: 10.1099/mic.0.000987.

[119] R. Plebani *et al.*, “Modeling pulmonary cystic fibrosis in a human lung airway-on-a-chip: Cystic fibrosis airway chip,” *J. Cyst. Fibros.*, vol. 21, no. 4, pp. 606–615, 2021, doi: 10.1016/j.jcf.2021.10.004.

[120] ISO, “Biological evaluation of medical devices - Part 5: Tests for in vitro cytotoxicity.” 2009, [Online]. Available: https://www.iso.org/standard/36406.html.

[121] A. J. Huang, C. L. O’Brien, N. Dawe, A. Tahir, A. J. Scott, and B. M. Leung, “Characterization of an engineered mucus microenvironment for *in vitro* modeling of host–microbe interactions,” *Sci. Rep.*, vol. 12, no. 1, pp. 1–14, 2022, doi: 10.1038/s41598-022-09198-6.

[122] I. Wiegand, K. Hilpert, and R. E. W. Hancock, “Agar and broth dilution methods to determine the minimal inhibitory concentration (MIC) of antimicrobial substances,” *Nat. Protoc.*, vol. 3, no. 2, pp. 163–175, 2008, doi: 10.1038/nprot.2007.521.

[123] M. Boon *et al.*, “Morphometric analysis of explant lungs in cystic fibrosis,” *Am. J. Respir. Crit. Care Med.*, vol. 193, no. 5, pp. 516–526, 2016, doi: 10.1164/rccm.201507-1281OC.

[124] G. Tomaiuolo *et al.*, “A new method to improve the clinical evaluation of cystic fibrosis patients by mucus viscoelastic properties,” *PLoS One*, vol. 9, no. 1, p. e82297, 2014, doi: 10.1371/journal.pone.0082297.

[125] C. M. Fernandez-Petty *et al.*, “A glycopolymer improves vascoelasticity and mucociliary transport of abnormal cystic fibrosis mucus,” *JCI Insight*, vol. 4, no. 8, 2019, doi: 10.1172/jci.insight.125954.

[126] A. Horsley *et al.*, “Reassessment of the importance of mucins in determining sputum properties in cystic fibrosis,” *J. Cyst. Fibros.*, vol. 13, no. 3, pp. 260–266, 2014, doi: 10.1016/j.jcf.2013.11.002.

[127] B. Vukosavljevic, X. Murgia, K. Schwarzkopf, U. F. Schaefer, C. M. Lehr, and M. Windbergs, "Tracing molecular and structural changes upon mucolysis with N-acetyl cysteine in human airway mucus," *Int. J. Pharm.*, vol. 533, no. 2, pp. 373–376, 2017, doi: 10.1016/j.ijpharm.2017.07.022.

[128] J. Patarin *et al.*, "Rheological analysis of sputum from patients with chronic bronchial diseases," *Sci. Rep.*, vol. 10, no. 1, pp. 1–10, 2020, doi: 10.1038/s41598-020-72672-6.

[129] D. J. Serisier, M. P. Carroll, J. K. Shute, and S. A. Young, "Macrorheology of cystic fibrosis, chronic obstructive pulmonary disease & normal sputum," *Respir. Res.*, vol. 10, pp. 1–8, 2009, doi: 10.1186/1465-9921-10-63.

[130] Valerius NH, Koch C, and N. Hoiby, "Prevention of chronic *Pseudomonas aeruginosa* colonisation in cystic fibrosis by early treatment," *Lancet*, vol. 338, pp. 725–726, 1991, doi: 10.1016/0140-6736(91)91446-2.

[131] G. Taccetti, S. Campana, F. Festini, M. Mascherini, and G. Döring, "Early eradication therapy against *Pseudomonas aeruginosa* in cystic fibrosis patients," *Eur. Respir. J.*, vol. 26, no. 3, pp. 458–461, 2005, doi: 10.1183/09031936.05.00009605.

[132] S. C. Langton Hewer *et al.*, "Intravenous or oral antibiotic treatment in adults and children with cystic fibrosis and *Pseudomonas aeruginosa* infection: the TORPEDO-CF RCT," *Health Technol. Assess. (Rockv).*, vol. 25, no. 65, pp. VII–67, 2021, doi: 10.3310/hta25650.

[133] T. Kopač, A. Ručigaj, and M. Krajnc, "The mutual effect of the crosslinker and biopolymer concentration on the desired hydrogel properties," *Int. J. Biol. Macromol.*, vol. 159, pp. 557–569, 2020, doi: 10.1016/j.ijbiomac.2020.05.088.

[134] J. S. Suk *et al.*, "The penetration of fresh undiluted sputum expectorated by cystic fibrosis patients by non-adhesive polymer nanoparticles," *Biomaterials*, vol. 30, no. 13, pp. 2591–2597, 2009, doi: 10.1016/j.biomaterials.2008.12.076.

[135] Q. Xu *et al.*, "Impact of surface polyethylene glycol (PEG) density on biodegradable nanoparticle transport in mucus *ex vivo* and distribution *in vivo*," *ACS Nano*, vol. 9, no. 9, pp. 9217–9227, 2015, doi: 10.1021/acsnano.5b03876.

[136] M. Falavigna, P. C. Stein, G. E. Flaten, and M. P. Di Cagno, "Impact of mucin on drug diffusion: Development of a straightforward in vitro method for the determination of drug diffusivity in the presence of mucin," *Pharmaceutics*, vol. 12, no. 2, 2020, doi: 10.3390/pharmaceutics12020168.

[137] T. Mezger, "8. Oscillatory tests," in *The Rheology Handbook: For users of rotational and oscillatory rheometers*, Hannover, Germany: Vincentz Network, 2020, pp. 153–247. [Online]. doi: 10.1515/9783748603702.

[138] S. Liu, H. Li, B. Tang, S. Bi, and L. Li, "Scaling law and microstructure of alginate hydrogel," *Carbohydr. Polym.*, vol. 135, pp. 101–109, 2016, doi: 10.1016/j.carbpol.2015.08.086.

[139] C. Ridley *et al.*, "Assembly of the respiratory Mucin MUC5B a new model for a gel-forming Mucin," *J. Biol. Chem.*, vol. 289, no. 23, pp. 16409–16420, 2014, doi: 10.1074/jbc.M114.566679.

[140] E. Y. T. Chen, N. Yang, P. M. Quinton, and W. C. Chin, "A new role for bicarbonate in mucus formation," *Am. J. Physiol. - Lung Cell. Mol. Physiol.*, vol. 299, no. 4, pp. 542–549, 2010, doi: 10.1152/ajplung.00180.2010.

[141] B. D. E. Raynal, T. E. Hardingham, J. K. Sheehan, and D. J. Thornton, "Calcium-dependent protein interactions in MUC5B provide reversible cross-links in salivary mucus," *J. Biol. Chem.*, vol. 278, no. 31, pp. 28703–28710, 2003, doi: 10.1074/jbc.M304632200.

[142] J. P. Frampton, J. B. White, A. T. Abraham, and S. Takayama, "Cell co-culture patterning using aqueous two-phase systems.," *J. Vis. Exp.*, no. 73, pp. 16–20, 2013, doi: 10.3791/50304.

[143] Y. Liu, R. Lipowsky, and R. Dimova, "Concentration dependence of the interfacial tension for aqueous two-phase polymer solutions of dextran and polyethylene glycol," *Langmuir*, vol. 28, no. 8, pp. 3831–3839, 2012, doi: 10.1021/la204757z.

[144] T. Yaguchi *et al.*, "Aqueous two-phase system-derived biofilms for bacterial interaction studies," *Biomacromolecules*, vol. 13, no. 9, pp. 2655–2661, 2012, doi: 10.1021/bm300500y.

[145] M. Dwidar, B. M. Leung, T. Yaguchi, S. Takayama, and R. J. Mitchell, "Patterning bacterial communities on epithelial cells," *PLoS One*, vol. 8, no. 6, pp. 1–14, 2013, doi: 10.1371/journal.pone.0067165.

[146] J. P. Barraza and M. Whiteley, "A *Pseudomonas aeruginosa* antimicrobial affects the biogeography but not fitness of *Staphylococcus aureus* during coculture," *MBio*, vol. 12, no. 2, pp. e00047-21, 2021, doi: 10.1128/mBio.00047-21.

[147] M. Fazli *et al.*, "Nonrandom distribution of *Pseudomonas aeruginosa* and *Staphylococcus aureus* in chronic wounds," *J. Clin. Microbiol.*, vol. 47, no. 12, pp. 4084–4089, 2009, doi: 10.1128/JCM.01395-09.

[148] P. M. Alves, E. Al-Badi, C. Withycombe, P. M. Jones, K. J. Purdy, and S. E. Maddocks, "Interaction between *Staphylococcus aureus* and *Pseudomonas aeruginosa* is beneficial for colonisation and pathogenicity in a mixed biofilm," *Pathog. Dis.*, vol. 76, no. 1, pp. 1–10, 2018, doi: 10.1093/femspd/fty003.

[149] E. Chi, T. Mehl, D. Nunn, and S. Lory, "Interaction of *Pseudomonas aeruginosa* with A549 pneumocyte cells," *Infect. Immun.*, vol. 59, no. 3, pp. 822–828, 1991, doi: 10.1128/iai.59.3.822-828.1991.

[150] S. Moreau-Marquis *et al.*, "The ΔF508-CFTR mutation results in increased biofilm formation by *Pseudomonas aeruginosa* by increasing iron availability," *Am. J. Physiol. - Lung Cell. Mol. Physiol.*, vol. 295, no. 1, pp. 25–37, 2008, doi: 10.1152/ajplung.00391.2007.

[151] G. G. Anderson, S. Moreau-Marquis, B. A. Stanton, and G. A. O'Toole, "*In vitro* analysis of tobramycin-treated *Pseudomonas aeruginosa* biofilms on cystic fibrosis-derived airway epithelial cells," *Infect. Immun.*, vol. 76, no. 4, pp. 1423–1433, 2008, doi: 10.1128/IAI.01373-07.

[152] J. Jyot *et al.*, "Type II secretion system of *Pseudomonas aeruginosa*: *In vivo* evidence of a significant role in death due to lung infection," *J. Infect. Dis.*, vol. 203, no. 10, pp. 1369–1377, 2011, doi: 10.1093/infdis/jir045.

[153] G. Horna and J. Ruiz, "Type 3 secretion system of *Pseudomonas aeruginosa*," *Microbiol. Res.*, vol. 246, no. January, p. 126719, 2021, doi: 10.1016/j.micres.2021.126719.

[154] C. G. Korea *et al.*, "Staphylococcal Esx proteins modulate apoptosis and release of intracellular *Staphylococcus aureus* during infection in epithelial cells," *Infect. Immun.*, vol. 82, no. 10, pp. 4144–4153, 2014, doi: 10.1128/IAI.01576-14.

[155] K. Stelzner *et al.*, "Intracellular *Staphylococcus aureus* employs the cysteine protease staphopain A to induce host cell death in epithelial cells," *PLoS Pathog.*, vol. 17, no. 9, p. e1009874, 2021, doi: 10.1371/journal.ppat.1009874.

[156] B. C. Kahl *et al.*, "*Staphylococcus aureus* RN6390 replicates and induces apoptosis in a pulmonary epithelial cell line," *Infect. Immun.*, vol. 68, no. 9, pp. 5385–5392, 2000, doi: 10.1128/IAI.68.9.5385-5392.2000.

[157] J. Baishya, J. A. Everett, W. J. Chazin, K. P. Rumbaugh, and C. A. Wakeman, "The innate immune protein calprotectin interacts with and encases biofilm communities of *Pseudomonas aeruginosa* and *Staphylococcus aureus*," *Front. Cell. Infect. Microbiol.*, vol. 12, p. 898796, 2022, doi: 10.3389/fcimb.2022.898796.

[158] P. Briaud, L. Camus, S. Bastien, A. Doléans-Jordheim, F. Vandenesch, and K. Moreau, "Coexistence with *Pseudomonas aeruginosa* alters *Staphylococcus aureus* transcriptome, antibiotic resistance and internalization into epithelial cells," *Sci. Rep.*, vol. 9, no. 1, pp. 1–14, 2019, doi: 10.1038/s41598-019-52975-z.

[159] P. Gao *et al.*, "Subinhibitory concentrations of antibiotics exacerbate staphylococcal infection by inducing bacterial virulence," *Microbiol. Spectr.*, vol. 10, no. 4, 2022, doi: 10.1128/spectrum.00640-22.

[160] M. Alhede *et al.*, "Phenotypes of non-attached *Pseudomonas aeruginosa* aggregates resemble surface attached biofilm," *PLoS One*, vol. 6, no. 11, 2011, doi: 10.1371/journal.pone.0027943.

[161] B. J. Staudinger *et al.*, "Conditions associated with the cystic fibrosis defect promote chronic *Pseudomonas aeruginosa* infection," *Am. J. Respir. Crit. Care Med.*, vol. 189, no. 7, pp. 812–824, 2014, doi: 10.1164/rccm.201312-2142OC.

[162] M. Caldara, R. S. Friedlander, N. L. Kavanaugh, J. Aizenberg, K. R. Foster, and K. Ribbeck, "Mucin biopolymers prevent bacterial aggregation by retaining cells in the free-swimming state," *Curr. Biol.*, vol. 22, no. 24, pp. 2325–2330, 2012, doi: 10.1016/j.cub.2012.10.028.

[163] A. Crabbé, P. Ø. Jensen, T. Bjarnsholt, and T. Coenye, "Antimicrobial tolerance and metabolic adaptations in microbial biofilms," *Trends Microbiol.*, vol. 27, no. 10, pp. 850–863, 2019, doi: 10.1016/j.tim.2019.05.003.

[164] F. Jean-Pierre, M. A. Henson, and G. A. O'Toole, "Metabolic modeling to interrogate microbial disease: A tale for experimentalists," *Front. Mol. Biosci.*, vol. 8, p. 634479, 2021, doi: 10.3389/fmolb.2021.634479.

[165] A. Crabbé *et al.*, "Host metabolites stimulate the bacterial proton motive force to enhance the activity of aminoglycoside antibiotics," *PLoS Pathog.*, vol. 15, no. 4, p. e1007697, 2019, doi: 10.1371/journal.ppat.1007697.

[166] Y. Wang *et al.*, "Two NAD-independent l-lactate dehydrogenases drive l-lactate utilization in *Pseudomonas aeruginosa* PAO1," *Environ. Microbiol. Rep.*, vol. 10, no. 5, pp. 569–575, 2018, doi: 10.1111/1758-2229.12666.

[167] M. Ulrich *et al.*, "Localization of *Staphylococcus aureus* in infected airways of patients with cystic fibrosis and in a cell culture model of *S. aureus* adherence," *Pneumologie*, vol. 52, no. 12, p. 729, 1998, doi: 10.1165/ajrcmb.19.1.3137.

[168] V. L. Thomas, B. A. Sanford, and M. A. Ramsay, "Calcium- and mucin-binding proteins of staphylococci," *J. Gen. Microbiol.*, vol. 139, no. 3, pp. 623–629, 1993, doi: 10.1099/00221287-139-3-623.

[169] J. Shuter, V. B. Hatcher, and F. D. Lowy, "*Staphylococcus aureus* binding to human nasal mucin," *Infect. Immun.*, vol. 64, no. 1, pp. 310–318, 1996, doi: 10.1128/iai.64.1.310-318.1996.

[170] D. Trivier, N. Houdret, R. J. Courcol, G. Lamblin, P. Roussel, and M. Davril, "The binding of surface proteins from *Staphylococcus aureus* to human bronchial mucins," *Eur. Respir. J.*, vol. 10, no. 4, pp. 804–810, 1997, doi: 10.1183/09031936.97.10040804.

[171] K. Schilcher and A. R. Horswill, "Staphylococcal biofilm development: Structure, regulation, and treatment strategies," *Am. Soc. Microbiol.*, vol. 84, no. 3, pp. 00026–19, 2020, doi: 10 .1128/MMBR.00026-19.

[172] M. Tognon, T. Köhler, A. Luscher, and C. Van Delden, "Transcriptional profiling of *Pseudomonas aeruginosa* and *Staphylococcus aureus* during *in vitro* co-culture," *BMC Genomics*, vol. 20, no. 30, 2019, doi: 10.1186/s12864-018-5398-y.

[173] M. Pazgier, D. M. Hoover, D. Yang, W. Lu, and J. Lubkowski, "Human β-defensins," *Cell. Mol. Life Sci.*, vol. 63, no. 11, pp. 1294–1313, 2006, doi: 10.1007/s00018-005-5540-2.

[174] J. Harder, J. Bartels, E. Christophers, and J. M. Schroder, "A peptide antibiotic from human skin," *Nature*, vol. 387, no. 6636, p. 861, 1997, doi: 10.1038/43088.

[175] J. Harder, J. Bartels, E. Christophers, and J. M. Schröder, "Isolation and characterization of human β-Defensin-3, a novel human inducible peptide antibiotic," *J. Biol. Chem.*, vol. 276, no. 8, pp. 5707–5713, 2001, doi: 10.1074/jbc.M008557200.

[176] L. Alekseeva *et al.*, "Inducible expression of beta defensins by human respiratory epithelial cells exposed to *Aspergillus fumigatus* organisms," *BMC Microbiol.*, vol. 9, 2009, doi: 10.1186/1471-2180-9-33.

[177] K. Midorikawa *et al.*, "*Staphylococcus aureus* susceptibility to innate antimicrobial peptides, β-defensins and CAP18, expressed by human keratinocytes," *Infect. Immun.*, vol. 71, no. 7, pp. 3730–3739, 2003, doi: 10.1128/IAI.71.7.3730-3739.2003.

[178] K. R. Parducho *et al.*, "The antimicrobial peptide human Beta-Defensin 2 inhibits biofilm production of *Pseudomonas aeruginosa* without compromising metabolic activity," *Front. Immunol.*, vol. 11, no. May, pp. 1–16, 2020, doi: 10.3389/fimmu.2020.00805.

[179] A. P. Magalhães, S. P. Lopes, and M. O. Pereira, "Insights into cystic fibrosis polymicrobial consortia: The role of species interactions in biofilm development, phenotype, and response to in-use antibiotics," *Front. Microbiol.*, vol. 7, p. 2146, 2017, doi: 10.3389/fmicb.2016.02146.

[180] T. M. Zarrella and A. Khare, "Systematic identification of molecular mediators of interspecies sensing in a community of two frequently coinfecting bacterial pathogens," *PLoS Biol.*, vol. 20, no. 6, p. e3001679, 2022, doi: 10.1371/journal.pbio.3001679.

[181] T. Samad, J. Y. Co, J. Witten, and K. Ribbeck, "Mucus and mucin environments reduce the efficacy of polymyxin and fluoroquinolone antibiotics against *Pseudomonas aeruginosa*," *ACS Biomater. Sci. Eng.*, vol. 5, no. 3, pp. 1189–1194, 2019, doi: 10.1021/acsbiomaterials.8b01054.

[182] C. E. Price, D. G. Brown, D. H. Limoli, V. V. Phelan, and G. A. O'Toole, "Exogenous alginate protects *Staphylococcus aureus* from killing by *Pseudomonas aeruginosa*," *Am. Soc. Microbiol.*, vol. 202, no. 8, pp. e00559-19, 2020, doi: 10.1128/JB .00559-19.

[183] R. L. Neve, B. D. Carrillo, and V. V. Phelan, "Impact of artificial sputum medium formulation on *Pseudomonas aeruginosa* secondary metabolite production," *J. Bacteriol.*, vol. 203, no. 21, 2021, doi: 10.1128/JB.00250-21.

[184] A. Crabbé *et al.*, "Antimicrobial efficacy against *Pseudomonas aeruginosa* biofilm formation in a three-dimensional lung epithelial model and the influence of fetal bovine serum," *Sci. Rep.*, vol. 7, no. January, pp. 1–13, 2017, doi: 10.1038/srep43321.

[185] Q. Yu, E. F. Griffin, S. Moreau-Marquis, J. D. Schwartzman, B. A. Stanton, and G. A. O'Toole, "*In vitro* evaluation of tobramycin and aztreonam versus *Pseudomonas aeruginosa* biofilms on cystic fibrosis-derived human airway epithelial cells," *J. Antimicrob. Chemother.*, vol. 67, no. 11, pp. 2673–2681, 2012, doi: 10.1093/jac/dks296.

[186] R. G. Doggett, "Incidence of mucoid *Pseudomonas aeruginosa* from clinical sources.," *Appl. Microbiol.*, vol. 18, no. 5, pp. 936–937, 1969, doi: 10.1128/aem.18.5.936-937.1969.

[187] S. S. Pedersen, N. Hoiby, F. Espersen, and C. Koch, "Role of alginate in infection with mucoid *Pseudomonas aeruginosa* in cystic fibrosis," *Thorax*, vol. 47, no. 1, pp. 6–13, 1992, doi: 10.1136/thx.47.1.6.

[188] A. Mena *et al.*, "Genetic adaptation of *Pseudomonas aeruginosa* to the airways of cystic fibrosis patients is catalyzed by hypermutation," *J. Bacteriol.*, vol. 190, no. 24, pp. 7910–7917, 2008, doi: 10.1128/JB.01147-08.

[189] M. del M. Cendra, N. Blanco-Cabra, L. Pedraz, and E. Torrents, “Optimal environmental and culture conditions allow the *in vitro* coexistence of *Pseudomonas aeruginosa* and *Staphylococcus aureus* in stable biofilms,” *Sci. Rep.*, vol. 9, p. 16284, 2019, doi: 10.1038/s41598-019-52726-0.

[190] E. Y. Trizna *et al.*, “Bidirectional alterations in antibiotics susceptibility in *Staphylococcus aureus—Pseudomonas aeruginosa* dual-species biofilm,” *Sci. Rep.*, vol. 10, p. 14849, 2020, doi: 10.1038/s41598-020-71834-w.

Appendix A

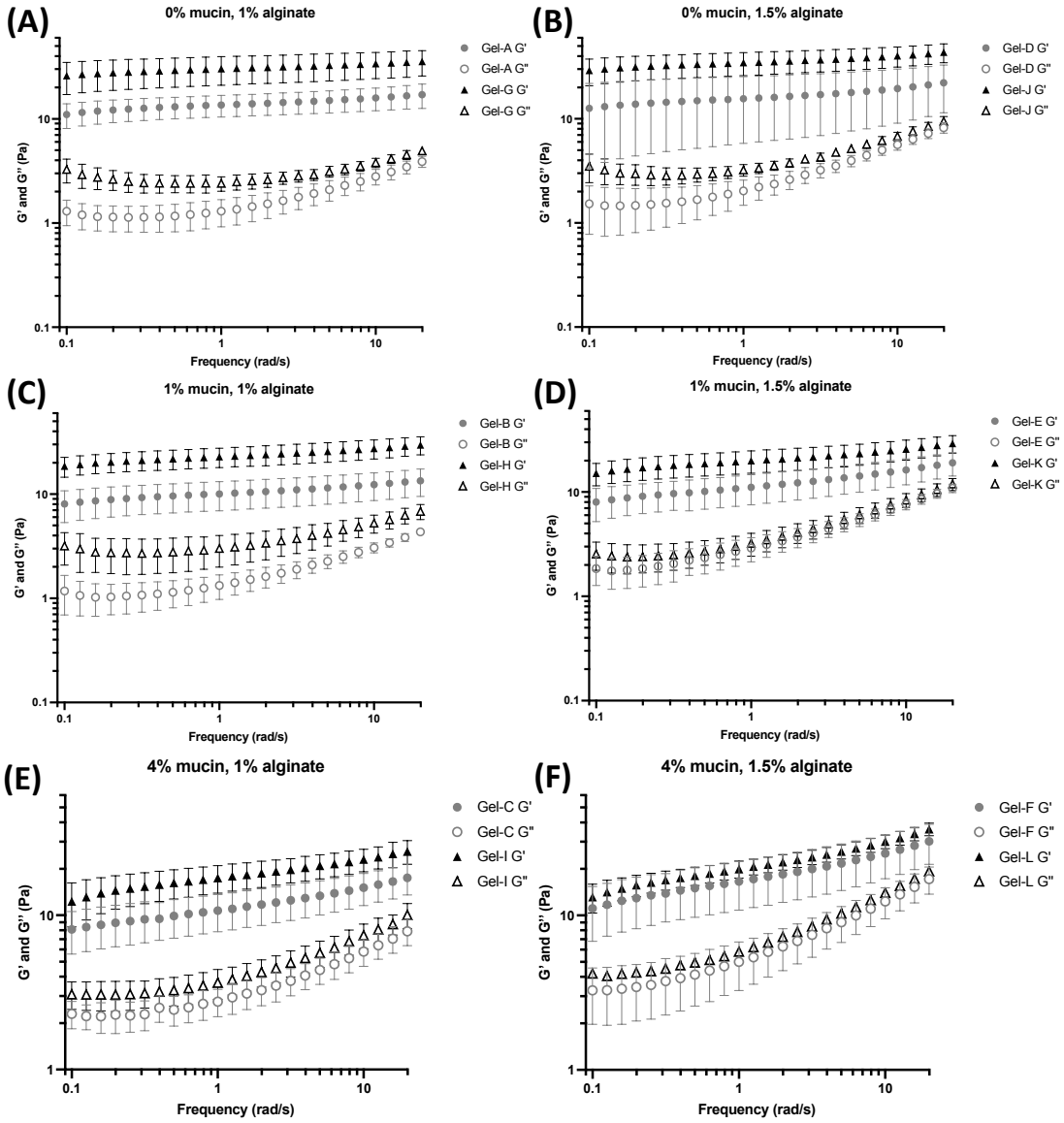

Figure 31: Viscoelastic properties of potential mucus-like hydrogel formulations paired by constant mucin and alginate concentrations to demonstrate how crosslinker concentration impacts viscoelastic properties. Grey icons represent formulations with 0.5 mg/ml $CaCl_2$ crosslinker and black icons represent formulations with 0.6 mg/ml $CaCl_2$ crosslinker. Storage moduli, G', represented by solid icons and loss moduli, G'', represented by open icons. Data shown from an angular frequency range of 0.1 to 20 rad/s. Values are the average ± SD from three independent measurements. **(A)** 0% mucin, 1% alginate. **(B)** 0% mucin, 1.5% alginate. **(C)** 1% mucin, 1% alginate. **(D)** 1% mucin, 1.5% alginate. **(E)** 4% mucin, 1% alginate. **(F)** 4% mucin, 1.5% alginate.

Appendix B

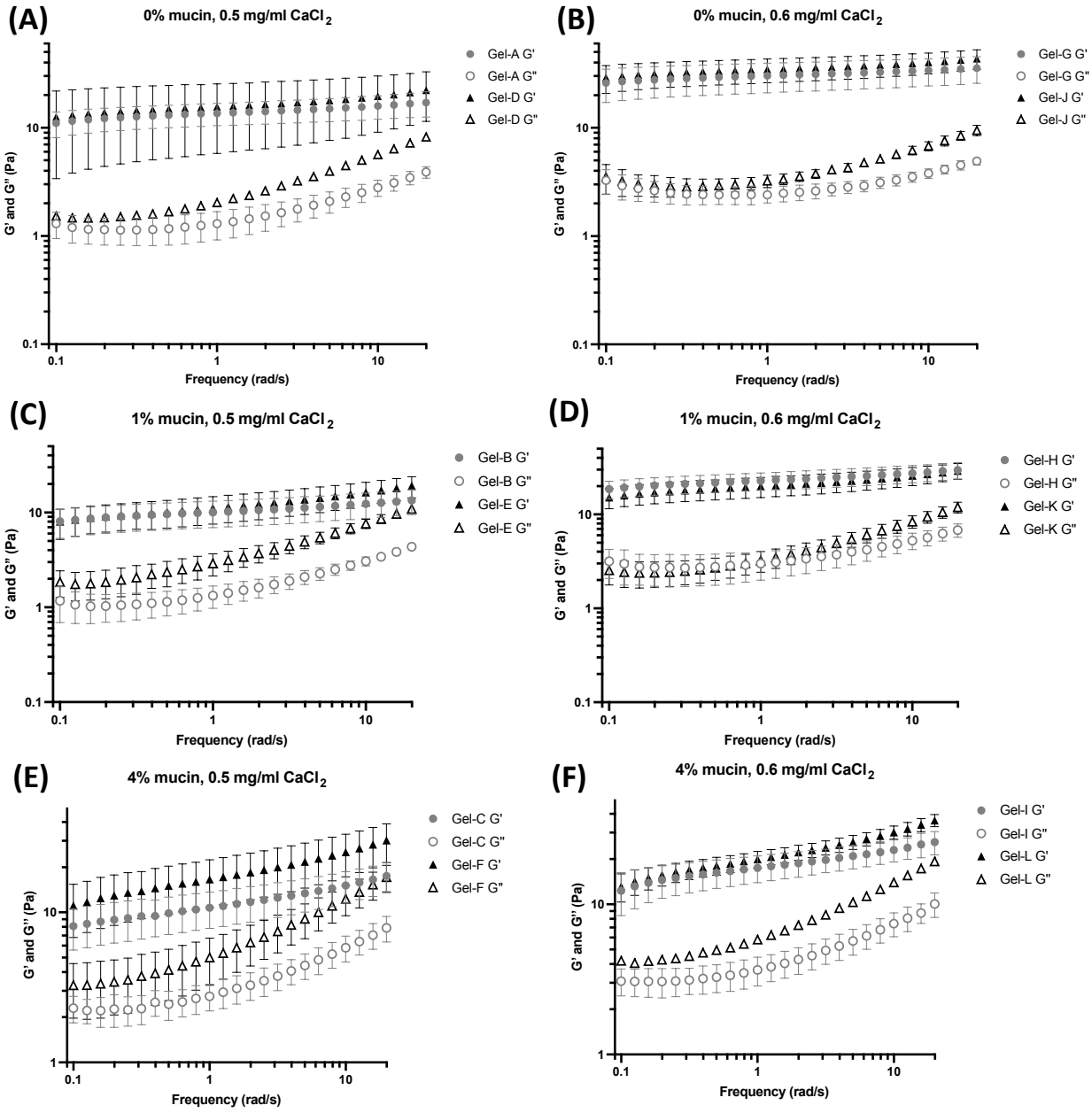

Figure 32: Viscoelastic properties of potential mucus-like hydrogel formulations paired by constant mucin and crosslinker concentrations to demonstrate how alginate concentration impacts viscoelastic properties. Grey icons represent formulations with 1% alginate and black icons represent formulations with 1.5% alginate. Storage moduli, G', represented by solid icons and loss moduli, G'', represented by open icons. Data shown from an angular frequency range of 0.1 to 20 rad/s. Values are the average ± SD from three independent measurements. **(A)** 0% mucin, 0.5 mg/ml $CaCl_2$. **(B)** 0% mucin, 0.6 mg/ml $CaCl_2$. **(C)** 1% mucin, 0.5 mg/ml $CaCl_2$. **(D)** 1% mucin, 0.6 mg/ml $CaCl_2$. **(E)** 4% mucin, 0.5 mg/ml $CaCl_2$. **(F)** 4% mucin, 0.6 mg/ml $CaCl_2$.

Appendix C

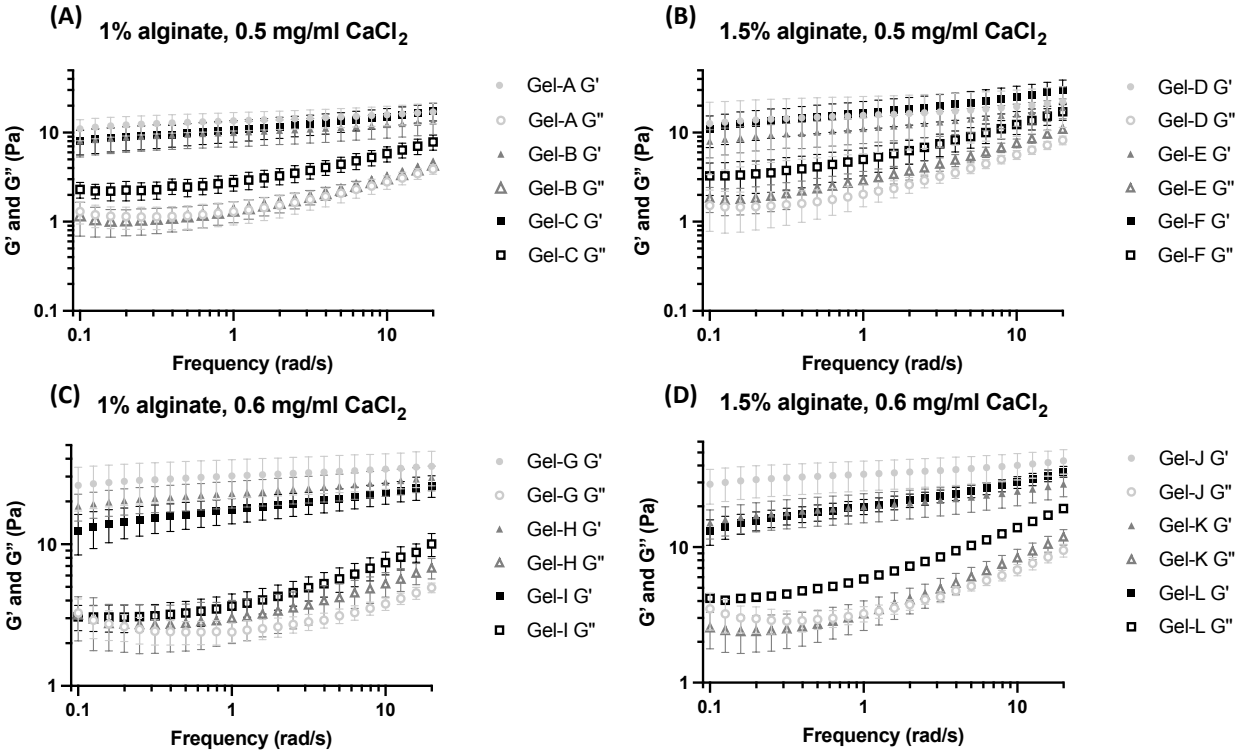

Figure 33: Viscoelastic properties of potential mucus-like hydrogel formulations paired by constant alginate and crosslinker concentrations to demonstrate how mucin concentration impacts viscoelastic properties. Lighter grey icons represent formulations with 1% mucin, darker grey icons represent formulations with 1% mucin, and black icons represent formulations with 4% mucin. Storage moduli, G', represented by solid icons and loss moduli, G'', represented by open icons. Data shown from an angular frequency range of 0.1 to 20 rad/s. Values are the average ± SD from three independent measurements. **(A)** 1% alginate, 0.5 mg/ml $CaCl_2$. **(B)** 1.5% alginate, 0.5 mg/ml $CaCl_2$. **(C)** 1% alginate, 0.6 mg/ml $CaCl_2$. **(D)** 1.5% alginate, 0.6 mg/ml $CaCl_2$.

Appendix D

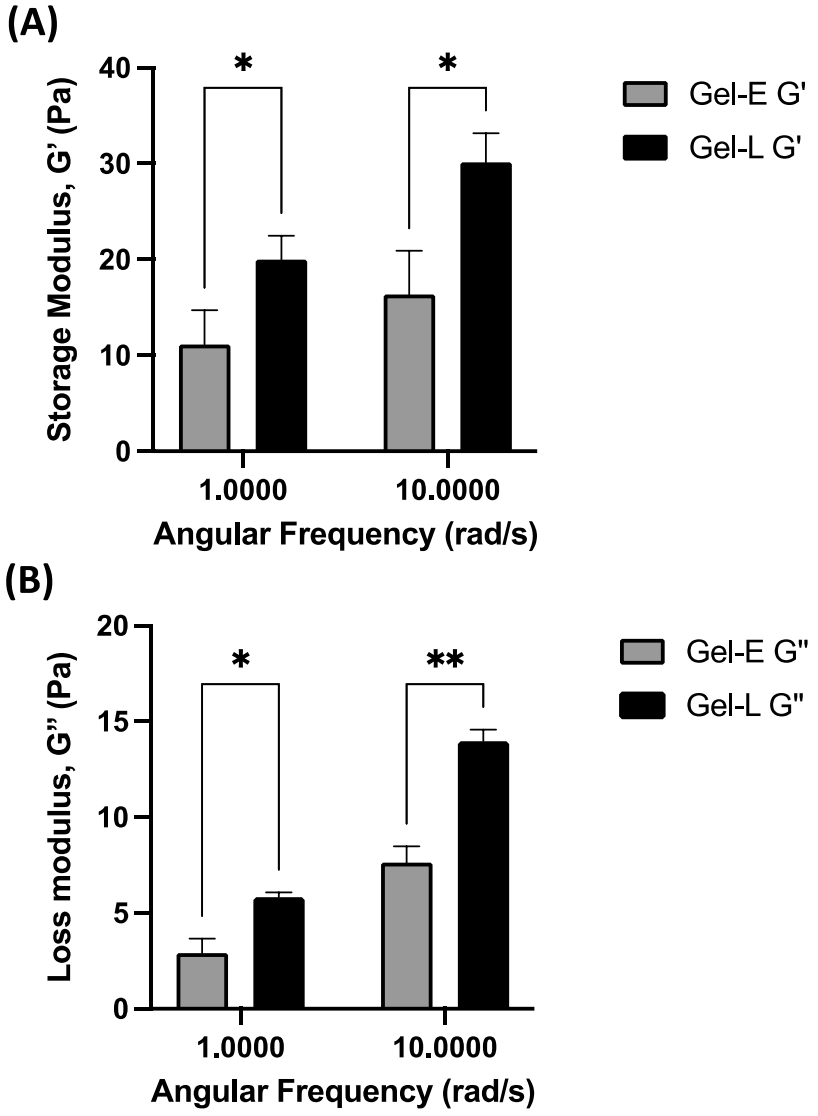

Figure 34: Comparison of the viscoelastic properties of the chosen mucus-like hydrogels at selected higher (10 rad/s) and lower (1 rad/s) angular frequencies. (A) Storage modulus, G'. **(B)** Loss modulus, G''. Statistical significance was determined using multiple t-test. *$p < 0.05$, **$p < 0.01$.